Universidade do Minho
Escola de Medicina

Olga Marisa da Silva Pereira

Metabolic networks and metabolism in acute myeloid leukemia

novembro de 2019

Olga Marisa da Silva Pereira **Metabolic networks and metabolism in acute myeloid leukemia**

UMinho | 2019

Universidade do Minho
Escola de Medicina

Olga Marisa da Silva Pereira

Metabolic networks and metabolism in acute myeloid leukemia

Tese de Doutoramento
Doutoramento em Envelhecimento e Doenças Crónicas

Trabalho efetuado sob a orientação da
Professora Doutora Paula Cristina da Costa Alves Monteiro Ludovico
e do
Doutor Henrique Manuel Paixão dos Santos Girão

novembro de 2019

AGRADECIMENTOS

"Life is not easy for any of us. But what of that? We must have perseverance and above all confidence in ourselves. We must believe that we are gifted for something and that this thing must be attained." – Marie Curie (1867-1934)

Gostaria de deixar um agradecimento especial,

À Professora Doutora Paula Ludovico, pela oportunidade e confiança atribuídas, pelo apoio e conhecimento transmitidos, pelos debates científicos, bem como, pela exigência e rigor impostos.

Ao Doutor Henrique Girão, por aceitar co-orientar este projecto, pelas sugestões dadas e pela disponibilidade sempre demonstrada.

Aos coordenadores do PhDOC, Professora Catarina Oliveira, Professora Margarida Correia-Neves, Professor Henrique Girão e Professor Duarte Barral, por todo o apoio prestado.

À Dra. Isabel Castro, pelos debates científicos e por toda a amabilidade e prontidão demonstradas.

A todos os membros do Concelho Científico da Escola de Medicina, com um agradecimento sentido à Professora Cecília Leão e ao Professor Jorge Pedrosa.

Aos meus amigos e familiares, por TUDO!

The present work was carried out at the Life and Health Sciences Research Institute (ICVS), School of Medicine, University of Minho, ICVS/3B's - PT Government Associate Laboratory, Braga/Guimarães, Portugal. Financial support was provided by a PhD grant from the Foundation for Science and Technology (FCT) - SFRH/BD/52292/2013. This work was developed under the scope of the project NORTE-01-0145-FEDER-000013, supported by the Northern Portugal Regional Operational Programme (NORTE 2020), under the Portugal 2020 Partnership Agreement, through the European Regional Development Fund (FEDER), through the Competitiveness Factors Operational Programme (COMPETE), and by National funds, through the Foundation for Science and Technology (FCT), under the scope of the project POCI-01-0145FEDER-007038.

FCT Fundação para a Ciência e a Tecnologia
MINISTÉRIO DA EDUCAÇÃO E CIÊNCIA

POPH PROGRAMA OPERACIONAL POTENCIAL HUMANO
QREN QUADRO DE REFERÊNCIA ESTRATÉGICO NACIONAL PORTUGAL 2007.2013
Governo da República Portuguesa
UNIÃO EUROPEIA Fundo Europeu de Desenvolvimento Regional

Cofinanciado por:
COMPETE 2020
PORTUGAL 2020
UNIÃO EUROPEIA Fundo Europeu de Desenvolvimento Regional
NORTE2020 PROGRAMA OPERACIONAL REGIONAL DO NORTE

STATEMENT OF INTEGRITY

I hereby declare having conducted this academic work with integrity. I confirm that I have not used plagiarism or any form of undue use of information or falsification of results along the process leading to its elaboration. I further declare that I have fully acknowledged the Code of Ethical Conduct of the University of Minho.

RESUMO - METABOLISMO E SUA SINALIZAÇÃO NA LEUCEMIA MIELOIDE AGUDA

A leucemia mieloide aguda (LMA) é um grupo heterogéneo de doenças caracterizado por alterações na diferenciação e/ou proliferação de células mieloides imaturas. A terapia usada na LMA tem aplicabilidade limitada nos idosos, a população mais afetada, tornando critica a elucidação dos mecanismos subjacentes a esta doença. Alterações no metabolismo energético, vias de sinalização celular (AMPK, mTORC1 e AKT) e/ou macroautofagia (doravante denominado autofagia) têm sido identificadas na LMA, com dados controversos reportados. Este trabalho caracterizou o perfil energético, metabólico e autofágico, bem como a sua interligação, em diferentes subtipos de LMA. Linhas celulares de LMA representativas de subtipos desta doença, HL-60 (FAB-M2), NB-4 (FAB-M3) e KG-1 (FAB-M6), foram usadas. Um fenótipo de fosforilação oxidativa associado a co-ativação do AMPK e mTORC1 e autofagia aumentada foi exibido pelas células KG-1, enquanto as células NB-4 e HL-60 apresentaram um fenótipo glicolítico associado a ativação do AKT/mTORC1 e autofagia diminuída. A inibição do AKT reduziu a viabilidade das células NB-4 e HL-60. Adaptações metabólicas distintas parecem, portanto, ocorrer entre diferentes subtipos de LMA, sendo o AKT um potencial alvo terapêutico em alguns cenários de LMA. Esta tese também caracterizou o padrão de expressão de genes autofágicos em subtipos distintos de LMA, usando mRNA da medula óssea de pacientes com LMA. Ao categorizar os pacientes com LMA de acordo com o subtipo FAB, grupo de risco citogenético ou cariótipo, uma expressão diferencial de genes autofágicos foi notada entre os grupos testados. Este estudo suporta, portanto, a ocorrência de perfis autofágicos distintos entre diferentes subtipos de LMA. A diabetes *mellitus* tipo 2 (doravante denominada DM) tem sido associada à ocorrência de LMA e a alterações nas células estromais da medula óssea (CEMO). Esta tese também avaliou o impacto que as alterações induzidas pela glucose nas CEMO têm na patogénese de diferentes subtipos de LMA. As células NB-4, HL-60 e KG-1 foram expostas de forma aguda ou crónica a meio condicionado produzido por CEMO com uma concentração de glucose normal ou elevada (CM-RG or CM-HG). Um fenótipo tumorigénico aumentado foi exibido pelas células NB-4, seguidas pelas células HL-60 e KG-1, após exposição crónica ao meio condicionado produzido pelas CEMO com concentração elevada de glucose. A exposição crónica às alterações promovidas pela glucose no secretoma das CEMO parece, portanto, contribuir para a patogénese de diferentes subtipos de LMA. O tratamento da LMA deve passar por uma terapia personalizada adaptada à heterogeneidade deste grupo de doenças.

PALAVRAS-CHAVE: Autofagia ▪ Leucemia mieloide aguda (LMA) ▪ Metabolismo ▪ Medula óssea

ABSTRACT - METABOLIC NETWORKS AND METABOLISM IN ACUTE MYELOID LEUKEMIA

Acute myeloid leukemia (AML) is a heterogeneous group of disorders characterized by arrested differentiation and/or uncontrolled proliferation of immature myeloid progenitor cells. Intensified therapy has limited applicability among elderly, the most affected population, making critical the elucidation of the mechanisms underlying AML pathogenesis. Altered energy metabolism, nutrient-sensing pathways, as AMPK, mTORC1 and AKT, and/or macroautophagy (hereinafter called autophagy) have been identified in AML, with controversial data reported. This work characterized the energetic, metabolic and autophagic profile as well as its crosstalk in distinct AML subtypes. Human AML cell lines HL-60 (FAB-M2 subtype), NB-4 (FAB-M3 subtype) and KG-1 (FAB-M6 subtype), representative of AML subtypes, were used. An oxidative metabolism associated with an AMPK and mTORC1 co-activation and an increased autophagy was displayed by KG-1 cells, while NB-4 and HL-60 cells exhibited a glycolytic phenotype associated with an AKT/mTORC1 activation and a decreased autophagy. Inhibition of AKT significantly reduced the NB-4 and HL-60 cells survival. Distinct metabolic adaptations seem therefore to occur among different AML subtypes, being AKT a potential therapeutic target in some AML scenarios. This work also characterized the expression pattern of autophagy-related genes in distinct AML subtypes, using mRNA samples from the bone marrow mononuclear cells of AML patients. By categorizing AML patients according to their FAB subtype, cytogenetic risk group or karyotype, a differential expression of autophagy-related genes was noticed among the tested groups. This study supports the occurrence of distinct autophagic signatures among different AML subtypes, highlighting the heterogeneity of AML. Type 2 diabetes *mellitus* (hereinafter called DM) has been associated with AML occurrence and bone marrow mesenchymal stromal cells (BM-MSCs) disturbances. This thesis also assessed the impact of glucose-induced changes in the BM-MSCs on the pathogenesis of distinct AML subtypes. NB-4, HL-60 and KG-1 cells were acutely or chronically exposed to the conditioned medium produced by human BM-MSCs under regular or high glucose concentrations (CM-RG or CM-HG). An increased tumorigenic phenotype was displayed by all tested AML cells upon chronic exposure to CM-HG, with NB-4 cells exhibiting the highest tumorigenic profile followed by HL-60 and KG-1 cells. Long-term exposure to high glucose promotes alterations in the BM-MSCs secretome that seem to contribute to the pathogenesis of distinct AML subtypes. The AML therapeutic approach must pass through personalized therapy adapted to the heterogeneity of this group of disorders.

KEYWORDS: Acute myeloid leukemia (AML) ▪ Autophagy ▪ Bone marrow niche ▪ Metabolism

TABLE OF CONTENTS

LIST OF ABBREVIATIONS AND ACRONYMS

Numbers and Symbols

2-DG - 2-Deoxy-D-glucose

2-HG - 2- hydroxyglutarate

α-KG - α-ketoglutarate

A

AML - Acute myeloid leukemia

ALL - Acute lymphoid leukemia

APL - Acute promyelocytic leukemia

ATRA - All-trans retinoic acid

ATO - Arsenic trioxide

AKT - Serine/threonine protein kinase B

AMPK - AMP-activated protein kinase

ACC - Acetyl-CoA carboxylase

ATG - Autophagy related

ATG12 - Autophagy related 12 homolog

ATG5 - Autophagy related 5 homolog

B

BM - Bone marrow

BAAL - Brain and acute leukemia

BSA - Bovine serum albumin

BM-MNC(s) - Bone marrow mononuclear cell(s)

BM-MSC(s) - Bone marrow mesenchymal stromal cell(s)

BCL2 - B-cell lymphoma/leukemia 2

BECLIN1 - Coiled-coil myosin-like BCL2-interacting protein

C

CML - Chronic myeloid leukemia

CLL - Chronic lymphoid leukemia

CEBPα - Enhancer-binding protein alpha

CR - Complete remission

CC - Compound C

CM - Conditioned medium

CM-HG - Conditioned medium produced by non-diabetic human bone marrow mesenchymal stromal cells under high glucose levels

CM-RG - Conditioned medium produced by non-diabetic human bone marrow mesenchymal stromal cells under regular glucose levels

D

dsDNA - Double strand deoxyribonucleic acid

DM - Type 2 diabetes *mellitus*

DMEM - Dulbecco's Modified Eagle Medium

DMEM-HG - Dulbecco's Modified Eagle Medium containing high glucose levels

DMEM-RG - Dulbecco's Modified Eagle Medium containing regular glucose levels

E

EPC(s) - Endothelial progenitor cell(s)

EVs - Extracellular vesicles

F

FLT3 - Fms-like tyrosine kinase 3

FAB - French-American-British

FBS - Fetal bovine serum

FADH - Reduced flavin adenine dinucleotide

G

GAPDH - Glyceraldehyde-3-phosphate dehydrogenase

GLS - Glutaminase

H

HSC(s) - Hematopoietic stem cell(s)

HSPCs - Hematopoietic stem and progenitor cells

HSCT - Hematopoietic stem cell transplantation

I

IDH - Isocitrate dehydrogenase

K

KIT - Feline sarcoma viral oncogene homolog

L

LSC(s) - Leukemic stem cell(s)

LC3 - Light chain 3

LKB1 - Liver kinase B1

M

MDS - Myelodysplastic syndrome

MLL - Mixed lineage leukemia

MDR - Multi-drug resistance

mTORC1/2 - Mammalian target of rapamycin complex 1/2

MNC(s) - Mononuclear cell(s)

MSC(s) - Mesenchymal stromal cell(s)

MAP1LC3B - Microtubule associated protein 1 light chain 3 beta

N

NPM1 - Nucleoplasmin 1

NTA - Nanotracking analysis

O

OXPHOS - Mitochondrial oxidative phosphorylation

OS - Overall survival

P

PBS - Phosphate- buffered saline

PI - Propidium iodide

PFA - Paraformaldehyde

PE - Phosphatidylethanolamine

PPP - Pentose phosphate pathway

PI3K - Phosphoinositide 3-kinase

Q

qPCR - Quantitative polymerase chain reaction

R

RAS - Rat sarcoma viral oncogene homolog

RXR - Retinoid X receptor

Rap - Rapamycin

RT-PCR - Reverse transcription polymerase chain reaction

RPMI - Roswell Park Memorial Institute

RFS - Relapse-free survival

RFS - Reactive oxygen species

Rheb - Ras homolog enriched in brain

S

ssDNA - Single strand deoxyribonucleic acid

SDS - Sodium dodecyl sulfate

S6K - Ribosomal protein S6 kinase

Ser - Serine

T

T-ALL - T cell acute lymphoblastic leukemia

TBS - Tris-buffered saline

Thr - Threonine

TCA - Tricarboxylic acid cycle

TSC - Tuberous sclerosis complex

W

WT1 - Wilms tumor 1

WHO - World Health Organization

LIST OF FIGURES AND TABLES

Table

OBJECTIVES AND SCOPE OF THE THESIS

Acute myeloid leukemia (AML) comprises a group of clonal hematopoietic disorders characterized by an excessive proliferation of immature myeloid progenitor cells that fail to differentiate normally, leading to hematopoietic failure. Current AML therapies result in poor outcomes among the elderly, the most affected population, making critical the elucidation of the mechanisms underlying the AML pathogenesis. Alterations in the cellular energy metabolism, nutrient-sensing pathways, as AMPK, mTORC1 and AKT, and macroautophagy (hereinafter called autophagy) have been identified in the AML scenario. However, their exact role in the AML pathogenesis is still controversial. Accordingly, the work presented in this thesis aimed to obtain new insights on the contribution of these metabolic adaptations to the AML development.

The presence of type 2 diabetes *mellitus* (hereinafter called DM) has been associated with the occurrence and poor prognosis of AML, however, the molecular mechanisms underlying this association are still unclear. DM has also been identified as promoting disturbances in the function of bone marrow mesenchymal stromal cells (BM-MSCs). Accordingly, the present thesis also aimed to clarify the impact of glucose-induced changes in the BM-MSCs on the AML pathogenesis.

To drive the reader through the main achievements, this thesis was organized in five chapters:

In **chapter 1**, a general introduction focused on the broad knowledge about AML, including epidemiology, etiology, clinical presentation, diagnosis, therapy and outcomes, will be given. A review of current knowledge on cellular energy metabolism, nutrient-sensing pathways and autophagy will be also presented. Recent data on the contribution of energy metabolism, nutrient-sensing pathways and autophagy to AML initiation, progression and therapy resistance will be also discussed.

In **chapter 2**, entitled "Interplay between energy metabolism, nutrient-sensing pathways and autophagy on distinct acute myeloid leukemia cell types", the energetic, metabolic and autophagic signatures, as well as its crosstalk and regulation, were assessed in three different AML cell lines. An exclusive energetic, metabolic and autophagic network was proposed for each subtype of AML. AKT was pointed as a potential therapeutic target in specific AML subtypes, since the pharmacological inhibition of this metabolic player promoted a drastic reduction in the viability of both NB-4 and HL-60 cells.

In **chapter 3**, entitled "Autophagy in acute myeloid leukemia patients: a retrospective cohort study", the expression pattern of critical autophagy-associated genes was determined in distinct subtypes

of AML. The gene expression of core autophagy players was shown to be decreased in the BM-MNCs of all tested FAB AML subtypes, but a differential expression of autophagy-related genes was also noticed among the BM-MNCs of the different tested FAB AML subtypes, cytogenetic risk groups or karyotypes. Autophagy was also referred as a promising target for therapeutic intervention in AML, due to the reduced expression of autophagy-related genes displayed by the BM-MNCs of the AML subjects.

In **chapter 4**, entitled "Human bone marrow mesenchymal stromal cells under high glucose concentrations: impact on the tumorigenicity of distinct acute myeloid leukemia cell types", the impact of glucose-induced changes in the BM-MSCs secretome on the pathogenesis of distinct AML subtypes was evaluated. NB-4, HL-60 and KG-1 cells were acutely and chronically exposed to the conditioned medium produced by non-diabetic human BM-MSCs under regular or high glucose levels. Chronic exposure to the changes promoted by high glucose levels in the secretome of BM-MSCs was identified as a contributor to the pathogenesis of different AML subtypes.

All the materials and methods used in this work will be referred within chapter 2, chapter 3 and chapter 4.

Finally, the **chapter 5** will comprise an integrative discussion focused on the main contributions of the present work combined with future perspectives.

CHAPTER 1

General introduction

1. LEUKEMIA

Leukemia (*White blood*, from Greek) comprises a group of clonal hematopoietic disorders characterized by an uncontrolled expansion of hematopoietic stem cells (HSCs) and/or committed myeloid/lymphoid progenitor cells that fail to differentiate normally, resulting in the accumulation of nonfunctional immature hematopoietic cells in the bone marrow (BM) with subsequent dissemination into the blood circulation and other organs [1-3]. In addition to the proliferative advantages, malignant cells also acquire enhanced self-renewal capacity [4, 5].

The first case of leukemia was reported in 1845 by the pathologist John Bennett, who called this disease as "leucocythaemia" (white cell blood) [6]. Nevertheless, only in 1847, the pathologist Rudolph Virchow used the term "leukemia" (white blood) for the first time after observing an absence of red blood cells and an excess of white/colorless cells in a patient who presented fatigue, nosebleeds and swelling on legs and abdomen [6, 7]. A few years later, discoveries of the pathologist Paul Ehrlich (1877) and the hematologist Otto Naegeli (1900) allowed a significant advance in the classification of leukemia by dividing it into two classes according to the origin of the cells: leukemia evolving from myeloblasts was termed myeloid leukemia, whereas lymphoblasts were identified as giving rise to lymphoid leukemia (Fig. 1) [6]. By the end of the 19th century, leukemia was no longer recognized as a single disease but rather as four distinct entities depending on the cell of origin and its stage of development: acute/chronic myeloid leukemia (AML/CML) and acute/chronic lymphoid leukemia (ALL/CLL) (Fig. 1) [6, 7]. Chronic leukemias are derived from more mature blasts than acute leukemias [7]. This thesis will focus on AML.

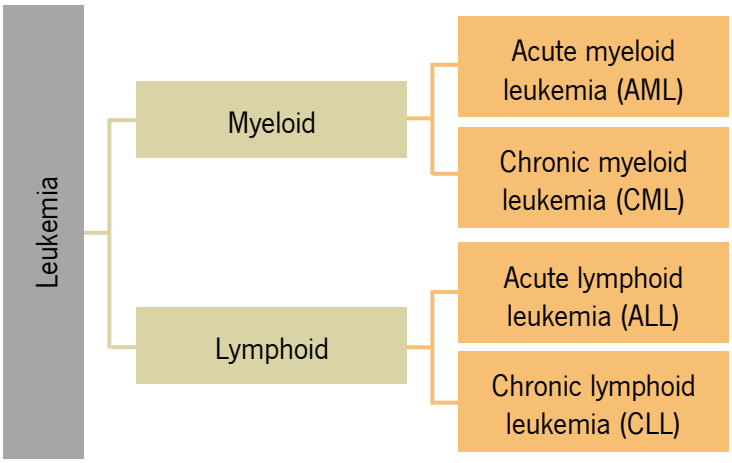

Fig. 1. Schematic representation of the major subtypes of leukemia. From the late 19th century to the present, leukemia has been grouped into four major subtypes: acute myeloid leukemia (AML), chronic myeloid leukemia (CML), acute lymphoid leukemia (ALL) and chronic lymphoid leukemia (CLL).

1.1. Acute myeloid leukemia

1.1.1. Etiology, epidemiology and clinical presentation

AML is a clonal hematopoietic disorder characterized by an impaired differentiation, exacerbated proliferation and enhanced self-renewal of the HSCs and/or committed myeloid precursor cells, leading to the accumulation of leukemic myeloblasts in the BM and consequent failure of the normal blood cells production [8-11]. Three possible scenarios have been postulated for the transformation of normal hematopoietic cells into leukemic myeloblasts: i) a normal HSC undergoes an initial mutation that leads to the formation of a pre-leukemic stem cell (pre-LSC), which suffers secondary mutation(s) giving rise to a LSC (Fig. 2i); ii) an initial mutation occurs at the HSC level resulting in the formation of a pre-leukemic myeloid progenitor cell, which generates a LSC upon secondary mutation(s) (Fig. 2ii) and iii) a normal HSC differentiates into a normal myeloid progenitor cell, which undergoes primary and secondary mutations to ultimately originate a LSC (Fig. 2iii) [3]. In all three scenarios, the generation of a LSC with arrested differentiation, excessive proliferation, increased self-renewal capacity and resistance to death signals leads to the development and accumulation of leukemic myeloblasts in the BM (Fig. 2) [3]. This accumulation reduces the BM's ability to produce healthy white and red blood cells as well as platelets [8-11]. Throughout the disease progression, the accumulation of leukemic myeloblasts occurs not only in the BM but also in the blood and organs such as brain, skin and gums [8-11]. The AML symptoms are nonspecific and include loss of appetite and weight, weakness and fatigue, anemia, lethargy, dyspnea, fever and bleeding as a result of erythropenia, neutropenia and thrombocytopenia [12, 13]. Pain in the bones may also occur due to the BM infiltration with leukemic myeloblasts [12, 13]. Common physical features may include pallor, epistaxis, gingivitis, splenomegaly, hepatomegaly and bone tenderness [12].

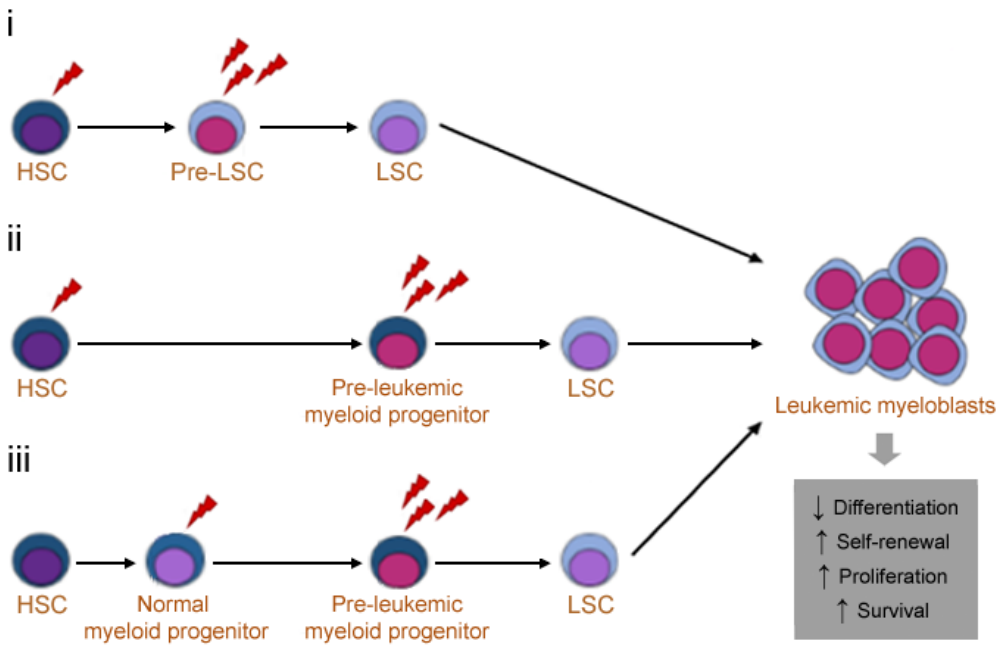

Fig. 2. Schematic representation of the models for the acute myeloid leukemia development. Three possible scenarios have been described for the evolution of acute myeloid leukemia (AML)(i-iii). Hematopoietic stem cells (HSCs) or normal myeloid progenitor cells bearing a single mutation are termed "pre-leukemic cells", which upon undergoing subsequent mutations give rise to leukemic stem cells (LSCs), which in turn generate leukemic myeloblasts.

AML can arise *de novo* or secondarily, either due to the progression of other malignancies (such as myelodysplastic syndrome (MDS) or chronic BM stem cell disorders) [10, 14] or due to the treatment with cytotoxic agents or radiotherapy (10-15% of patients with AML develop this disorder after treatment with chemotherapy used against solid tumors) [15, 16].

AML comprises the most common type of acute leukemia in adults, being rarely diagnosed in the childhood [17-19]. Indeed, the AML incidence augments with age, presenting a marked increase after the 40 years and displaying a median age of diagnosis of 65 years (Fig. 3, 4) [17-19]. From 2011 to 2015, the United States AML incidence in the <65 years age group was 2.0 cases per 100.000 individuals, whereas in the ≥65 years age group was 20.1 cases per 100.000 individuals (Fig. 3) [17]. In Portugal, data published in 2015 and referring to 2010 reported an AML incidence of 2.1 and 9.4 cases per 100.000 individuals in the <65 and ≥65 years age group, respectively (Fig. 4) [19]. In AML, a slight male predominance was also registered (Fig. 3, 4) [17, 19]. In the United States (2011 to 2015), the AML incidence in the females and males group was 3.6 and 5.2 cases per 100.000 individuals, respectively (Fig. 3) [17]. In Portugal (2010), 3.1 and 3.8 AML cases per 100.000 individuals were reported in the females and males group, respectively (Fig. 4) [19]. Although AML is the most common type of leukemia in adults and presents elevated incidence

rates, this malignancy still has the lowest survival rate among all leukemias [18]. The AML incidence is expected to increase in the future in line with the population's age [18, 20].

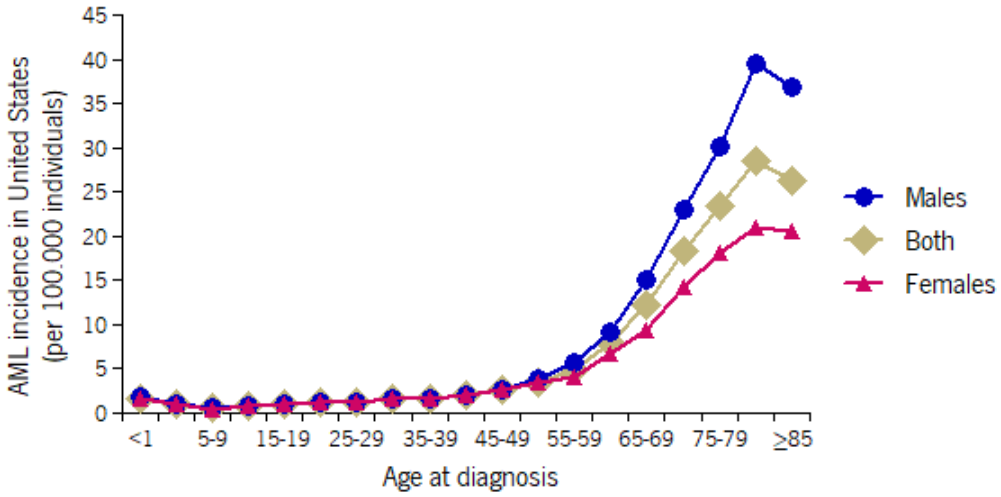

Fig. 3. Acute myeloid leukemia: Age-specific incidence rates by gender in the United States population, 2011-2015. The graph represents the most recent published data [17]. The horizontal axis shows 5-year age intervals. The vertical axis shows the frequency of new AML cases per 100.000 individuals in a given age and sex-group. Blue, pink and brown lines represent males, females and both, respectively.

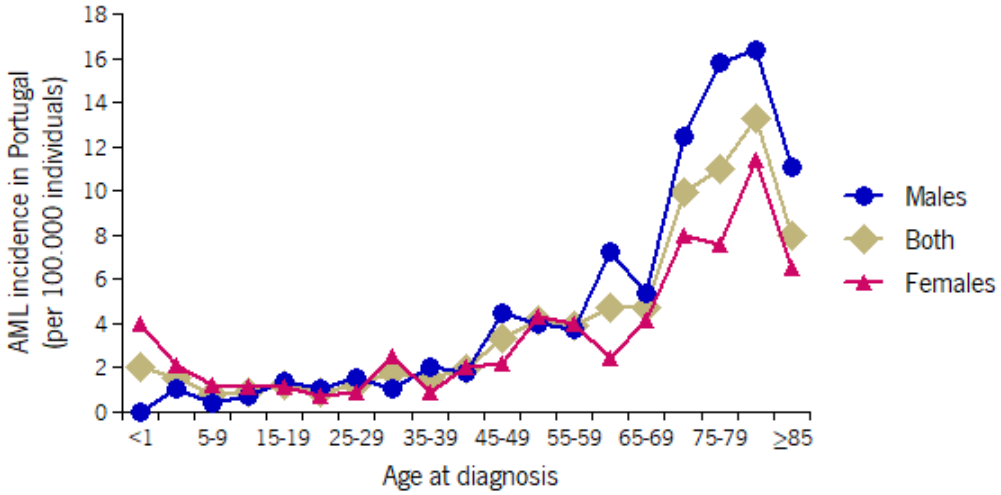

Fig. 4. Acute myeloid leukemia: Age-specific incidence rates by gender in the Portuguese population, 2010. The graph represents the most recent published data [19]. The horizontal axis shows 5-year age intervals. The vertical axis shows the frequency of new AML cases per 100.000 individuals in a given age and sex-group. Blue, pink and brown lines represent males, females and both, respectively.

1.1.2. Diagnosis and classification

The two systems commonly used in the classification of AML are the French-American-British (FAB) system, initially proposed in 1976 [21], and the World Health Organization (WHO) system, introduced for the first time in 1999 [13, 22] and reviewed in 2016 [23]. The FAB classification

system is based on the morphology, cytochemistry and maturation degree of the malignant blasts [24, 25], whereas the 2016 WHO classification system combines not only morphological and cytochemical features but also genetic, immunophenotypic, biological and clinical information [23]. The WHO classification system is therefore more complete, with the FAB classification system falling into disuse. Eight subtypes of AML (M0 to M7) are recognized by the FAB classification system (Table 1) [12, 24], while the 2016 WHO classification system identifies four main groups (AML with recurrent genetic abnormalities; AML with multilineage dysplasia; therapy-based AML; those that do not fall into any of these groups) that are further categorized into innumerous and complex AML subclasses [23]. While the current WHO classification system recognizes 20% of malignant blasts as the cutoff for a diagnosis of AML [23], the FAB classification system assumes 30% [12, 24].

Table 1. Classification of acute myeloid leukemia according to the French-American-British classification system [13].

FAB subtype	Morphological classification
M0	Undifferentiated acute myeloid leukemia
M1	Acute myeloid leukemia with minimal maturation
M2	Acute myeloid leukemia with maturation
M3	Acute promyelocytic leukemia
M4/M4 eos	Acute myelomonocytic leukemia/with eosinophilia
M5	Acute monocytic leukemia
M6	Acute erythroid leukemia
M7	Acute megakaryoblastic leukemia

1.1.3. Cytogenetic abnormalities

AML comprises a heterogeneous hematological malignancy with respect to chromosome abnormalities, gene mutations and changes in the expression of multiple genes and microRNAs [13]. By correlating these cytogenetic/molecular genetic alterations with the patient's clinical data, four different genetic risk groups were established: favorable, intermediate I, intermediate II and adverse (Table 2) [26]. Approximately 50-60% of the newly diagnosed AML individuals present cytogenetic abnormalities [27], most of them associated with non-random chromosomal

translocations [28]. Such translocations often result in gene rearrangements leading to the expression of fusion proteins which, by changing the expression of myeloid development-related genes, contribute to AML transformation [28, 29]. t(15; 17) and t(8; 21), with an incidence of 10%, and inv(16), with an incidence of 5%, constitute the most described chromosomal translocations in AML [13, 27]. The t(15; 17), t(8; 21) and inv(16) result in the expression of PML-RARα , RUNX1-RUNX1T1 (also called AML1-ETO [30]) and CBFβ-MYH11 oncofusion proteins, respectively. These proteins, through different mechanisms [13, 27, 30], act as transcriptional repressors that interfere with the expression of differentiation-related genes, impairing the normal maturation of myeloid hematopoietic cells [31-35]. AML individuals presenting these chromosomal translocations are included into the favorable genetic risk group (Table 2) [27]. Around 40-50% of AML patients have a normal karyotype [36]. However, although without karyotype alterations, not all of these patients exhibit the same response to treatment, mainly due to a large variability of gene mutations. These mutations are normally clustered into two classes: I and II [13]. The class I includes mutations in signal transduction pathways responsible for the survival and/or proliferation of hematopoietic myeloid progenitor cells. Mutations in *KIT* (feline sarcoma viral oncogene homolog), *FLT3* (Fms-like tyrosine kinase 3) and *RAS* (rat sarcoma viral oncogene homolog) fall into this group [13]. The class II comprises mutations that affect transcription factors and components of the cell cycle machinery, blocking the normal myeloid differentiation. Mutations in *MLL* (mixed lineage leukemia), *BAAL* (brain and acute leukemia), *WT1* (wilms tumor 1), *CEBPα* (enhancer-binding protein α) and *NPM1* (nucleoplasmin 1) belong to this group [13]. The cytogenetic/molecular genetic analysis of AML has become critical for disease diagnosis, classification, prognostic stratification and treatment guidance.

Table 2. Genetic risk groups established through the correlation between the cytogenetic/molecular genetic alterations of AML and the patient's clinical data [26].

Genetic risk group	Genetic alterations
Favorable	t(8;21)(q22;q22); RUNX1-RUNX1T1 inv(16)(p13.1q22) or t(16;16)(p13.1;q22); CBFB-MYH11 Mutated NPM1 without FLT3-ITD (normal karyotype) Mutated CEBPA (normal karyotype)
Intermediate I	Mutated NPM1 and FLT3-ITD (normal karyotype) Wild-type NPM1 and FLT3-ITD (normal karyotype) Wild-type NPM1 without FLT3-ITD (normal karyotype)
Intermediate II	t(9;11)(p22;q23); MLLT3-MLL Cytogenetic abnormalities not classified as favorable or adverse
Adverse	inv(3)(q21q26.2) or t(3;3)(q21;q26.2); RPN1-EVI1 t(6;9)(p23;q34); DEK-NUP214 t(v;11)(v;q23); MLL rearranged – 5 or del(5q); – 7; abnl(17p); Complex karyotype

1.1.4. THERAPY AND OUTCOMES

Acute leukemia is a fatal disorder that if untreated has a median survival of 3 months or less, being the early diagnosis and treatment imperative to obtain better outcomes [12]. The AML treatment comprises two distinct phases: the remission induction therapy and the post-remission/consolidation therapy [12, 13]. While the remission induction therapy intents to eradicate all the leukemic myeloblasts from the BM and peripheral blood in order to recover normal hematopoiesis, the post-remission therapy is initiated weeks after the remission induction therapy has ended and aims to prevent disease relapse [12, 13]. The mainstay for initial AML treatment was developed more than 40 years ago and consists in the combination of two largely unspecific cytotoxic agents that remain the worldwide gold standard of the AML therapy: high doses of a cytosine analogue (such as cytarabine) combined with an anthracycline antibiotic (such as doxorubicin, daunorubicin or idarubicin) [37-39]. Cytarabine (cytosine arabinoside or ara-C) is a deoxycytidine analogue that is easily taken up by malignant cells and subsequently metabolized

into the nucleoside triphosphate form (ara-CTP), which is a substrate for DNA polymerase [40]. The incorporation of ara-CTP instead of deoxycytidine into the nascent DNA strand during DNA replication promotes the inhibition of DNA strand elongation with consequent single strand DNA (ssDNA) breaks and unsuccessful DNA replication [41, 42]. On the other hand, doxorubicin is a hydroxylated daunorubicin derivative that impairs DNA replication and transcription processes [43]. This compound is rapidly taken up into the nucleus where it binds with high affinity to DNA by the classical intercalation between base pairs, acting as a DNA topoisomerase II inhibitor [44-46]. Doxorubicin is commonly described as inhibiting the DNA re-ligation step, leading to the accumulation of enzyme-linked dsDNA breaks and consequent DNA replication/transcription failure [45-47]. In general, cytarabine and doxorubicin promote severe DNA damage that prevents survival, division and proliferation of AML cells. The standard regimen used during the remission induction therapy is termed as "7 + 3" regimen, which includes 7 days of continuous cytarabine infusion (100-200mg/m^2) combined with an anthracycline (45-60mg/m^2) administered intravenously for 3 days [37-39]. After this phase, it is expected that AML patients achieve complete remission (CR), which is defined as a BM with less than 5% of blasts and a neutrophil and platelet count greater than 1000 and 100.000, respectively [48]. Approximately 70-80% of AML patients aged <60 years [39, 49] and 40-50% of AML patients aged >60 years [50-52] reach CR upon the "7 + 3" regimen. AML patients who achieve CR should advance to the post-remission therapy, since it was described that patients who do not receive this treatment relapse within 6 to 9 months [53]. The post-remission therapy includes courses of chemotherapy, autologous hematopoietic stem cell transplantation (HSCT) or allogeneic HSCT, which are applied depending on the patient's age, comorbidities, cytogenetic-based relapse chance and whether the patient has a suitable donor for HSCT [8]. For AML patients aged <60 years, the post-remission chemotherapy consists in high doses of cytarabine (2-3g/m^2) twice a day on days 1, 3 and 5 for a total of 3-5 cycles [8]. However, AML patients aged >60 years receive a less intensive chemotherapeutic scheme, characterized by 5 days of cytarabine (100mg/m^2) and 2 days of an anthracycline (45mg/m^2) for a total of 2 cycles [8, 10], due to the elevated cerebellar toxicity promoted by the high doses of cytarabine in this aged group [54, 55]. These chemotherapeutic schemes present minor alterations and adaptations depending on the clinical center. HSCT is also associated with an increased risk of transplant-related morbidity and mortality, being this approach less used in AML patients aged >60 years [56]. Concerning the treatment outcomes, AML patients aged >60 years present lower CR rates, shorter relapse-free survival (RFS), lower overall survival (OS) and higher incidence of early death

during chemotherapy than AML patients aged <60 years [51, 52, 57]. The increased prevalence of unfavorable cytogenetics, elevated incidence of multi-drug resistance (MDR) and highly frequent comorbidities are risk factors that contribute to the poor outcomes exhibited by old AML patients [8]. Thus, while young patients tolerate intensified treatment strategies and have good outcomes, AML treatment is highly toxic and has limited application and poor outcomes among old individuals. Accordingly, current clinical trials have focused on preserving the therapy efficacy while reducing its toxicity in old AML patients. The identification of specific gene mutations, chromosomal translocations and changes in signaling pathways has led to the development of several targeted agents, such as histone deacetylase inhibitors, FLT3 inhibitors, ubiquitin-proteasome system inhibitors and DNA methyl transferase inhibitors (Table 3) [58, 59]. Nevertheless, during the last decades, the majority of therapeutic advances for AML have not come from the introduction of novel therapeutics but rather from optimizing the use of traditional drugs with the potential to be efficacious without impairing patients' quality of life [13]. Different concentrations and new formulations are examples of older drugs optimization [60, 61]. Unfortunately, the development of an efficient AML therapeutic strategy still remains a major challenge in the elderly individuals, the most affected population.

Although the standard AML therapy is applied to the most AML subtypes, the acute promyelocytic leukemia (APL; recognized as M3 subtype by the FAB classification system) is differently treated [62]. APL is characterized by the t(15;17) chromosomal translocation that leads to the fusion of the PML and RARα sequences with subsequent expression of the PML-RARα fusion oncoprotein [62, 63]. The PML-RARα in turn binds to the nuclear retinoid X receptor (RXR) originating the PML-RARα/RXR repressor complex that disrupts the transcription of differentiation-related genes with consequent blockage of the normal promyelocytic maturation [62, 64, 65]. APL patients are currently treated with all-trans retinoic acid (ATRA), a non-cytotoxic agent capable of differentiating promyelocytes into mature granulocytes [66, 67]. Since ATRA have a transient effect when administered as a single agent [66, 68], the current APL standard treatment consists in the combination of ATRA with anthracycline-based chemotherapy [69]. APL patients treated with this combinatorial approach present similar increased CR rates (80-90%) but significantly lower relapse rates than those treated with ATRA monotherapy [70]. Interestingly, arsenic trioxide (ATO) also demonstrated activity against APL, displaying CR rates above 80% [71, 72]. It was also showed that APL patients submitted to ATO plus ATRA present similar CR rates but shorter time to achieve CR and greater reduction of the disease burden than those only treated with ATO [73].

Table 3. Therapeutic strategies investigated in the treatment of acute myeloid leukemia [13].

Therapeutic approach	Examples
Epigenetic regulation	- Histone deacetylase inhibitors: vorinostat, panobinostat, belinostat - DNA methyl transferase inhibitors: vidaza, dacogen
Differentiation-inducing therapeutics	- Retinoid X receptor agonists - Arsenic trioxide
Angiogenesis inhibition	- Inhibition of angiogenesis: velcade - Immunomodulatory agents: thalomid, revlimid
Inhibition of signaling pathways	- Tyrosine kinase inhibitors: midostaurin, lestaurtinib, sorafenib, KW-2449, AC220 - Cell cycle inhibitors: ON 01910.Na - Farnesyl transferase inhibitors: zarnestra, sarasar - mTOR inhibitors: afinitor, PI-103, temsirolimus, GSK21110183 - PARP inhibitors: ABT-888 - MEK1/2 inhibitors: AZD6244, AS703026, PD98059, GSK1120212 - Bcl-2 inhibitors: oblimersen, obatoclax, ABT-263 - XIAP inhibitors: AEG-35156 - Aminopeptidase inhibitors (tosedostat)
Modulation of drug resistance	- Chemosensitizer agents: valspodar, zosuquidar
Modified traditional drugs	- Nucleoside analogs: clofarabine, sapacitabine, elacytarabine - Alkylating drugs: irofulven, temodar, onrigin - Topoisomerase inhibitors: hycamtin
Immune therapy	- Antibodies: mylotarg, lintuzumab, avastin, T-cell targeted therapy

2. METABOLIC REGULATION IN ACUTE MYELOID LEUKEMIA

2.1. GLYCOLYSIS VERSUS MITOCHONDRIAL OXIDATIVE PHOSPHORYLATION

Under normal conditions, mammalian cells primarily rely on both glycolysis and mitochondrial oxidative phosphorylation (OXPHOS) to generate energy in the form of ATP from the breakdown of glucose and other carbohydrates [74]. Briefly, in the cytoplasm, glucose is converted into pyruvate in a ten-step pathway called glycolysis (Fig. 5A) [75]. In this process, a net of two molecules of ATP, two molecules of pyruvate and two molecules of NADH is produced from one molecule of glucose (Fig. 5A) [75]. In the presence of oxygen, pyruvate, the end product of glycolysis, goes from cytoplasm to mitochondria where each pyruvate molecule is oxidatively decarboxylated into

an acetyl-CoA molecule by the pyruvate dehydrogenase complex (Fig. 5A) [76]. For each pyruvate oxidation, one molecule of NADH and one molecule of CO_2 are produced (Fig. 5A). The condensation of acetyl-CoA with oxaloacetate by the citrate synthase occurs in the mitochondria and comprises the first step of the tricarboxylic acid (TCA) cycle, also known as the citric acid cycle or Krebs cycle (Fig. 5A) [76]. The TCA cycle consists of a series of enzymatic redox reactions that, for each acetyl-CoA molecule, produces three molecules of NADH, two molecules of CO_2, one molecule of ATP and one molecule of $FADH_2$ (Fig. 5A) [76]. The TCA cycle is followed by the oxidation of the NADH and $FADH_2$ molecules on the mitochondrial electron transport chain and by the generation of a mitochondrial membrane electrochemical potential that culminates in the production of ATP by OXPHOS (Fig. 5A) [76]. Globally, under normoxic conditions, about 36 molecules of ATP are generated per glucose breakdown, with OXPHOS accounting for over 80% of the produced ATP [76]. Under low oxygen tension conditions, mammalian cells mainly rely on glycolysis, with pyruvate being reduced to lactate by the lactate dehydrogenase A (LDHA) in the cytoplasm, a metabolic process called lactate fermentation (Fig. 5B) [74]. Once produced, the lactate molecules are excreted into the extracellular space, while the recycled NAD+ molecules are used to sustain a high glycolytic flux [74]. Although glycolysis yields a lower amount of ATP per glucose molecule when compared to OXPHOS, the former generates ATP at a faster rate than the latter, resulting in higher ATP production per time unit [77]. Indeed, it was claimed that the rate of ATP production may be 100 times faster with glycolysis than with OXPHOS [77]. The ratio between glycolysis and OXPHOS for the total ATP yield varies according to cell type, growth state and microenvironment [74]. This metabolic flexibility demonstrates the cooperative relationship between glycolysis and OXPHOS to adapt the mechanisms of energy production to environmental pressures and cellular features [74]. Indeed, under hypoxic conditions, glycolysis becomes enhanced to compensate for the weakened function of OXPHOS [74]. Cancer cells continuously reprogram their metabolic phenotypes to adapt to microenvironmental changes and alterations of growth conditions [78]. This metabolic plasticity provides both the energy and the intermediates for biosynthetic processes required for the enhanced tumor cells survival, proliferation and growth [78]. Glycolysis has been identified as the predominant energy production pathway of various cancer cell types, even in the presence of oxygen (Fig. 5B) (reviewed in [78]). The metabolic switch from OXPHOS to glycolysis in tumor cells was first described by Otto Warburg in the 1920s and is currently recognized as the “Warburg effect” [79]. Although Otto Warburg originally claimed that cancer cells employ a less efficient metabolic pathway (glycolysis) due to a permanent impairment

of OXPHOS [79], a growing number of studies have abrogate this hypothesis by revealing an intact OXPHOS function in most cancer cell types [80-84]. Curiously, some authors, by showing that OXPHOS activity of tumor cells can be restored upon glycolysis inhibition, argued that the reduced OXPHOS phenotype displayed by cancer cells is due to enhanced glycolysis suppressing OXPHOS rather than defects in OXPHOS [81]. Although glycolysis plays an important role in cancer energy metabolism, accumulating evidence have shown that a considerable amount of tumors use OXPHOS as the main pathway of energy production, as reviewed by Moreno-Sánchez, R., *et al.* [85]. Tumors have therefore heterogeneous metabolic phenotypes: while some cancer cell types depend mainly on glycolysis for ATP production, others equally or predominantly rely on OXPHOS [85]. Accordingly, to identify metabolic vulnerabilities susceptible to therapeutic targeting, cancer energy metabolism should be analyzed for each particular type of cancer cells.

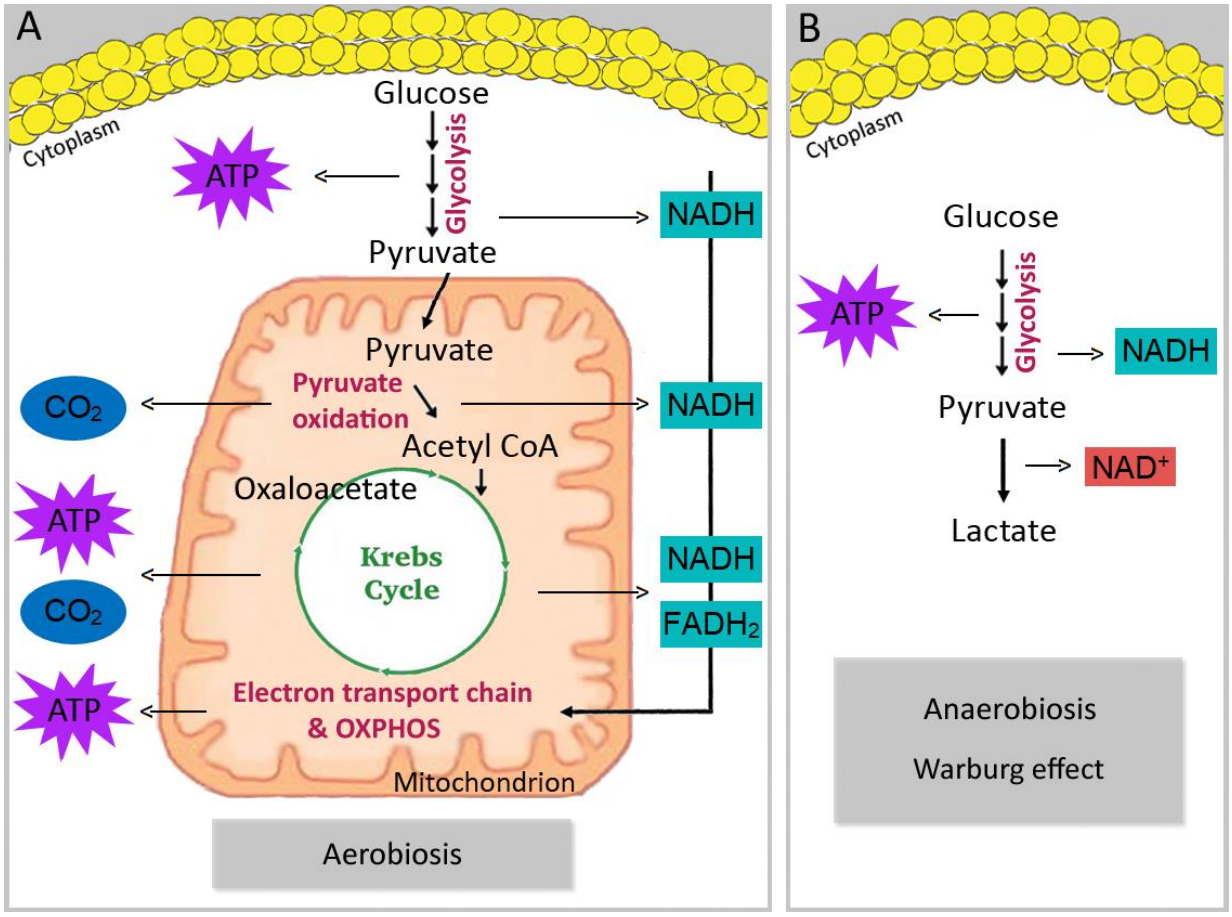

Fig. 5. Schematic representation of ATP synthesis by mammalian cells. The generation of ATP by mammalian cells is initiated in the cytoplasm by the broken down of carbohydrate molecules, namely glucose, into pyruvate in a ten-step reaction called glycolysis. A) Under normal oxygen tension conditions (aerobiosis), pyruvate enters the mitochondria and is oxidatively decarboxylated to acetyl-CoA, which by condensation with oxaloacetate initiates the Krebs cycle. The mitochondrial electron transport chain is then followed by the mitochondrial oxidative phosphorylation (OXPHOS). The NADH and $FADH_2$ molecules produced during glycolysis, pyruvate oxidation and Krebs cycle act as electron carrier

molecules during the mitochondrial electron transport chain, with the free energy released during its oxidation driving ATP synthesis during OXPHOS. Although glycolysis and Krebs cycle generate ATP, OXPHOS accounts for over 80% of the produced ATP per glucose breakdown. B) Under low oxygen tension conditions (anaerobiosis), pyruvate remains in the cytoplasm and is reduced to lactate with the regeneration of NAD+ molecules, in a process called lactate fermentation. Regardless of oxygen availability, some cancer cell types primarily rely on glycolysis to generate ATP (Warburg effect). Per glucose unit, a net of about 36 ATP molecules is produced under aerobiosis, while a net of 2 ATP molecules is generated under anaerobiosis or Warburg effect.

Alterations in the energy metabolism of AML cells have been recently described, with the metabolic reprogramming towards glycolysis being extensively reported. Indeed, by performing a serum metabolomic study focused on the glucose metabolism, Chen, W.L., *et al.* found increased levels of glycolytic metabolites in AML patients when compared to control donors [86]. By using several human AML cell lines and human BM-derived AML blasts, these authors also proposed an association between augmented glycolysis and AML cells resistance to cytarabine [86]. In line with these observations, other studies have established an association between increased glycolysis and AML cells chemoresistance [87-90]. For example, by showing that daunorubicin-resistant HL-60 cells exhibit high glycolytic activity when compared to daunorubicin-sensitive HL-60 cells and that glycolysis inhibition results in the apoptosis of daunorubicin-resistant HL-60 cells without affecting the viability of their sensitive counterparts, Ohayon, D., *et al.* reinforced the role of glycolysis in promoting AML cells chemoresistance [89]. Ju, H. K. and colleagues, by testing several human AML cell lines, mononuclear cells (MNCs) isolated from the peripheral blood of AML patients and an AML mouse model, reported that mutations in the *FLT3* gene, which occur in approximately 30% of all AML cases, promote induction of glycolysis and that combination of glycolytic inhibitors with the FLT3 inhibitor sorafenib enhances the sorafenib-induced cytotoxicity [90]. An association between enhanced glycolysis and leukemogenesis was also proposed by Wang, Y. H. and co-workers, after observing the inhibition of leukemia initiation through depletion of either pyruvate kinase M2 isoform (PKM2), an enzyme involved in the final step of glycolysis, or LDHA, needed for NADH re-oxidation in conditions of high glycolytic flux rates [91]. These authors claimed that depletion of PKM2 or LDHA enforced a metabolic shift from glycolysis to OXPHOS, compromising AML induction in mice [91]. The relevance of glycolysis in leukemogenesis was also identified by Saito, Y., *et al.* which, by using a mouse model of AML, reported a high dependency of leukemia-initiating cells on glycolytic metabolism [92]. By using BM-derived MNCs of AML subjects and an AML mouse model, Watson, A. S. and colleagues reported an association between high glycolytic flux, low autophagy level and aggressive AML phenotype [93]. Finally, Poulain, L., *et al.*, by testing several human AML cell lines and human BM-derived AML blasts, described that

mammalian target of rapamycin complex 1 (mTORC1) signaling, which is constantly overactivated in AML cells, specifically promotes glycolysis in the AML context [94]. Over the past few years, an increasing number of publications have also referred a metabolic reprogramming of AML cells towards OXPHOS. Briefly, Lagadinou, E. D., *et al.,* by using BM-derived MNCs of AML patients and an AML mouse model, found that LSCs are highly reliant on OXPHOS rather than glycolysis for energy generation and that inhibition of Bcl2-mediated OXPHOS specifically eradicates LSCs [95]. By showing that inhibition of OXPHOS increases the apoptosis and decreases the proliferation of several human AML cell lines, Scotland, S., *et al.* [96] and Molina, J. R., *et al.* [97] elucidated the dependence of AML cells on OXPHOS. Finally, Farge, T. and co-workers described that cytarabine-resistant AML cells exhibit a high OXPHOS status and that OXPHOS inhibition strongly enhances cytarabine-induced antileukemic effects both *in vitro* and *in vivo*, highlighting the relevance of OXPHOS in the AML cells metabolism [98]. Dysregulation of glycolysis or OXPHOS can therefore be exploited to develop effective AML treatments. The combination of currently used antileukemia agents with inhibition of specific metabolic addictions must be privileged. Importantly, the high plasticity of AML cells, which allows their adaptation to unfavorable environments, should be considered during therapeutic strategies design. The heterogeneous energy metabolism of AML cells should also be considered.

In addition to ATP production, glycolysis provides tumor cells with intermediates required for biosynthetic pathways during cellular division, including ribose for nucleotides, citrate/glycerol for lipids, nonessential amino acids for proteins and, via the oxidative pentose phosphate pathway (PPP), NADPH, which acts as a reducing agent during nucleotide, amino acid and lipid synthesis [99]. Likely glycolysis, TCA cycle also exerts a key role in sustaining the high metabolic demands of cancer cells by acting as a hub for biosynthesis [100]. Indeed, malignant cells use TCA cycle intermediates as biosynthetic precursors of lipids, proteins and nucleic acids, which support their increased proliferation, growth and survival [100]. While oxaloacetate and α-ketoglutarate (α-KG) supply the intracellular pools of nucleotides and nonessential amino acids to be used in the synthesis of nucleic acids and proteins, citrate is required for the synthesis of fatty acids and cholesterol needed for bio-membranes [100]. To sustain TCA cycle function in the face of a continuous efflux of TCA cycle intermediates to biosynthetic pathways, replenishment of TCA cycle intermediates occurs mainly via pyruvate carboxylation, which generates oxaloacetate from pyruvate, and glutaminolysis, which produces α-KG from glutamine [101]. Mutations of TCA-associated enzymes, namely cytosolic isocitrate dehydrogenase 1 (IDH1) and its mitochondrial

homolog IDH2, have been identified in AML patients [102-107]. Instead of catalyzing the reversible oxidative decarboxylation of isocitrate to α-KG, the mutated IDH1/2 catalyzes the abnormal NADPH-dependent reduction of α-KG to 2-hydroxyglutarate (2-HG), which, by acting as a competitive inhibitor of multiple α-KG-dependent enzymes, functions as an oncometabolite [108]. Indeed, Figueroa, M. E., *et al.*, by performing a genetic, epigenetic and transcriptional profiling study in a large cohort of *de novo* AML patients, claimed that 2-HG generated by the IDH1/2-mutant AML cells promotes aberrant DNA hypermethylation through the inhibition of the α-KG-dependent and DNA demethylase enzyme TET2, resulting in a blockade of cellular differentiation and consequent leukemic transformation [106]. The contribution of mutant IDH1/2-produced 2-HG to leukemogenesis was also suggested by other authors [102, 107]. Targeting mutant-IDH2 enzymes was proposed by Wang, F. and co-workers as a potential therapeutic strategy against AML, after observing the *in vitro* differentiation of AML cells through selective inhibition of mutant-IDH2 proteins by the AGI-6780 compound [103]. Several clinical trials featuring drugs that inhibit mutant-IDH1/2 enzymes are currently ongoing with promising results in the AML scenario, as recently reviewed by Castro, I., *et al.* [109]. For example, a selective small-molecule inhibitor of mutant-IDH2 enzymes (enasidenib) have been recently developed, with early-phase clinical trials showing hematological responses in patients with relapsed or refractory AML [104, 105]. The induction of myeloblasts differentiation was revealed as driving the clinical efficacy of enasidenib [104, 105]. The knowledge that AML cells harboring IDH1/2 mutations become addicted to glutamine as the main cellular source of α-KG points to glutaminase (GLS), enzyme that catalyzes the first reaction of glutaminolysis, as an attractive target for AML therapy. Indeed, GLS inhibition in IDH1/2-mutant AML cells has been explored, with anti-leukemia activity demonstrated [110, 111].

Deciphering and targeting metabolic abnormalities/addictions that are specific of AML cells, or mechanisms underlying these processes, represents a promising strategy that could lead to therapeutic applications in AML.

2.2. Nutrient-sensing pathways

The metabolic rewiring in cancer cells is mainly driven by deregulation of the nutrient-sensing pathways AMP-activated protein kinase (AMPK), mammalian target of rapamycin complex 1 (mTORC1) and serine/threonine protein kinase B (AKT) [112]. AMPK is an evolutionarily conserved heterotrimeric complex composed of a catalytic subunit, AMPKα, and two regulatory subunits,

AMPKβ and AMPKγ, that plays a central role in maintaining cellular homeostasis by acting as a nutrient availability- and energy status-sensing mechanism [113]. Indeed, AMPK activation occurs in response to metabolic stresses, such as glucose starvation, amino acid deprivation, growth factor withdrawal, hypoxia and compounds that affect ATP synthesis [114]. These cellular stresses reduce ATP production or accelerate ATP consumption, rising AMP/ATP and ADP/ATP ratios [114]. The accumulation of AMP results in its allosteric binding to the regulatory γ-subunit of AMPK, which induces a major conformational change in the AMPK heterotrimeric complex, allowing the exposure of the threonine 172 (Thr172) residue located in the catalytic α-subunit of AMPK to the action of upstream kinases, namely liver kinase B1 (LKB1) (Fig. 6) [114]. Upon activation, AMPK acts to restore nutrient/energy balance by promoting catabolism (e.g. macroautophagy (hereinafter referred to as autophagy), glycolysis and fatty acid oxidation) and down-regulating anabolism (e.g. fatty acid, protein and glycogen synthesis) [114]. Like AMPK, mTORC1 is also a serine/threonine protein kinase that functions as a key sensor of cellular nutrient availability [115, 116]. Nevertheless, mTORC1 signaling is activated by high levels of amino acids, glucose and/or growth factors; positively regulates anabolic programs while suppresses catabolism; and promotes cell proliferation/growth [115, 116]. In response to nutrient availability, inactive mTORC1 is translocated from the cytoplasm to the lysosomal outer surface where, through phosphorylation at the serine 2448 (Ser2448) residue, it is activated by the Ras homolog enriched in brain (Rheb) GTPase (Fig. 6) [115, 116]. Rheb in turn is negatively controlled by the heterodimeric tuberous sclerosis complex (TSC), whose TSC2 component carries a GTPase-activating protein (GAP) function for the mTORC1-activating protein Rheb, converting it from the active GTP- to the inactive GDP-bound state (Fig. 6) [115, 116]. mTORC1 consists of the mTOR kinase plus multiple protein partners, including Raptor, which plays an essential role during mTORC1 activation by mediating its recruitment to the lysosomal surface [115, 116]. Once activated, mTORC1 exerts broad regulatory effects by phosphorylating numerous downstream effector proteins. For example, active mTORC1 phosphorylates the ribosomal protein S6 kinase 1 (p70 S6K1) at the Thr389 residue and the eukaryotic initiation factor 4E (eIF4E) binding protein 1 (4E-BP1) at several Thr and Ser residues, triggering protein synthesis [115, 116]. The opposing actions of AMPK and mTORC1 in cellular metabolism demands a close and tight regulation between these two metabolic hubs to avoid uncoordinated synthesis and degradation processes. Indeed, AMPK negatively controls mTORC1 signaling by promoting Rheb inactivation via TSC2 GAP activity and by preventing Raptor mediated-mTORC1 recruitment to the lysosomal surface (Fig. 6) [117]. AMPK directly

phosphorylates both TSC2 (Ser1387 and Thr1227) and Raptor (Ser722 and Ser792) to suppress mTORC1 kinase activity (Fig. 6) [117]. AKT is a serine/threonine protein kinase that, by transducing extracellular signals from growth factors, cytokines and hormones, contributes to the regulation of numerous cellular processes, such as glucose homeostasis, lipid metabolism, protein synthesis, cell proliferation/growth and cell survival [118, 119]. Upon stimulation of receptor tyrosine kinases (RTKs), cytokine receptors (CRs) or G-protein-coupled receptors (GPCRs) by extracellular ligand binding, inactive AKT is translocated from the cytoplasm to the plasma membrane where it is activated via a phosphoinositide 3-kinase (PI3K)-dependent mechanism (Fig. 6) [118, 119]. Full AKT activation requires its phosphorylation at the Thr308 residue located in the kinase domain by phosphoinositide-dependent protein kinase 1 (PDK1) and at the Ser473 residue located in the C-terminal regulatory domain by mTOR complex 2 (mTORC2) (Fig. 6) [118, 119]. Once activated, AKT phosphorylates a wide spectrum of downstream targets, either positively or negatively affecting their functions. For example, AKT allows Rheb-mediated mTORC1 activation by inhibiting the TSC2 GAP activity (Fig. 6); promotes direct mTORC1 activation through its phosphorylation at the Ser2448 residue (Fig. 6); induces glycolysis by up-regulating the expression of glucose transporters and by stimulating glycolytic enzymes; allows glycogen synthesis by inhibiting the activity of glycogen synthase kinase 3 (GSK3); and inhibits the induction of apoptosis and cell cycle arrest by suppressing the function of Forkhead Box O (FoxO) transcription factors [118, 119]. Unlike AMPK, PI3K/AKT signaling cascade positively controls mTORC1 activity, enhancing protein synthesis and down-regulating autophagy [118, 119]. Through a variety of shared and distinct downstream targets, AKT and AMPK have opposing roles on cellular metabolism, with AKT stimulating ATP-consuming anabolic processes and AMPK blocking anabolic metabolism in favor of ATP-generating catabolic processes. AMPK, mTORC1 and AKT compose therefore a tightly regulated kinase triad that works to closely monitor and maintain cellular homeostasis.

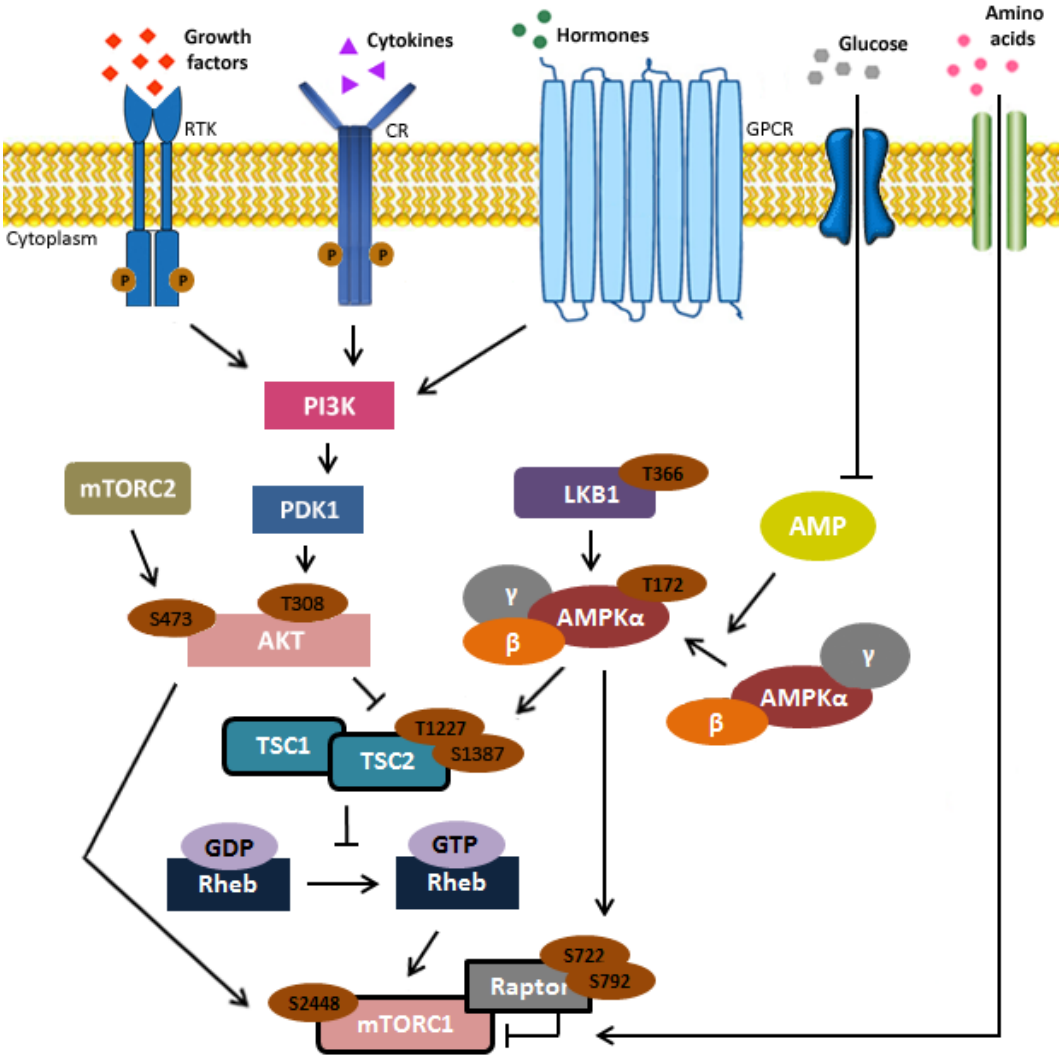

Fig. 6. Schematic representation of AMPK, mTORC1 and AKT regulation. Distinct stimuli conduct to the activation of different nutrient-sensing pathways. The AMPK signaling pathway is activated in response to metabolic stresses that, by reducing ATP production or accelerating ATP consumption, increase the levels of intracellular AMP. Under lowered intracellular ATP levels, AMP binds to the γ-subunit of AMPK, leading to an AMPK conformational change that exposures the threonine 172 (T172) residue located at the α-subunit of AMPK to the action of LKB1. Once activated, AMPK negatively controls mTORC1 activity, by directly phosphorylating raptor at the serine 722 and serine 792 (S722 and S792) residues or TSC2 at the threonine 1227 and serine 1387 (T1227 and S1387) residues, and positively regulates catabolism. In nutrient-rich conditions (e.g. amino acids), mTORC1 is activated and drives cells growth by stimulating anabolic processes. The PI3K/AKT signal transduction pathway is activated in response to extracellular signals, such as growth factors, cytokines and hormones. Phosphorylation of AKT at the threonine 308 (T308) residue by PDK1 and at the serine 473 (S473) residue by mTORC2 leads to full AKT activation. Once activated, AKT mediates several downstream responses, including cell survival and growth. By phosphorylating mTORC1 at the serine 2448 (S2448) residue or inhibiting TSC2 activity, AKT stimulates mTORC1. RTK: receptor tyrosine kinase; CR: cytokine receptor; GPCR: G-protein-coupled receptor.

Dysregulated AMPK, mTORC1 and/or AKT pathways have been extensively reported in AML, with both pro- and anti-tumoral activities suggested [92, 94, 120-136]. Briefly, Green, A. S. and colleagues, by using human BM-derived AML blasts and an AML mouse model, identified the

LKB1/AMPK signaling pathway as a tumor suppressor axis in AML cells through the repression of mTORC1-dependent oncogenic mRNA translation [120]. In addition, these authors claimed that the LKB1/AMPK pathway is consistently functional in AML cells and that its activation with metformin results in a strong anti-leukemic activity [120]. The role of AMPK in leukemogenesis suppression was also proposed by Kawashima, I. and co-workers [121]. By using a mouse model of AML, Saito, Y., *et al.* reported that AMPK protects leukemia-initiating cells from dietary restriction-caused metabolic stress in the BM and that combination of AMPK inhibition with physiological metabolic stress potently blocks leukemogenesis, elucidating the contribution of AMPK to AML development [92]. These authors also established an association between energy metabolism and nutrient-sensing pathways [92]. Activation of AMPK in AML cells exhibiting constitutive mTORC1 activation was proposed by Sujobert, P. and co-workers as a potential therapeutic strategy against AML [122]. Indeed, AMPK and mTORC1 co-activation resulted in a synthetic lethal interaction across a range of human AML cell lines and human primary AML samples [122]. An aberrant mTORC1 activation has been observed in the majority of the primary AML cases, with the inhibition of mTORC1 signaling, through rapamycin or rapamycin analogs, being exploited as a potential anti-leukemia strategy (reviewed in [123]). Although in preclinical and clinical settings mTORC1 inhibition alone elicited a modest inhibitory effect on AML cells growth [124, 125], the combination of mTORC1 inhibitors with conventional chemotherapy has shown a significant improvement in the median disease-free survival and median OS of AML patients [126, 127]. The recent identification of mTORC1 as a positive regulator of glycolysis in the AML context, pointed to the combination of glycolytic inhibitors with currently used chemotherapy as a new promising therapeutic strategy in mTORC1-overactivated AML cells [94]. A constitutive activation of PI3K/AKT signaling pathway has also been detected in 50-80% of AML cases [128-130]. In preclinical studies, PI3K/AKT inhibitors have demonstrated activity against AML, by markedly increasing the sensitivity of human AML cell lines and human primary AML cells to etoposide- or cytarabine-induced cytotoxicity [131, 132]. However, despite the theoretical potential of PI3K/AKT inhibitors as anti-leukemia agents, their clinical effects have been limited, as shown in phase I clinical trials [133-135]. Considerable efforts have been made to elucidate the molecular mechanisms underlying AML cells resistance to PI3K/AKT inhibitors. In a recent report, Nepstad, I., *et al.*, by performing a non-targeted metabolite profiling in human primary AML cells susceptible or resistant to *in vitro* PI3K/AKT inhibition, established an association between altered cellular metabolism and AML cells resistance to pharmacological PI3K/AKT inhibition [136]. Indeed, differences in the levels of metabolites

involved in energy, amino acid and lipid metabolism were detected between resistant and susceptible AML blasts [136]. Interestingly, an association between energy metabolism and nutrient-sensing pathways in the AML context was proposed by Scotland, S. *et al.*, by showing that AKT activation promotes glycolysis in the U937 AML cell line [96].

Targeting metabolic processes that are critical in AML biology and that may constitute an *Achilles heels* of AML cells is therefore viewed as a potential strategy to fight AML. Indeed, autophagy, an important downstream target of AMPK, mTORC1 and AKT, has been extensively implicated in the development, progression and drug-resistance of AML.

2.3. AUTOPHAGY

Autophagy is an evolutionarily conserved self-degradative process in which cytoplasmic contents, including cytotoxic proteins and superfluous/damaged organelles, are delivered to lysosomes for degradation [137]. This cellular catabolic pathway involves at least five steps (Fig. 7): 1 - initiation/nucleation (isolation of a small double-membrane called phagophore and mobilization of proteins required for the phagophore expansion); 2 - elongation/expansion of the phagophore; 3 - closure/maturation of the phagophore into a completed double-membrane-bound compartment termed autophagosome; 4 - fusion of the autophagosome with a lysosome originating an autolysosome; and 5 - degradation of the autolysosome content [137-139]. Several Atg (autophagy-related genes) proteins are involved in this process and constitute the core of the "autophagy machinery" essential for the execution of this dynamic process [137-139]. The initiation/nucleation phase of autophagy is mainly regulated by two complexes: Unc-51 like autophagy activating kinase 1/2 (ULK1/2) and vacuolar protein sorting 34 (hVPS34)/Beclin1 (Fig. 7). While the phosphorylation of ULK1 at Ser757 by mTORC1 and Beclin1 at Ser234 and Ser295 by AKT leads to autophagy inhibition, AMPK positively controls autophagy by directly phosphorylating ULK1 at the Ser317 and Ser777 residues (Fig. 7) [140-143]. Once activated, AMPK and AKT may also regulate autophagy through mTORC1-dependent pathways (Fig. 7) [142]. The activation of ULK1 has been identified as responsible for the isolation of the phagophore, whereas the activation of hVPS34/Beclin1 has been implicated in the recruitment of Atg5 and Atg12 proteins into this structure [137-139]. The elongation/expansion of the phagophore requires two essential ubiquitin-like conjugation systems: the conjugation of Atg12 to Atg5, mediated by the ubiquitin-like modifier-activating enzymes Atg7 (E1 enzyme) and Atg10 (E2 enzyme), and the conjugation of LC3-I to phosphatidylethanolamine (PE), mediated by the E1 enzyme Atg7 and E2 enzyme Atg3 (Fig. 7)

[137-139]. Note that before LC3-I/PE conjugation, the cysteine protease Atg4 cleaves the C-terminal portion of a nascent pro-LC3, leading to the formation of LC3-I (Fig. 7) [137-139]. Upon conjugation, the Atg12/Atg5 complex binds to Atg16 generating the Atg12/Atg5/Atg16 trimeric complex, which binds to the phagophore (Fig. 7) [137-139]. This trimeric complex recruits cytosolic LC3-I/PE (also called LC3-II) to the edges of the phagophore, allowing the elongation and curvature of this structure (Fig. 7) [137-139]. By serving as a scaffold, the cargo also contributes to the expansion of the phagophore [137-139]. During the closure/maturation phase of autophagy, the Atg12/Atg5/Atg16 trimeric complex redistributes and concentrates mostly on the outer side of the phagophore, while LC3-II is distributed symmetrically on both sides of this structure (Fig. 7) [137-139]. The proteins located at the outer side of the membrane are then released into the cytoplasm and the uncoated autophagosome is fused with the lysosome originating the autolysosome (Fig. 7) [137-139]. The acid hydrolases supplied by the lysosome promote the acidification of the autophagosome environment, allowing the degradation of the autolysosome contents, namely the cargo and the LC3-II trapped in the lumen of this structure (Fig. 7) [137-139]. The macromolecules resulting from this degradation are transported through permeases to cytoplasm for recycling or energy production [137-139]. The LC3-II present in the autophagosomes can be easily monitored by immunoblotting and immunofluorescence, being the most widely used marker for autophagy detection [144].

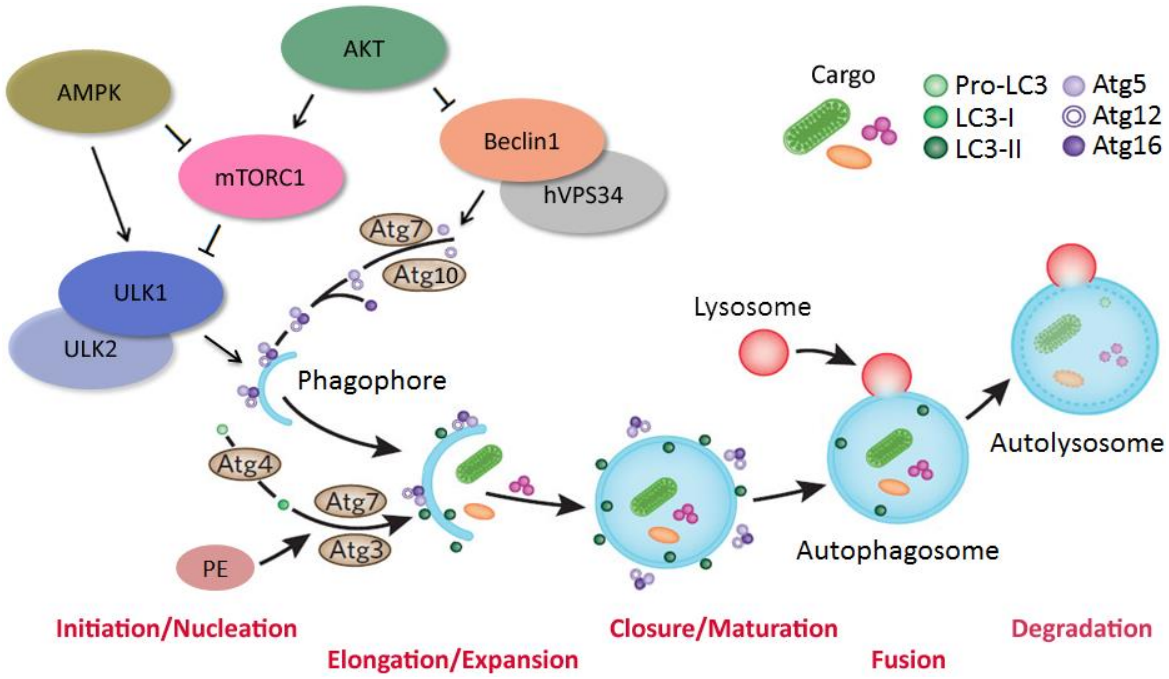

Fig. 7. Schematic representation of macroautophagy. Macroautophagy, hereinafter called autophagy, is a multi-step degradative system that delivers cytoplasmic constituents to the lysosome. This catabolic process involves at least five

steps: 1) initiation/nucleation; 2) elongation/expansion; 3) closure/maturation; 4) fusion; and 5) degradation. The initiation/nucleation step of autophagy involves the participation of ULK1/2 and hVPS34/Beclin1 complexes, whose activities are mainly regulated by the AMPK, mTORC1 and AKT upstream kinases. The Atg12, Atg5, Atg16 and LC3-II autophagy-related proteins, as well as the E1 enzyme Atg7 and the E2 enzymes Atg10 and Atg3, exert a critical role during the elongation/expansion phase of autophagy. Pro-LC3 is processed by the cysteine protease Atg4 into LC3-I, which by conjugation with the phosphatidylethanolamine (PE) originates the LC3-I/PE (also called LC3-II). The closure/maturation step of autophagy consists in the completion of a phagophore into an autophagosome, which by fusing with a lysosome gives rise to an autolysosome. Nonfunctional proteins and organelles are finally degraded in the autolysosome compartment by lysosomal hydrolases.

Under physiological conditions, autophagy occurs at basal levels for the removal of harmful or surplus cytoplasmic components, such as protein aggregates, dysfunctional/long-lived organelles and intracellular pathogens, playing a vital role in maintaining cellular homeostasis [145, 146]. In the presence of stressful conditions, such as starvation and hypoxia, autophagy is up-regulated functioning as an adaptive response that, by recycling and generating basic components as amino acids, nucleotides and fatty acids, allows temporary cell survival [145, 146]. Autophagy is therefore primarily viewed as a pro-survival mechanism. Nevertheless, this cytoprotective role of autophagy does not occur indefinitely and when the cellular stress leads to continuous or excessive autophagy, this "self-eating" process can be lethal due to extensive self-digestion [146]. It is therefore imperative to maintain a tightly regulated autophagy, since cell survival or death may happen depending on the duration and severity of this process.

Over the last years, extensive attention has been devoted to understanding the paradoxical roles of autophagy in the AML initiation, progression and drug resistance. It is currently accepted that autophagy plays a multi-layered role in the AML scenario (anti- and pro-leukemic) that is highly dependent on both cell type and cellular context. Briefly, Mortensen, M. and co-workers, by showing that deletion of the *ATG7* autophagy gene in mouse HSCs results in loss of normal HSC functions, BM failure, severe myeloproliferation and eventually death, claimed that impairment of autophagy promotes the transformation of normal HSCs into a pre-leukemic state [147]. The recognition of autophagy as a suppressor of leukemic transformation was also made by Watson, A. S. *et al.*, who found that heterozygous loss of the *ATG5* autophagy gene in mouse HSCs potentiates AML initiation, progression and aggressiveness [93]. By detecting that bone marrow mononuclear cells (BM-MNCs) of AML patients exhibit reduced expression levels of essential autophagy genes, such as *MAP1LC3B* (*microtubule associated protein 1 light chain 3 beta*), when compared to the BM-MNCs of control donors, these authors reinforced the AML suppressor function of autophagy [93]. With distinct AML and control cohorts, Brigger, D. and colleagues also noticed lower expression

levels of autophagy-associated genes in AML individuals than in non-hematological subjects, identifying them as tumor suppressor genes in the AML context [148]. The role of autophagy in promoting leukemogenesis was reported by Liu, Q. *et al.*, who noticed that deletion of *ATG5* in BM cells transduced with the MLL (mixed lineage leukemia)-AF9 fusion gene prevents the efficient initiation of AML in mice [149]. However, according to some authors, upon leukemic transformation, autophagy is no longer required for the maintenance of AML [149-151]. In contrast, Sumitomo, Y. and co-workers, by observing that deletion of the *ATG7* or *ATG5* autophagy genes reduces the tumorigenic phenotype of a MLL-ENL-induced murine AML model, claimed that autophagy is critical for the maintenance of established AML [152]. By detecting that autophagy promotes the survival of AML cells under hypoxia, Dirkje, W. H., *et al.* also ascribed an AML-promoting role to autophagy [153]. Altogether, these contradictory data highlight the highly complex and context-dependent role of autophagy in AML initiation and progression.

This chapter summarized current knowledge on the regulation of energy metabolism, nutrient-sensing pathways and autophagy in both normal and AML scenarios. Relevant data on the impact of metabolic alterations on the AML development, progression and therapy resistance were extensively reviewed.

Despite recent advances in cancer cell metabolism, the exact role of metabolic changes in the AML context remains debatable. On the next chapters, results on the metabolic networks operating in distinct AML cell types will be presented and discussed. With these findings we hope to provide new insights that contribute to the development of targeted and effective therapies against AML.

CHAPTER 2

Interplay between energy metabolism, nutrient-sensing pathways and autophagy on distinct acute myeloid leukemia cell types

SOME RESULTS PRESENTED IN THIS CHAPTER WERE PUBLISHED AS FOLLOW:

- Olga Pereira, Alexandra Teixeira, Belém Sampaio-Marques, Isabel Castro, Henrique Girão and Paula Ludovico. *Signaling mechanisms that regulate metabolic profile and autophagy of acute myeloid leukemia cells*. J Cell Mol Med., 2018.

THE RESULTS DESCRIBED IN THIS CHAPTER WERE PRESENTED IN THE FOLLOWING NATIONAL AND INTERNATIONAL CONGRESSES:

- National congresses:
  - Olga Pereira, Belém Sampaio-Marques, Henrique Girão and Paula Ludovico. *Metabolic characterization of distinct acute myeloid leukemia cell lines*. Poster communication. XIX National Congress of Biochemistry (SPB2016 Meeting). Guimarães, Portugal, 2016.
- International congresses:
  - Olga Pereira, Alexandra Teixeira, Sara Fernandes, Ângela Mesquita, Belém Sampaio-Marques, Isabel Castro, Henrique Girão and Paula Ludovico. *Interplay between energetic metabolism and autophagic regulation in acute myeloid leukemia cells*. Poster communication. 1st Meeting on Vesicular Biology. Coimbra, Portugal, 2018.
  - Olga Pereira*, Sara Fernandes*, Alexandra Teixeira, Ângela Mesquita, Belém Sampaio-Marques, Isabel Castro, Henrique Girão and Paula Ludovico. *Metabolic cell signaling pathways and autophagy regulation in acute myeloid leukemia cells.* Poster communication. ESH 4th International Conference on ACUTE MYELOID LEUKEMIA "MOLECULAR AND TRANSLATIONAL": ADVANCES IN BIOLOGY AND TREATMENT. Estoril, Portugal, 2017. (*The authors equally contributed for this work).
  - Olga Pereira*, Alexandra Teixeira*, Sara Fernandes, Ângela Mesquita, Belém Sampaio-Marques, Isabel Castro, Henrique Girão and Paula Ludovico. *Energy metabolism in acute myeloid leukemia cells*. Oral communication. SINAL 2017 - 8th Meeting on Signal Transduction. Lisboa, Portugal, 2017. (*The authors equally contributed for this work).
  - Olga Pereira*, Alexandra Teixeira*, Sara Fernandes, Ângela Mesquita, Belém Sampaio-Marques, Isabel Castro, Henrique Girão and Paula Ludovico. *Energy metabolism in acute myeloid leukemia cells*. Poster communication. SINAL 2017 - 8th Meeting on Signal Transduction. Lisboa, Portugal, 2017. (*The authors equally contributed for this work).
  - Sara Fernandes*, Olga Pereira*, Alexandra Teixeira, Ângela Mesquita, Ângela Fernandes, Belém Sampaio-Marques, Isabel Castro, Henrique Girão and Paula Ludovico. *Cell signaling pathways and autophagy regulation in acute myeloid leukemia*. Poster communication. SINAL 2017 - 8th Meeting on Signal Transduction. Lisboa, Portugal, 2017. (*The authors equally contributed for this work).
  - Olga Pereira, Belém Sampaio-Marques, Henrique Girão and Paula Ludovico. *Autophagy and metabolism of acute myeloid leukemia cells*. Poster communication. 3rd PROTEOSTASIS Action Meeting: "Proteostasis and its Biological Implications". Lisboa, Portugal, 2016.

2.1. Abstract

Acute myeloid leukemia (AML) comprises a group of heterogeneous hematopoietic neoplasms characterized by impaired differentiation and excessive proliferation of hematopoietic stem and/or myeloid progenitor cells, resulting in their accumulation in the bone marrow (BM) with subsequent dissemination to other organs. The metabolic switch from mitochondrial oxidative phosphorylation (OXPHOS) to a more glycolytic dependent metabolism has been extensively associated with the high survival and proliferation rates of cancer cells, including AML cells. This metabolic reprogramming is mainly driven by deregulation of the nutrient-sensing pathways serine/threonine protein kinase B (AKT), mammalian target of rapamycin complex 1 (mTORC1) and AMP-activated protein kinase (AMPK), which control fundamental cellular processes as macroautophagy (hereinafter referred to as autophagy). Despite the innumerous studies concerning the AML cells metabolism, the role of these metabolic adaptations on the AML cells survival, proliferation and chemoresistance remains controversial. The present work aimed to characterize the metabolic status and the respective metabolic networks operating in distinct AML cell types. Three different human AML cell lines representative of three distinct AML subtypes, HL-60 (FAB-M2 AML), NB-4 (FAB-M3 AML) and KG-1 (FAB-M6 AML), were used. KG-1 cells exhibited an OXPHOS phenotype accompanied by a constitutive AMPK and mTORC1 co-activation and an increased autophagy flux, whereas NB-4 and HL-60 cells displayed a highly glycolytic profile associated with an AKT/mTORC1 activation and a low autophagy flux. Inhibition of AKT was disclosed as a promising therapeutic target in some scenarios, while inhibition of AMPK or mTORC1 had no major impact on KG-1 cells survival. The results highlight an exclusive metabolic pattern for each tested AML cell type as well as its impact on the determination of the anti-leukemia efficacy.

Keywords: Acute myeloid leukemia (AML) ▪ Energy metabolism ▪ Glycolysis ▪ Mitochondrial oxidative phosphorylation (OXPHOS) ▪ Nutrient-sensing pathways ▪ Macroautophagy.

2.2. Introduction

Acute myeloid leukemia (AML) comprises a group of heterogeneous hematopoietic disorders characterized by a multitude of genetic and epigenetic aberrations associated with altered differentiation, proliferation and self-renewal of hematopoietic stem and/or myeloid progenitor cells [8-11]. AML intensive chemotherapy regimens result in different patient responses, with favorable outcomes in young patients [154] but limited application and poor outcomes among elderly, the most affected population [155-157]. Given the genetic, epigenetic, immunophenotypic and clinical

diversity among the AML patients, the development of targeted therapies remains a major challenge [158]. Accordingly, the elucidation of the mechanisms underlying AML pathogenesis is demanding.

A switch from mitochondrial oxidative phosphorylation (OXPHOS) to glycolytic metabolism, the well-recognized "Warburg effect", is a common strategy used by cancer cells to overcome their high bioenergetic needs [159-162]. This metabolic reprograming provides tumor cells with advantages, such as the rapid generation of ATP and intermediates for the synthesis of nucleotides, amino acids and fatty acids, that sustain their increased survival and proliferation rates [159-162]. A distinct glucose metabolism signature was recently identified in serum samples from the peripheral blood of AML patients when compared to control individuals [86]. Indeed, Chen, W.L. and co-workers identified 6 serum metabolite markers with prognostic value in cytogenetically normal AML patients [86]. By testing several AML cell lines (U937, OCI-AML3, HL-60 and KG-1) and human bone marrow (BM) AML blasts, these authors also proposed an association between metabolic reprograming towards glycolysis and AML cells chemoresistance by showing that enhanced glycolysis decreases AML cells sensitivity to cytarabine while the inhibition of glycolysis potentiates the cytotoxicity of this anti-leukemia agent [86]. The impact of augmented glycolysis in promoting AML cells drug resistance was also reported by other authors [87-90]. By showing that leukemia-initiating cells are highly dependent on glycolysis and that disruption of glycolysis inhibits leukemia initiation, Wang, Y. H., *et al.* [91] and Saito, Y., *et al.* [92] attributed a pro-leukemogenic role to glycolysis. As reported in several tumors, these findings also point to increased metabolic reprograming towards glycolysis as critical for the pathogenesis and therapy resistance of AML.

The metabolic reprogramming in tumor cells is mainly driven by deregulation of the nutrient-sensing pathways serine/threonine protein kinase B (AKT), mammalian target of rapamycin complex 1 (mTORC1) and AMP-activated protein kinase (AMPK) [112]. By testing several AML cell lines and human BM AML blasts, Poulain, L. *et al.* identified mTORC1 as a promoter of the glycolytic metabolism [94]. AKT was also recognized by Scotland, S. *et al.* as promoting glycolysis in the U937 AML cell line [96]. In T cell acute lymphoblastic leukemia (T-ALL), Kishton, R. J. *et al.* pointed to AMPK as an inducer of the OXPHOS [163]. AKT pathway is often found activated in AML, while mTORC1 seems to be active in all reported AML cases. [128, 130]. The possibility of a concomitant mTORC1 and AMPK constitutive activation independent of AKT illustrates the complexity of the nutrient-sensing pathways network in the AML context [123, 164]. Globally, it is still debatable and controversial whether AKT, mTORC1 and/or AMPK acts as a tumor-suppressor or -promoter in the

AML scenario [92, 120, 122, 128, 164-168]. Nevertheless, once activated, AKT [142, 143] and AMPK [140-142] may control macroautophagy in mTORC1-(in)dependent pathway(s). Macroautophagy, hereinafter referred to as autophagy, is a multi-step self-degradative process by which cytoplasmic content, such as long-lived proteins and superfluous/damaged organelles, is delivered to lysosomes for degradation [137]. Deregulation of autophagy has been widely described in AML, with both pro- and anti-tumoral functions identified [93, 147, 148, 152, 153, 169-172]. The elucidation of the interplay between energy metabolism, nutrient-sensing players and autophagy is therefore of major relevance in understanding AML pathogenesis and drug resistance. Results herein presented provide evidence for distinct metabolic signatures among different AML cell types. Indeed, whereas KG-1 cells displayed a preferential oxidative metabolism mainly associated with a constitutive AMPK and mTORC1 co-activation and an increased autophagy flux, NB-4 and HL-60 cells exhibited a glycolytic phenotype mainly associated with an AKT/mTORC1 activation and a reduced autophagy flux. Inhibition of AKT was disclosed as a promising target for therapeutic intervention in some scenarios, while inhibition of AMPK or mTORC1 had no major impact on the survival of KG-1 cells.

2.3. Material and methods

2.3.1. Human acute myeloid leukemia cell lines

Three distinct human acute myeloid leukemia (AML) cell lines, NB-4, HL-60 and KG-1, were used in the present work. NB-4 is a promyelocytic cell line, a French-American-British (FAB)-M3 subtype, that was established in 1989 from a 23-year-old female [63]. HL-60 is an AML cell line with maturation, a FAB-M2 subtype, that was established in 1976 from a 35-year-old female [173, 174]. KG-1 is an erythroleukemia cell line, a FAB-M6 subtype, that was established in 1977 from a 59-year-old male [175]. NB-4, HL-60 and KG-1 cells grow in culture suspensions and present a doubling time from 35h to 45h, 25h to 45h and 40h to 50h, respectively [63, 173-175].

NB-4, HL-60 and KG-1 cell lines were obtained from the German Collection of Microorganisms and Cell cultures (DSMZ® - Deutsche Sammlung von Mikroorganismen und Zellkulturen - German). Cells were maintained in Roswell Park Memorial Institute (RPMI) 1640 medium (Biochrom® - Merck Millipore) supplemented with 10% heat-inactivated fetal bovine serum (FBS) (Biochrom® - Merck Millipore) and 1% antibiotic-antimycotic solution (Invitrogen®) in a humidified, 37°C, 5% CO_2 atmosphere. Cells in exponential phase of growth (passages from 5 to 20) were used for the experimental approaches presented in this chapter.

2.3.2. Treatments

Compound C (CC), an AMPK inhibitor [176], and 2-Deoxy-D-glucose (2-DG), a synthetic glucose analog that cannot undergo glycolysis [177], were purchased from Sigma-Aldrich® and dissolved in dH_2O. Rapamycin (Rap), an mTORC1 inhibitor [178], and bafilomycin A1, an autophagy flux inhibitor [179], were also obtained from Sigma-Aldrich® but dissolved in DMSO. MK-2206, an AKT inhibitor [180], was purchased from Bertin Pharma® and prepared in DMSO. Final concentration: CC - 2.5µM; 2-DG - 11mM; Rap - 2µM; Bafilomycin A1 - 10nM; MK-2206 - 20µM.

NB-4 and HL-60 cells were submitted to MK-2206, while KG-1 cells were exposed to CC or Rap. All tested AML cells were treated with bafilomycin A1 for the assessment of autophagy flux. To study the AML cells glycolytic dependence, NB-4, HL-60 and KG-1 cells were cultured for 24h or 48h in RPMI 1640 medium no glucose (Alfagene®) supplemented with 10% heat-inactivated FBS (Biochrom® - Merck Millipore), 1% antibiotic-antimycotic solution (Invitrogen®) and 11mM 2-DG (Sigma-Aldrich®) in a humidified, 37°C, 5% CO_2 atmosphere.

2.3.3. Determination of the extracellular glucose and lactate levels

NB-4, HL-60 and KG-1 cells were plated at $0.5x10^6$ cells/mL/well, cultured for 24h with or without the respective treatment(s), collected and the supernatant reserved. Measurement of the extracellular glucose and lactate levels was then performed using the glucose test kit from R-Biopharm® and the lactate test kit from Spinreact® according to the manufacturer's instructions. At least, three independent biological replicates were performed.

2.3.4. Quantification of the intracellular ATP levels

NB-4, HL-60 and KG-1 cells were plated at $0.5x10^6$ cells/mL/well, cultured for 24h, collected and the pellet reserved. Intracellular ATP levels were determined using the ENLITEN ATP Assay System from Promega® according to the manufacturer's instructions. At least, three independent biological replicates were performed.

2.3.5. Measurement of cell survival - Annexin V/PI by flow cytometry

NB-4, HL-60 and KG-1 cells were plated at $0.5x10^6$ cells/mL/well, cultured for 24h or 48h with or without the respective treatment(s) and collected. Cells were then washed with 800µL of phosphate-buffered saline (PBS) followed by the addition of 100µL of binding buffer (100mM HEPES (pH 7.4), 140mM NaCl and 2.5mM $CaCl_2$). An incubation with 5µL of annexin V (BD

Biosciences®) and 10µL of propidium iodide (PI) at 50µg/mL (Invitrogen®) was then performed for 15min at room temperature and in the dark. 200µL of binding buffer was added once again to each sample. PI signal was measured using the FACS LSRII flow cytometer (BD Biosciences®) with a 488nm excitation laser. The annexin V signal was collected through a 488nm blocking filter, a 550nm long-pass dichroic with a 525nm band pass. Signals from 10.000 cells/sample were captured and FACS Diva was used as the acquisition software. Analysis of the results was performed using the FlowJo 7.6 (Tree Star®) software. At least, three independent biological replicates were done.

2.3.6. Immunoblotting analysis

NB-4, HL-60 and KG-1 cells were plated at $0.5x10^6$ cells/mL/well, cultured for 24h with or without the respective treatment(s), collected and the pellet reserved. Protein extraction was then performed by shaking and sonicating samples with 100µL of lysis buffer (1% NP-40, 500mM Tris HCl, 2.5M NaCl, 20mM EDTA, phosphatase and protease inhibitors (Roche®); pH 7.2). 20µg of the total protein were resolved in a 12% sodium dodecyl sulfate (SDS) polyacrylamide gel and transferred to a nitrocellulose membrane for 7min or 12min in the Trans-Blot Turbo Transfer System (Bio-Rad®). Membranes were blocked for 1h in tris-buffered saline (TBS) with 0.1% tween 20 (TBS-T) containing 5% bovine serum albumin (BSA) (Sigma-Aldrich®) and afterwards incubated overnight at 4°C with the polyclonal primary antibodies at 1:1000 in 1% BSA - Rabbit anti-phospho-AMPKα (Thr172) antibody; Rabbit anti-AMPKα antibody; Rabbit anti-phospho-ACC (Ser79) antibody; Rabbit anti-ACC antibody; Rabbit anti-phospho mTORC1 (Ser2448) antibody; Rabbit anti-mTORC1 antibody; Rabbit anti-phospho-p70 S6K (Thr389) antibody; Rabbit anti-p70 S6K antibody; Rabbit anti-phospho-AKT (Ser473) antibody; Rabbit anti-AKT antibody; Rabbit anti-LC3A/B antibody; Rabbit anti-p62 antibody; Rabbit anti-Beclin-1 antibody; Rabbit anti-Atg7 antibody; Rabbit anti-Atg5-Atg12 antibody; Rabbit anti-Atg16L1 antibody; Rabbit anti-GAPDH antibody (all from Cell Signaling Technology®); Rabbit anti-Atg10 antibody (Sigma-Aldrich®) and Mouse anti-Actin antibody (Abcam®). After washing with TBS-T, membranes were incubated with the respective secondary antibodies, IgG anti-Mouse antibody (Chemicon International®) for Actin and IgG anti-Rabbit antibody (Cell Signaling Technology®) for all the others, at 1:5000 in 1% skim milk for 1h20min at room temperature. Protein levels were detected after incubation with Clarity Western ECL Substrate (Bio-Rad®) or SuperSignal West Femto Maximum Sensitivity Substrate (Thermo

Fisher Scientific®). Digital images were obtained in the ChemiDoc XRS System (Bio-Rad®) with the Quantity One software (Bio-Rad®). At least, three independent biological replicates were done.

2.3.7. Immunostaining assay

Upon 24h of culture, NB-4, HL-60 and KG-1 cells (50.000 cells/well) were re-suspended in PBS and concentrated on a slide using the cytospin technique. Fixation was then performed using 2% paraformaldehyde (PFA). Cells were washed, permeabilized with 0.1% Triton X-100 in 0.1% sodium citrate and blocked with 4% BSA in PBS 0.05% Tween. Incubation with the primary antibody, Rabbit anti-mouse LC3 A/B (Cell Signaling Technology®), was performed overnight at 4°C. Goat anti-Rabbit IgG Alexa Fluor 588 (red-fluorescent dye; Molecular Probes®) was used as secondary antibody. Cells were also exposed to DAPI (4',6-diamidino-2-phenylindole), a nuclear counterstain with blue fluorescence. An epifluorescence microscope (BX61 microscope with an Olympus DP70 camera) was used to slide visualization and images were analyzed with the ImageJ® Software (National Institutes of Health). At least, three independent biological replicates were done.

2.3.8. Statistical analysis

All data is reported as the mean ± standard error of the mean (SEM). Statistical analysis was performed using the two-away ANOVA and Bonferroni post hoc tests to denote significant differences between the tested groups for the annexin V/PI approach. The Student's t-test was applied to compare the densitometric analysis of the Beclin-1/GAPDH, Atg7/GAPDH, Atg10/GAPDH, Atg5-Atg12/GAPDH and Atg16L1/GAPDH ratios between HL60 and KG-1 cells, as well as, to compare the extracellular glucose and lactate levels between untreated and MK-2206-treated HL-60 or NB-4 cells. The one-way ANOVA and Tukey post hoc tests were used to compare the tested groups for all the other approaches. A p value lower than 0.05 was assumed to denote a significant difference. Statistical analysis was conducted using the Prism software (GraphPad Software, San Diego, CA®).

2.4. RESULTS AND DISCUSSION

2.4.1. Energy metabolism of acute myeloid leukemia cells

Despite acute myeloid leukemia (AML) be a heterogeneous group of neoplasms, the association between energy metabolism and the pathogenesis of each AML subtype remains largely unknown. To better understand energy metabolism and its implication in the pathogenesis of different AML

subtypes, AML cell lines derived from patients diagnosed with FAB-M2 (HL-60 cell line), FAB-M3 (NB-4 cell line) and FAB-M6 (KG-1 cell line) AML subtypes were used and several metabolic parameters were evaluated. Determination of the extracellular glucose and lactate levels revealed distinct energy requirements for the different tested AML cell types. NB-4 cells presented lower extracellular glucose levels associated with higher extracellular lactate concentration than HL-60 and KG-1 cells (Fig. 8A, B), indicating a high glucose consumption and lactate production by NB-4 cells. In contrast, KG-1 cells displayed lower glucose uptake and lactate release than NB-4 and HL-60 cells (Fig. 8A, B). Accordingly, tested AML cell types can be sorted from a preferential glycolytic metabolism, presented by NB-4 cells, to a high oxidative metabolism, exhibited by KG-1 cells, assuming HL-60 cells an intermediate position. This AML glycolytic phenotype was supported by the ratio obtained between the extracellular lactate and glucose levels ([Lactate]/[Glucose]), which was clearly high for NB-4 cells followed by HL-60 cells and finally KG-1 cells (Fig. 8C). Consistently, data showed NB-4 cells as those exhibiting the highest intracellular ATP levels followed by HL-60 and KG-1 cells (Fig. 8D), in agreement with the enhanced production of ATP by time unit as result of their glycolytic rates (Fig. 8).

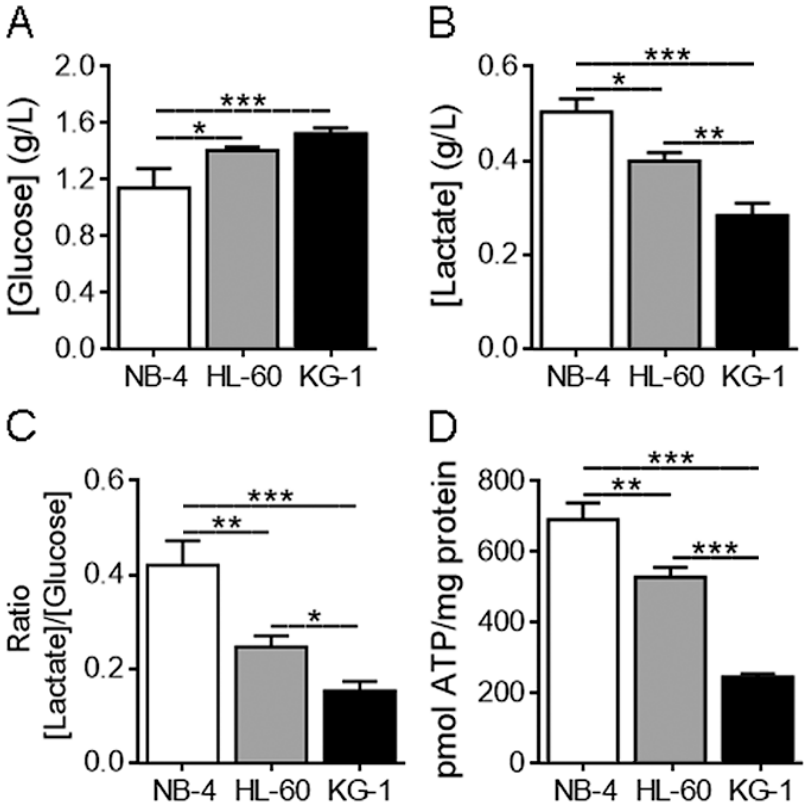

Fig. 8. NB-4 and HL-60 cells display a glycolytic phenotype while KG-1 cells exhibit an oxidative metabolism. NB-4, HL-60 and KG-1 cells were maintained for 24h in normal growth medium. (A) Extracellular glucose and (B) lactate levels were determined using glucose and lactate enzymatic detection kits. (C) The ratio between the extracellular lactate

and glucose levels ([Lactate]/[Glucose]) was calculated. (D) Intracellular ATP levels were quantified using the ENLITEN ATP Assay System. The results are shown as mean+/-SEM of, at least, three independent biological replicates. One-way ANOVA and Tukey post hoc test were used to compare the extracellular glucose and lactate levels, the ratio [Lactate]/[Glucose] and the intracellular ATP levels between NB-4, HL60 and KG-1 cells. *p <0.05; **p <0.01; ***p <0.001.

To further confirm the distinct energy requirements of the tested AML cell types, NB-4, HL-60 and KG-1 cells were exposed to 2-Deoxy-D-glucose (2-DG), a synthetic glucose analog that cannot undergo glycolysis [177]. Upon 24h, results showed a drastic reduction of NB-4 and HL-60 cells viability with no major impact on the survival of KG-1 cells, as revealed by the annexin V/PI assay (Fig. 9A). A similar cell viability profile was obtained upon 48h of 2-DG exposure, with KG-1 cells still displaying an increased survival pattern (Fig. 9B). The elevated sensitivity of NB-4 and HL-60 cells to the glycolytic inhibitor 2-DG reinforces the previous findings concerning their high glycolytic dependence (Fig. 8A-C). On the other hand, the resistance of KG-1 cells to 2-DG reveals not only the low relevance of glycolysis in these cells but also suggests mitochondrial oxidative phosphorylation (OXPHOS) as the main energy-generating cellular process.

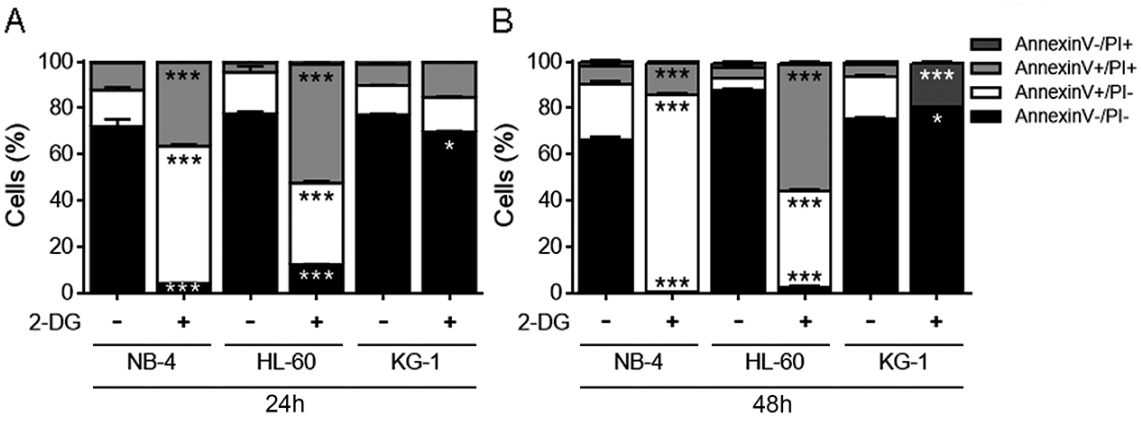

Fig. 9. The glycolytic inhibitor 2-DG promotes a drastic reduction on the NB-4 and HL-60 cells survival with no major impact on the KG-1 cells viability. NB-4, HL-60 and KG-1 cells were cultured for (A) 24h or (B) 48h in normal growth medium or in medium containing 2-DG instead of glucose. Cell viability was determined by flow cytometry analysis of annexin V- and propidium iodide (PI)-stained NB-4, HL-60 or KG-1 cells untreated or treated with 2-DG. The results are shown as mean+/-SEM of, at least, three independent biological replicates. Annexin V/PI data were analyzed using two-way ANOVA and Bonferroni post hoc test. *p <0.05; ***p <0.001.

Results herein presented with different AML cell lines propose that distinct AML cell types display specific energy requirements. Indeed, while NB-4 and HL-60 cells seem to be highly dependent on glycolysis, KG-1 cells appear to be more dependent on OXPHOS.

2.4.2. Complexity of the nutrient-sensing pathways network of acute myeloid leukemia cells

The reprogramming of energy metabolism in tumor cells is mainly driven by deregulation of the nutrient-sensing pathways AKT, mTORC1 and AMPK [112]. The occurrence of mTORC1 constitutive activation independent of AKT and the additional possibility of AMPK activation illustrates the complexity of the interactions between the nutrient-sensing pathways in the AML scenario [123, 164]. To explore the crosstalk between the observed energy metabolism of tested AML cell types (Fig. 8, 9) and the activation pattern of their nutrient-sensing pathways, the activation status of AKT, mTORC1 and AMPK was evaluated. Immunoblotting analysis revealed an AKT activation in NB-4 and HL-60 cells, as noticed by the augmented levels of phosphorylated AKT (Fig. 10A). As expected, mTORC1 activation was observed in all tested AML cell types, as reflected by the elevated phosphorylated levels of mTORC1 and of ribosomal protein S6 kinase (S6K), a mTORC1 direct downstream target [181] (Fig. 10B, C). A consistent higher AMPK activation was detected in KG-1 cells, as noticed by the augmented phosphorylated levels of AMPK and of acetyl-CoA carboxylase (ACC), an AMPK direct downstream substrate [182] (Fig. 10D, E). Data concerning AMPK activation concurred with the detected intracellular ATP levels (Fig. 8D), since AMPK activation occurs in the context of energy stress (high AMP/ATP ratio) [183] and KG-1 cells were those displaying the lowest intracellular ATP levels (Fig. 8D).

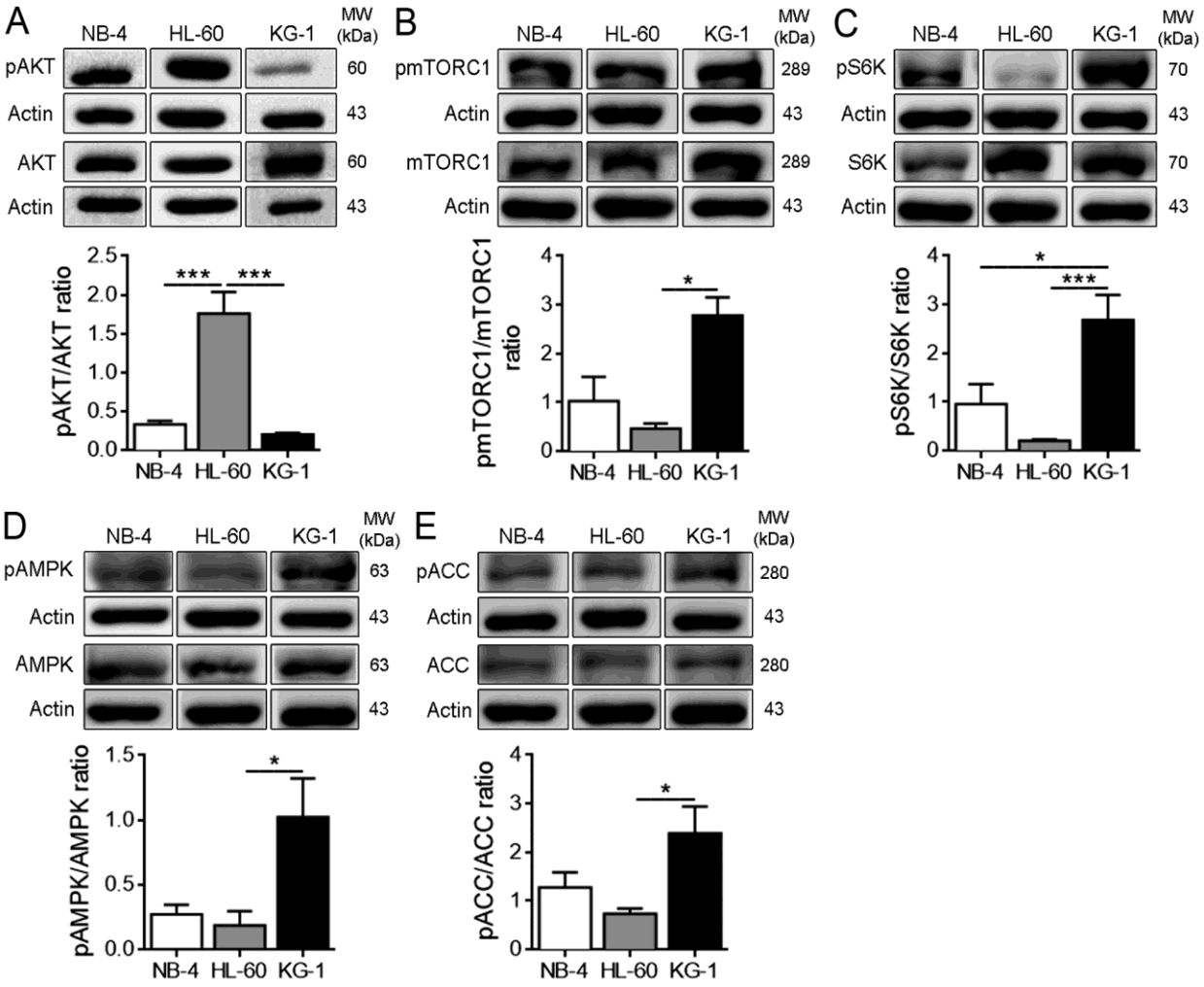

Fig. 10. NB-4 and HL-60 cells exhibit a constitutive AKT activation whereas KG-1 cells display a constitutive AMPK and mTORC1 co-activation. NB-4, HL-60 and KG-1 cells were maintained for 24h in normal growth medium. (A) Activation of AKT was determined by immunoblotting analysis of phosphorylated (Ser473) AKT levels. Activation of (B) mTORC1 and (C) S6K was assessed by immunoblotting analysis of phosphorylated (Ser2448) mTORC1 and phosphorylated (Thr389) S6K levels, respectively. Activation of (D) AMPK and (E) ACC was evaluated by immunoblotting analysis of phosphorylated (Thr172) AMPK and phosphorylated (Ser79) ACC levels, respectively. Actin was used as loading control. Densitometric analysis was performed and bands were quantified using the ImageLab4.1TM software. The results are shown as mean+/-SEM of, at least, three independent biological replicates. One-way ANOVA and Tukey post hoc test were used to compare the densitometric analysis of pAKT/AKT, pmTORC1/mTORC1, pS6K/S6K, pAMPK/AMPK and pACC/ACC ratios between NB-4, HL-60 and KG-1 cells. *p <0.05; ***p <0.001.

Although AMPK and mTORC1 have opposite effects on cellular metabolism [184], a concurrent activation of these two key metabolic players seems to occur in KG-1 cells. Knowing that AMPK may directly inhibit mTORC1 activity [185], this concomitant AMPK and mTORC1 activation appears to indicate a dissociative AMPK-mTORC1 axis in KG-1 cells. To the best of our knowledge, data herein presented showed for the first time a simultaneous constitutive activation of AMPK and mTORC1 in a specific subtype of AML cells. Interestingly, Kishton, R. J. *et al.* identified AMPK as an inducer of OXPHOS in T cell acute lymphoblastic leukemia (T-ALL) [163]. Using several AML

cell lines and human primary AML samples, Poulain, L. *et al.* also described mTORC1 as a promoter of glycolytic metabolism [94]. Plus, AKT was recognized by Scotland, S. *et al.* as promoting glycolysis in U937 AML cells [96]. Accordingly, data herein obtained propose AMPK as responsible for the increased oxidative metabolism exhibited by KG-1 cells (Fig. 8, 9) while suggest AKT-mTORC1 axis as sustaining the NB-4 and HL-60 cells glycolytic phenotype (Fig. 8, 9).
Altogether, data suggest that different AML cell types display distinct metabolic needs by showing a constitutive AKT activation in both NB-4 and HL-60 cells and a constitutive AMPK and mTORC1 co-activation in KG-1 cells.

2.4.3. Autophagy regulation of acute myeloid leukemia cells

The orchestrated metabolic network perpetuated by the nutrient-sensing pathways AKT, mTORC1 and AMPK converge on the control of cellular catabolic processes of high relevance to maintain cellular homeostasis, as macroautophagy (hereinafter referred to as autophagy) [138]. Given the central, although controversial, role of autophagy in the AML pathogenesis [93, 147, 148, 152, 153, 169-172], it is critical to understand not only its regulation but also its crosstalk with the metabolic signals. Autophagy flux was evaluated in the different AML cell types by immunoblotting analysis of both LC3 processing (I and II) and p62 protein levels after blocking the lysosomal degradation though the use of bafilomycin A1 [186]. KG-1 cells presented a higher autophagy flux than NB-4 and HL-60 cells, as reflected by the elevated LC3-II (Fig. 11A) and p62 (Fig. 11B) protein levels. Although p62 is a substract of autophagy [187], the concomitant increased levels of p62 and autophagy displayed by KG-1 cells results from the use of bafilomycin A1, which prevents the degradation of the autophagosome cargo, namely p62 [138]. Results herein obtained gave us an indicative of the autophagy flux up to the step of cargo delivery to lysosomes instead of the complete autophagy flux [186]. Indeed, to obtain an overall estimation of the autophagy flux, immunoblotting analysis should be performed in the presence and absence of lysosomal degradation/bafilomycin A1 [186]. The difference between the amount of LC3-II in the bafilomycin A1-treated and -untreated conditions would reflect the transit of LC3-II through the entire autophagy pathway [186]. Immunostaining of LC3 was also performed in the different tested AML cell types to assess autophagy by LC3 puncta visualization [186]. A higher number of LC3 puncta was observed in KG-1 cells than in NB-4 and HL-60 cells (Fig. 11C), corroborating the augmented autophagy flux of KG-1 cells revealed by the immunoblotting analysis. Data propose therefore that basal autophagy is higher in KG-1 cells than in NB-4 and HL-60 cells.

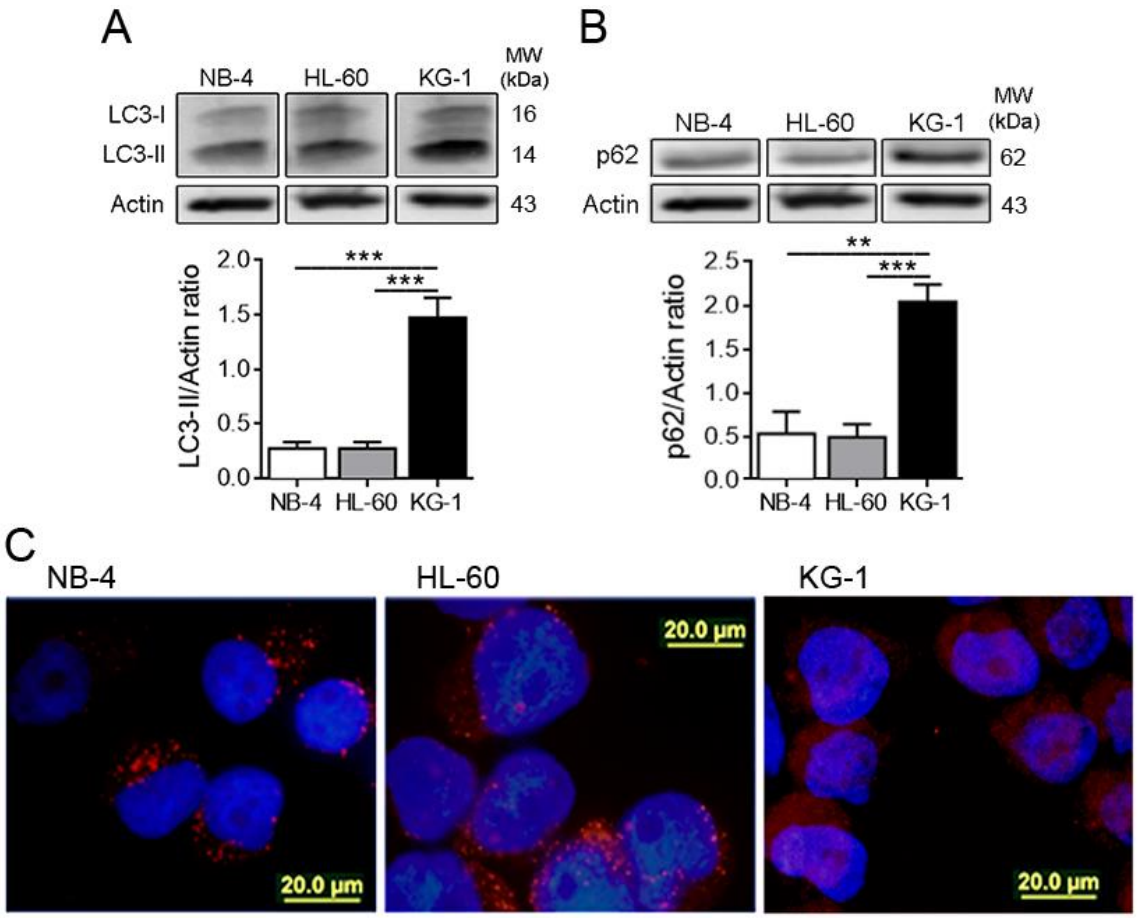

Fig. 11. NB-4 and HL-60 cells show reduced basal autophagy flux when compared to KG-1 cells. Autophagy flux was assessed by immunoblotting analysis of (A) LC3 processing (I and II) and (B) p62 protein levels in NB-4, HL-60 and KG-1 cells exposed for 24h to normal growth medium (all samples were incubated with 10nM of bafilomycin A1 for 2h before the end of the experiment to prevent lysosomal degradation and to allow LC3-II accumulation). Actin was used as loading control. Densitometric analysis was performed and bands were quantified using the ImageLab4.1TM software. The results are shown as mean+/-SEM of, at least, three independent biological replicates. One-way ANOVA and Tukey post hoc test were used to compare densitometric analysis of LC3-II/Actin and p62/Actin ratios between NB-4, HL60 and KG-1 cells. **p <0.01; ***p <0.001. (C) LC3 A/B-I/II puncta levels were visualized by immunostaining assay in NB-4, HL-60 and KG-1 cells submitted for 24h to normal growth medium. The tested AML cell types were stained with Goat LC3 anti-Rabbit IgG antibody (red fluorescence) and counterstained with DAPI (blue fluorescence). Representative images of the immunostaining assay are shown. Bar=20µm.

To better characterize the autophagy process, immunoblotting analysis of the autophagy-related proteins Beclin-1, Atg7, Atg10, Atg5-Atg12 complex and Atg16L1 was performed. Given the energetic, metabolic and autophagic similarities observed between the NB4 and HL-60 cells (Fig. 8-11), the assessment of the autophagy-related proteins was only done in HL-60 and KG-1 cells. Although no major differences were observed in the Beclin-1 protein levels between the tested AML cell types (Fig. 12A), lower Atg7 (Fig. 12B) and Atg10 (Fig. 12C) protein levels were detected in KG-1 cells than in HL-60 cells. However, higher Atg5-Atg12 complex (Fig. 12D) and Atg16L1 (Fig. 12E) protein levels were noticed in KG-1 cells than in HL-60 cells. Knowing that during the

elongation step of autophagy Atg12 is conjugated to Atg5 in an ubiquitin-like reaction that requires both Atg7 and Atg10 enzymes and that the Atg5-Atg12 conjugate is then noncovalently linked to Atg16L1 generating the Atg5-Atg12-Atg16L1 complex [188], these data reinforce the increased autophagy of KG-1 cells previously revealed by the immunoblotting (Fig. 11A, B) and immunostaining (Fig. 11C) assays.

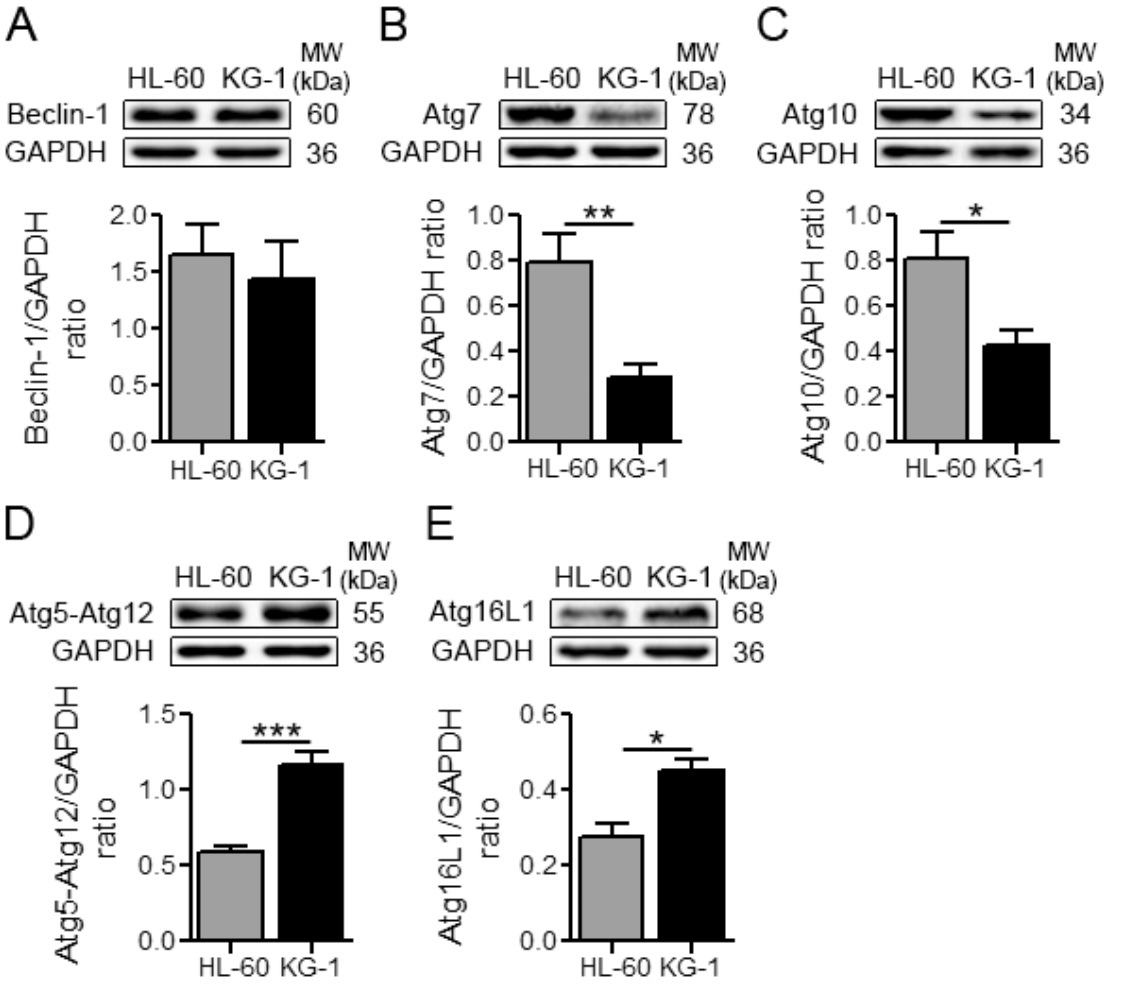

Fig. 12. HL-60 cells present decreased basal autophagy in comparison to KG-1 cells. Autophagy was evaluated by immunoblotting analysis of the autophagy-related proteins (A) Beclin-1, (B) Atg7, (C) Atg10, (D) Atg5-Atg12 complex and (E) Atg16L1 in HL-60 and KG-1 cells exposed for 24h to normal growth medium. GAPDH was used as loading control. Densitometric analysis was performed and bands were quantified using the ImageLab4.1TM software. The results are shown as mean+/-SEM of, at least, three independent biological replicates. Student's t-test was applied to compare the densitometric analysis of Beclin-1/GAPDH, Atg7/GAPDH, Atg10/GAPDH, Atg5-Atg12/GAPDH and Atg16L1/GAPDH ratios between HL60 and KG-1 cells. *p <0.05; **p <0.01; ***p <0.001.

The novel observation of a constitutive AMPK and mTORC1 co-activation in KG-1 cells (Fig. 10B-E) and its association with elevated autophagy (Fig. 11, 12) is striking. Knowing that AMPK can induce autophagy in mTORC1-independent pathways [140-142] and that mTORC1 is a negative regulator of autophagy [142], data herein presented propose a dissociative AMPK-mTORC1 axis with AMPK

directly sustaining autophagy in KG-1 cells. In contrast, NB-4 and HL-60 cells exhibited a constitutive activation of AKT (Fig. 10A) associated with reduced basal autophagy (Fig. 11, 12), suggesting that AKT and most probably mTORC1 are downregulating autophagy in these cells [142, 143]. Using human AML bone marrow mononuclear cells (BM-MNCs) and an AML mouse model, Watson, A. S. *et al.* showed that autophagy limits glycolytic metabolism in the AML context, being unclear the molecular mechanisms underlying this phenomenon [93]. Indeed, the increased glycolytic dependence displayed by NB-4 and HL-60 cells (Fig. 8, 9) was associated with a reduced autophagy (Fig. 11, 12), while in KG-1 cells a diminished glycolytic metabolism (Fig. 8, 9) was accompanied by an elevated autophagy (Fig. 11, 12). These findings highlight the contribution of autophagy in the regulation of energy metabolism, pointing to a role of autophagy in controlling the glycolytic metabolism of the different tested AML cell types. Taken together, data suggest that the activated AKT-mTORC1-autophagy axis may be responsible for the increased glycolytic status of both NB-4 and HL-60 cells, whereas the augmented oxidative metabolism of KG-1 cells may be controlled by the activated AMPK-autophagy axis.

Results herein obtained reveal a distinct autophagy signature among the different tested AML cell types by showing an elevated basal autophagy in KG-1 cells when compared to NB-4 and HL-60 cells.

Overall, data presented in sections 2.4.1 to 2.4.3 propose that different AML cell types exhibit distinct energetic, metabolic and autophagic requirements, which are highly interconnected between them. In fact, while NB-4 and HL-60 cells present a constitutive AKT activation associated with increased glycolysis and reduced autophagy, KG-1 cells display a constitutive AMPK and mTORC1 co-activation associated with both elevated OXPHOS and autophagy.

2.4.4. Manipulation of the nutrient-sensing pathways

2.4.4.1. Impact on the autophagy flux of acute myeloid leukemia cells

Data described above revealed a constitutive AKT activation associated with a decreased autophagy flux in both NB-4 and HL-60 cells, indicating AKT as the major autophagy regulator in these AML cell types. To clarify this metabolic coordination and regulation, NB-4 and HL-60 cells were submitted to the AKT inhibitor MK-2206 [180]. The status of the nutrient-sensing pathways and autophagy flux was then assessed by immunoblotting analysis. MK-2206 promoted a reduction of both AKT and mTORC1 activities, as noticed by the lowest AKT and S6K phosphorylated levels,

associated with an increase of autophagy flux, as reflected by the highest LC3 processing and p62 protein levels, (Fig. 13A, B). The AKT-mTORC1 axis appears therefore to play a critical role on the autophagy regulation of both NB-4 and HL-60 cells. Results presented in the previous sections also showed a constitutive AMPK and mTORC1 co-activation associated with an augmented autophagy flux in KG-1 cells, proposing AMPK as the major autophagy regulator in these cells. To decipher the relevance of this axis on the KG-1 cells metabolism, an AMPK inhibitor, compound C (CC) [176], or a mTORC1 inhibitor, rapamycin (Rap) [178], were used. The activation pattern of the nutrient-sensing pathways as well as the autophagy flux was evaluated by immunoblotting analysis. CC promoted a reduction of AMPK activation with no major impact on the mTORC1 activity but with a concomitant decline of the autophagy flux (Fig. 13C, left panel), proposing a dissociation of the AMPK-mTORC1 axis and reinforcing AMPK as the major autophagy regulator in KG-1 cells. As expected, Rap treatment induced a clear inhibition of mTORC1 activity with a further increase of autophagy flux (Fig. 13C, right panel), suggesting that although AMPK is the main autophagy regulator in KG-1 cells, mTORC1 is still able, to some degree, to negatively affect autophagy.

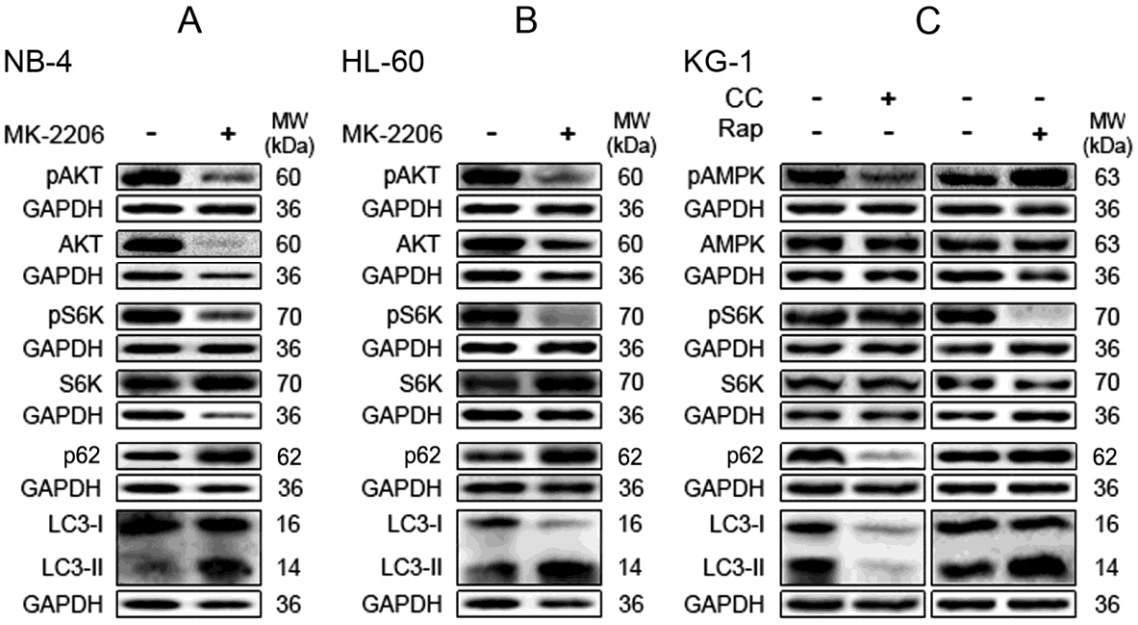

Fig. 13. Autophagy is mainly regulated by the AKT-mTORC1 axis in both NB-4 and HL-60 cells and by AMPK in KG-1 cells. NB-4 and HL-60 cells were maintained for 24h with or without 20μM of MK-2206 while KG-1 cells were cultured for 24h with or without 2.5μM of compound C (CC) or 2μM of rapamycin (Rap). (A-C) Activation of AMPK, AKT and S6K as well as autophagy flux was assessed by immunoblotting analysis. Activation of AMPK and AKT was evaluated by immunoblotting analysis of phosphorylated (Thr172) AMPK and phosphorylated (Ser473) AKT levels, respectively. Activation of S6K was determined by immunoblotting analysis of phosphorylated (Thr389) S6K levels. Autophagy flux was assessed by immunoblotting analysis of both LC3 processing (I and II) and p62 protein levels (all samples were incubated with 10nM of bafilomycin A1 for 2h before the end of the experiment to prevent lysosomal degradation and

to allow LC3-II accumulation). GAPDH was used as loading control. The results are representative of, at least, three independent biological replicates.

Data herein presented reinforce the identical metabolic and autophagic phenotype displayed by NB-4 and HL-60 cells, by pointing the AKT-mTORC1 axis as the major negative regulator of autophagy in both AML cell types, in contrast to KG-1 cells, in which autophagy is mainly positively controlled by AMPK.

2.4.4.2. Impact on the energy metabolism of acute myeloid leukemia cells

The impact of the nutrient-sensing pathways inhibition on the energy metabolism of the tested AML cell types was also assessed. Inhibition of AKT activity by MK-2206 promoted augmented extracellular glucose levels associated with reduced extracellular lactate concentrations in both NB-4 and HL-60 cells (Fig. 14A, B, D, E), proposing a decreased glucose consumption and lactate production by these cells. The reduced glycolytic metabolism observed in response to MK-2206 was confirmed by the calculated ratio between the extracellular lactate and glucose levels ([Lactate]/[Glucose]), which was lower in the MK-2206-treated NB-4 and HL-60 cells than in the untreated conditions (Fig. 14G, H). These data point to the AKT-mTORC1 axis as a positive regulator of the glycolytic metabolism displayed by NB-4 and HL-60 cells. Interestingly, the reduced glycolytic metabolism noticed in response to MK-2206 was accompanied by an increased autophagy flux (Fig. 13A, B), pointing to autophagy as a negative regulator of the NB-4 and HL-60 cells glycolytic process. These results agree with the Watson, A. S. *et al.* publication that identifies autophagy as limiting glycolysis in the AML context [93]. Data indicate therefore the AKT-mTORC1-autophagy axis as critical on the regulation of the NB-4 and HL-60 cells glycolytic metabolism. Treatment of KG-1 cells with CC or Rap resulted in increased extracellular glucose levels associated with no major alterations in the extracellular lactate concentrations (Fig. 14C, F, I). The maintenance of lactate concentrations associated with decreased glucose consumption suggests a glucose-independent source of lactate and is compatible with the predominant OXPHOS metabolism displayed by these cells (Fig. 8, 9).

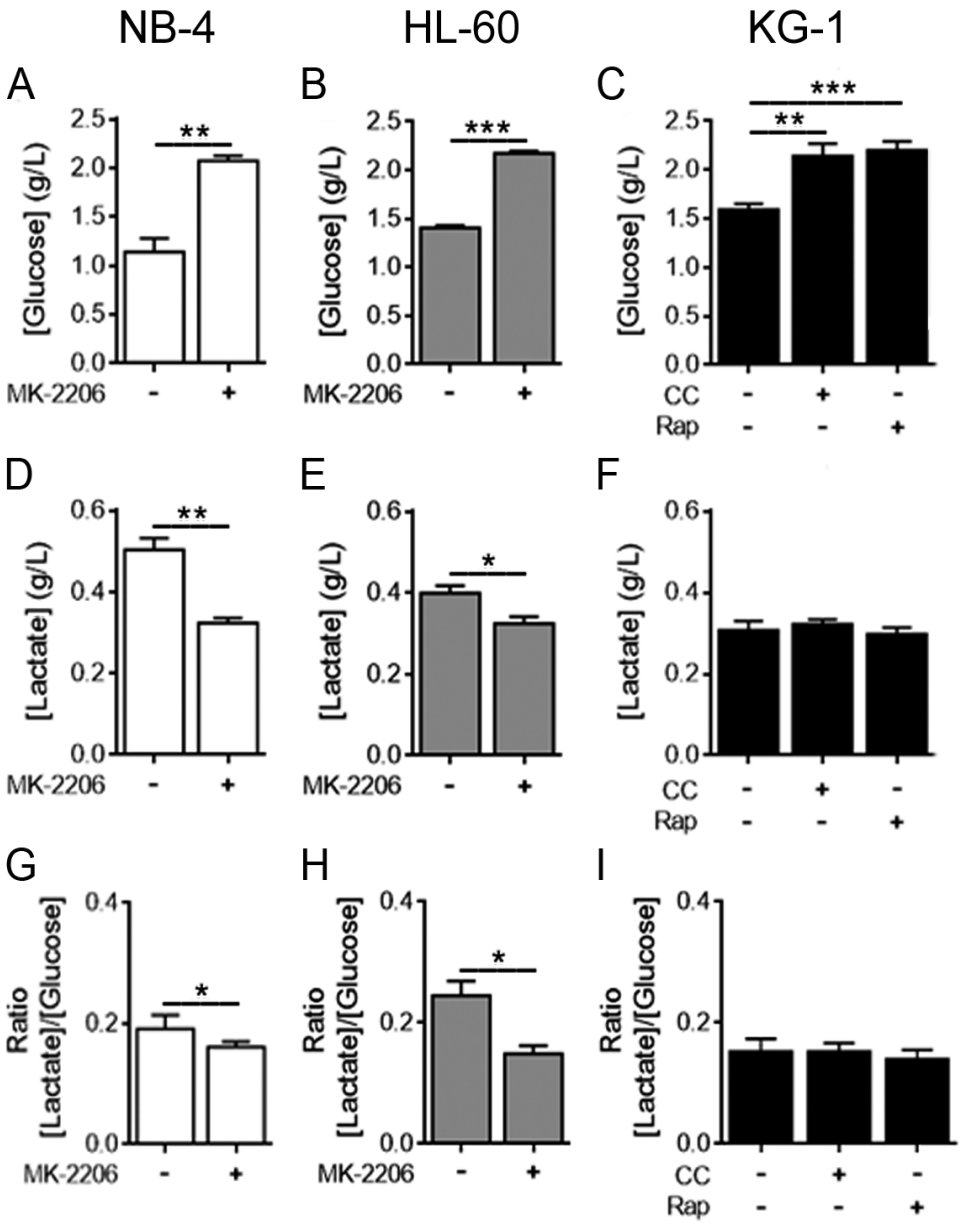

Fig. 14. Energy metabolism is mainly controlled by AKT in both NB-4 and HL-60 cells and by AMPK in KG-1 cells. NB-4 and HL-60 cells were maintained for 24h with or without 20μM of MK-2206 while KG-1 cells were cultured for 24h with or without 2.5μM of compound C (CC) or 2μM of rapamycin (Rap). (A-C) Extracellular glucose and (D-F) lactate levels were determined using glucose and lactate enzymatic detection kits. (G-I) The ratio between the extracellular lactate and glucose levels ([Lactate]/[Glucose]) was calculated. The results are shown as mean+/-SEM of, at least, three independent biological replicates. Student's t-test was applied to compare the extracellular glucose and lactate levels as well as the ratio [Lactate]/[Glucose] between untreated and MK-2206-treated NB-4 or HL-60 cells. One-way ANOVA and Tukey post hoc test were used to compare the extracellular glucose and lactate levels as well as the ratio [Lactate]/[Glucose] between untreated and CC- or Rap-treated KG-1 cells. *p <0.05; **p <0.01; ***p <0.001.

Results herein presented imply a key role of the AKT-mTORC1-autophagy axis in controlling glycolysis of both NB-4 and HL-60 cells while support the low relevance of this energetic process in KG-1 cells. Data also suggest a primordial role of OXPHOS in the KG-1 cells metabolism.

2.4.4.3. Impact on the survival of acute myeloid leukemia cells

Knowing that inhibition of AKT, mTORC1 or AMPK had a major impact on the autophagy flux (Fig. 13) and energy metabolism (Fig. 14) of all tested AML cell types, the viability of NB-4, HL-60 and KG-1 cells was also determined under the same conditions. Data revealed a significant decrease on the viability of NB-4 (Fig. 15A) and HL-60 (Fig. 15B) cells upon exposure to MK-2206, pointing to AKT as critical for the survival of both types of AML cells. Given that AKT inhibition induced an elevated autophagy flux in NB-4 and HL-60 cells (Fig. 13A, B), the MK-2206-promoted cell death may result from autophagy activation, implicating autophagy as an anti-tumoral process in both NB-4 and HL-60 cells. Treatment of KG-1 cells with CC or Rap resulted in a modest, although significant, decrease of their viability (Fig. 15C). Together with the distinct effects that these compounds had on autophagy flux (Fig. 13C) and with the independence of glycolysis (Fig. 8, 9), AMPK and mTORC1 do not seem to be an attractive target for KG-1 cells. Most probably, this phenomenon reflects the conflicting metabolic signals resulting from the constitutive AMPK and mTORC1 co-activation.

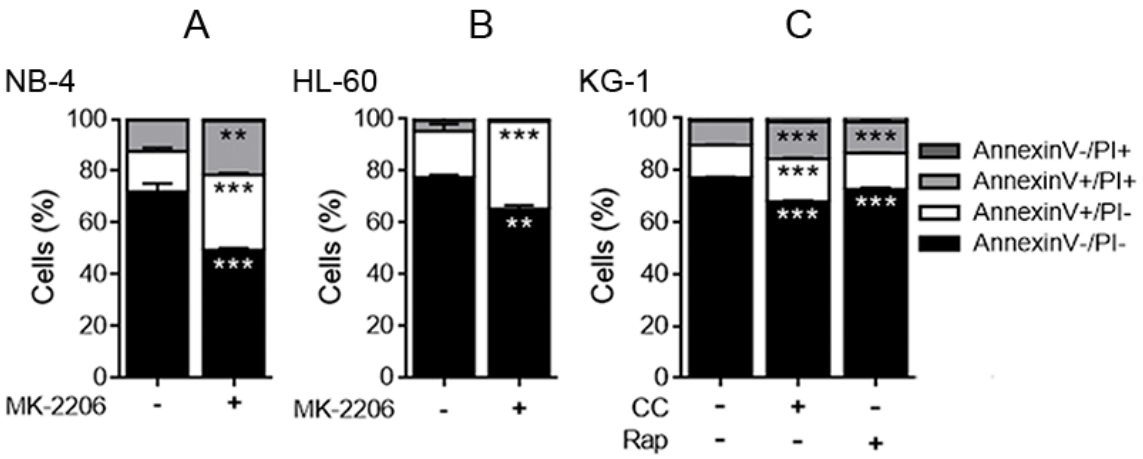

Fig. 15. AKT inhibition decreases NB-4 and HL-60 cell's viability whereas AMPK or mTORC1 inhibition has a minor effect on the survival of KG-1 cells. (A) NB-4 and (B) HL-60 cells were maintained for 24h with or without 20μM of MK-2206 while (C) KG-1 cells were cultured for 24h with or without 2.5μM of compound C (CC) or 2μM of rapamycin (Rap). Cell viability quantification was determined by flow cytometry analysis of annexin V- and propidium iodide (PI)-stained NB-4, HL-60 or KG-1 cells submitted to the different treatments. The results are shown as mean+/-SEM of, at least, three independent biological replicates. Annexin V/PI data were analyzed using the two-way ANOVA and Bonferroni post hoc test. **p <0.01; ***p <0.001.

Data herein presented reveal that targeting specific nutrient-sensing pathways sensitizes both NB-4 and HL-60 cells while has a minor impact on the survival of KG-1 cells.

By manipulating specific nutrient-sensing pathways, data presented in the section 2.4.4 support a similar metabolic, autophagic and energetic signature between NB-4 and HL-60 cells by pointing AKT-mTORC1 axis as a critical player on the regulation of both autophagy and energy metabolism. With a distinct phenotype, KG-1 cells seem to have AMPK as the main responsible for the regulation of autophagy and energy metabolism. The elevated sensitivity of NB-4 and HL-60 cells to the inhibition of AKT activity not only reinforces the similarities between these two AML cell types but also identifies AKT as a potential therapeutic target for the treatment of specific subtypes of AML.

Summing up, a schematic representation of the specific networks operating in NB-4, HL-60 and KG-1 cells is illustrated in Fig. 16. The occurrence of distinct energetic, metabolic and autophagic signatures among different subtypes of AML is proposed, highlighting the molecular heterogeneity of AML and the need to treat each AML subtype as a single disorder.

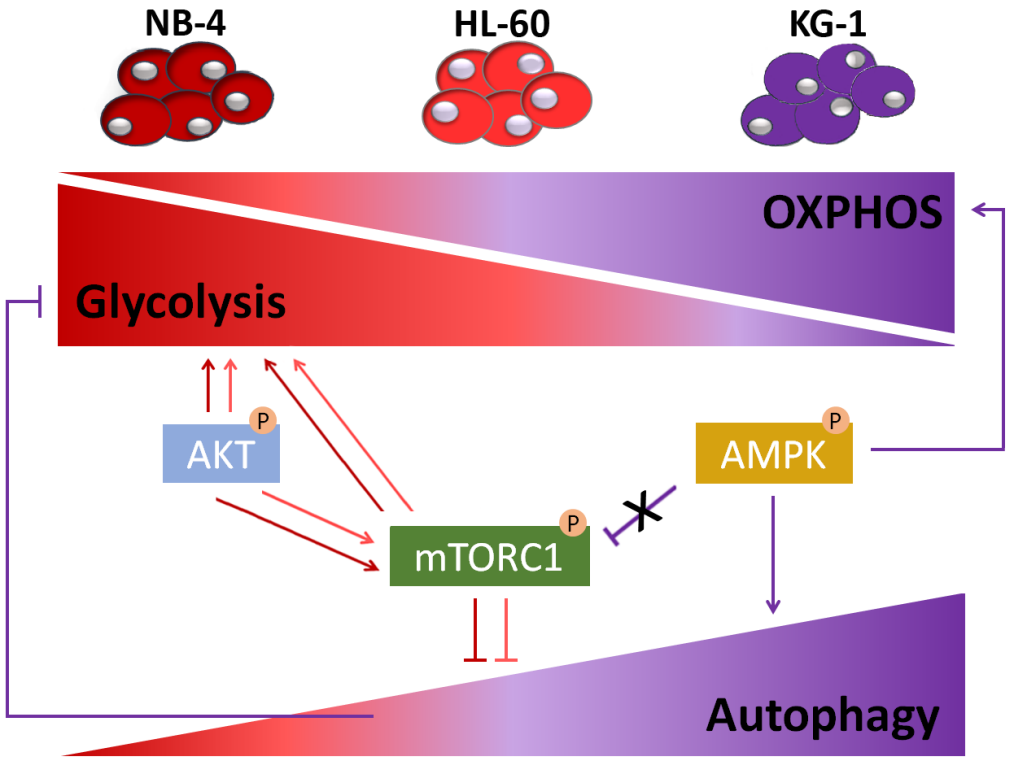

Fig. 16. Schematic representation of the specific networks operating in NB-4, HL-60 and KG-1 cells. An exclusive energetic, metabolic and autophagic signature is proposed for each tested AML cell type. While a glycolytic phenotype associated with an AKT-mTORC1 activation and a reduced autophagy pattern is suggested for NB-4 cells, an oxidative metabolism (OXPHOS) accompanied by a constitutive AMPK and mTORC1 co-activation and an augmented autophagy profile is indicated for KG-1 cells. For HL-60 cells, an intermediate state between NB-4 and KG-1 cells is identified. The

AKT-mTORC1 axis is viewed as a positive regulator of glycolysis and a negative regulator of autophagy in both NB-4 and HL-60 cells, whereas AMPK seems to positively control OXPHOS in KG-1 cells. Inhibition of glycolysis by autophagy is also proposed in KG-1 cells. AKT - serine/threonine protein kinase B; mTORC1 - mammalian target of rapamycin complex 1; AMPK - AMP-activated protein kinase. Dark red, light red and purple arrows represent NB-4, HL-60 and KG-1 cells, respectively.

CHAPTER 3

Autophagy in acute myeloid leukemia patients: a retrospective cohort study

3.1. Abstract

Acute myeloid leukemia (AML) is the most common type of acute leukemia in adults, being still fatal to 2/3 of young adults and to 90% of elderly. Macroautophagy, hereinafter referred to as autophagy, is a catabolic process that removes potentially dangerous cytoplasmic components, namely long-lived proteins and dysfunctional organelles, playing a vital role in maintaining cellular homeostasis. This self-degradative mechanism has been widely reported as critical for survival, proliferation and chemoresistance of AML cells. Nevertheless, the autophagy's role is still unclear with both pro- and anti-tumoral properties suggested. The present work aimed to characterize the expression pattern of core autophagy genes among distinct subtypes of AML. A retrospective cohort study was conducted with mRNA samples extracted from the bone marrow mononuclear cells (BM-MNCs) of 82 AML patients, clustered according to the French-American-British (FAB) classification system, and 39 control donors. The gene expression of critical autophagy players was shown to be decreased in the BM-MNCs of the AML individuals when compared to the BM-MNCs of the control subjects, proposing reduced autophagy as a hallmark of AML. Although without statistical significance, a differential expression of autophagy-related genes was noticed among the BM-MNCs of the tested AML subtypes, with the FAB-M3 AML patients exhibiting the highest autophagy phenotype followed by the FAB-M2 AML individuals and finally the FAB-M1, FAB-M3 and FAB-M5 AML subjects. By categorizing the AML patients according to the cytogenetic risk group, a distinct expression of essential autophagy genes was also detected, with the highest and lowest autophagy signature being displayed by the BM-MNCs of the favorable and intermediate II cytogenetic risk groups, respectively. Finally, an increased or a trend towards increased expression of autophagy-related genes was noticed in the BM-MNCs of the AML individuals with abnormal karyotype, when compared to the AML individuals with normal karyotype. The *in silico* analysis herein presented reveals the heterogeneity of AML, strongly suggesting the need to scrutinize and dissect AML as a group of heterogeneous disorders rather than a single malignancy.

Keywords: Acute myeloid leukemia (AML) ▪ Macroautophagy ▪ Autophagy-related genes ▪ Retrospective cohort study.

3.2. Introduction

Acute myeloid leukemia (AML) includes a heterogeneous group of hematological malignancies characterized by impaired differentiation and uncontrolled proliferation of hematopoietic stem and/or myeloid precursor's cells [8-11]. Such deregulation results in the accumulation of

nonfunctional immature cells in the bone marrow (BM) and disrupts the normal production of blood cells [8-11]. This group of neoplasms is the most common type of acute leukemia in adults, with a median age of diagnosis of 65 years, and presents a slight male predominance [17-19]. The AML incidence increases with age, being rarely diagnosed before the 40 years [17-19]. Accordingly, the number of AML cases is expected to increase in the future in line with the population's age.

Macroautophagy, hereinafter referred to as autophagy, is a self-degradative process by which cytoplasmic constituents, such as cellular proteins and organelles, are delivered to lysosomes for degradation [137]. Mechanistically, autophagy consists on a multistep process that starts with the initiation/nucleation phase, characterized by the isolation of a small double-membrane structure termed phagophore and by the mobilization of proteins required for the phagophore expansion. While the initiation step is regulated by the ULK1/2 complex, the nucleation phase demands the participation of Beclin1 complexes [137-139]. The elongation/expansion phase, characterized by the expansion of the phagophore, requires two essential ubiquitin-like conjugation systems: the conjugation of Atg12 to Atg5 via Atg7 and Atg10; and the conjugation of LC3-I to phosphatidylethanolamine (PE) via Atg7 and Atg3. Upon conjugation, the Atg12-Atg5 complex binds to Atg16 generating the Atg12-Atg5-Atg16 complex, which together with the LC3-I/PE, also called LC3-II, binds to the phagophore allowing its elongation and curvature [137-139]. Eventually, the expanding membrane closes to form the autophagosome (closure/maturation phase), which fuses with the lysosome originating the autolysosome (fusion phase), in which cargo is degraded (degradation phase) [137-139]. The macromolecules resulting from this degradation are recycled or used for energy production [137-139]. Under normal conditions, autophagy plays a vital role in maintaining cellular homeostasis [145, 146].

Autophagy has been widely recognized as a double-edged sword in the AML setting, with both tumor-suppressive and -promotive activities reported. Briefly, Mortensen, M. *et al.* attributed an anti-tumoral function to autophagy by showing that *ATG7* knockout mice develop a lethal pre-leukemic phenotype [147]. Autophagy-limiting leukemic transformation was also recognized by Watson, A. S. *et al.*, who found that heterozygous loss of *ATG5* potentiates disease progression and aggressiveness in an AML mouse model [93]. A marked reduction in the expression levels of the *GABARAPL1*, *GABARAPL2* and *MAP1LC3B* autophagy-related genes was also detected by Watson, A. S. *et al.* in the bone marrow mononuclear cells (BM-MNCs) of AML patients when compared to the BM-MNCs of control donors, identifying them as tumor suppressor genes in the AML context [93]. With distinct AML and control cohorts, Brigger, D. *et al.* also revealed lower

GABARAPL1 and *GABARAPL2* expression levels in AML individuals than in non-hematological subjects [148]. On the other hand, by testing several AML cell lines and AML blasts from the BM or peripheral blood of AML patients, Altman, J. K. *et al.* showed enhanced leukemic cell survival in response to autophagy induction, proposing autophagy as an oncogenic process [169]. By observing that autophagy promotes the survival and drug resistance of AML cells (AML cell lines) under hypoxia, Dirkje, W. H., *et al.* also ascribed a tumor-promoting role to autophagy [153]. Sumitomo, Y. *et al.* also suggested a pro-tumoral function to autophagy by detecting that inactivation of autophagy through *ATG7* or *ATG5* depletion reduces the tumorigenic phenotype of an AML mouse model [152]. It is therefore commonly accepted that autophagy plays a versatile role in AML disorders, which may depend on both cell type and cellular context. Accordingly, the characterization of the autophagy pattern among the distinct AML subtypes is useful to understand the survival, proliferation and therapy resistance of the different AML cell types.

A retrospective cohort study was herein conducted with mRNA samples extracted from the BM-MNCs of AML patients and control donors. A decrease in the expression of critical autophagy genes was noticed in the BM-MNCs of the AML subjects when compared to the BM-MNCs of the control individuals, pointing to reduced autophagy as a signature of AML. In the AML patients, a differential expression of autophagy-related genes was detected among the BM-MNCs of distinct FAB subtypes, cytogenetic risk group or karyotypes, supporting AML as a group of highly heterogeneous diseases.

3.3. Material and methods

3.3.1. Human biological specimens

3.3.1.1. mRNA samples

mRNA samples extracted from the bone marrow mononuclear cells (BM-MNCs) of 82 acute myeloid leukemia (AML) patients diagnosed and treated at IPO-Porto from 2005 to 2014 were kindly provided.

3.3.1.2. Bone marrow samples

BM samples were collected from 39 individuals without hematological malignancy (control donors) during a routine cardiac surgery at Hospital da Arrábida - Porto from 2014 to 2016.

The research projects related to sections 3.3.1.1 and 3.3.1.2 were submitted and approved by the ethics committees of the involved institutions. All the individuals enrolled in the studies provided written informed consent in accordance with the Declaration of Helsinki.

3.3.2. Extraction of human bone marrow mononuclear cells

Mononuclear cells (MNCs) from the BM samples of the 39 control donors were isolated by standard density gradient centrifugation, as described in the PhD thesis of Ângela Fernandes (*The functional crosstalk of proteolytic systems and metabolism in acute myeloid leukemia*, 2016, University of Minho).

3.3.3. Quantitative mRNA expression

All the experimental approaches required to determine the mRNA expression levels of the autophagy-associated genes *MAP1LC3B* (*microtubule associated protein 1 light chain 3 beta*), *ATG12* (*autophagy related 12 homolog*), *ATG5* (*autophagy related 5 homolog*), *BECLIN1* (*coiled-coil myosin-like BCL2-interacting protein*) and *BCL2* (*B-cell lymphoma/leukemia 2*) in the BM-MNCs of both control donors and AML subjects were performed as described in the PhD thesis of Ângela Fernandes (*The functional crosstalk of proteolytic systems and metabolism in acute myeloid leukemia*, 2016, University of Minho).

3.3.4. Statistical analysis

All data is reported as the mean ± standard error of the mean (SEM). Statistical analysis was performed using the Student's t-test and Mann-Whitney post hoc test to compare the mRNA expression levels of *MAP1LC3B*, *ATG12*, *ATG5*, *BECLIN1* or *BCL2* between the control donors and the AML subjects, as well as, between the normal and the abnormal karyotypes. One-way ANOVA and Dunns post hoc test were applied to compare the mRNA expression levels of *MAP1LC3B*, *ATG12*, *ATG5*, *BECLIN1* or *BCL2* between the different tested FAB AML subtypes as well as between the different cytogenetic risk groups. The Spearman's rank correlation method was used to calculate the strength of association between the mRNA expression levels of *BCL2* and *MAP1LC3B*, *ATG12*, *ATG5* or *BECLIN1* in the total AML group and in the FAB-M2 and FAB-M3 AML subtypes. A *p* value lower than 0.05 was assumed to denote a significant difference. Statistical analysis was conducted using Prism software (GraphPad Software, San Diego, CA®).

3.4. Results and discussion

3.4.1. Clinical characterization of both acute myeloid leukemia and control cohorts

Results obtained with different human acute myeloid leukemia (AML) cell lines representative of distinct AML subtypes indicated a similar autophagy profile between the NB-4 and HL-60 cells while

suggested a completely distinct autophagy phenotype for the KG-1 cells (Chapter 2). Accordingly, to better characterize the autophagy pattern among different AML subtypes, the assessment of critical autophagy-related players was performed in mononuclear cells (MNCs) isolated from the bone marrow (BM) samples of AML patients diagnosed and treated at IPO-Porto from 2005 to 2014. The clinical characteristics of 196 AML patients at diagnosis were recorded and analyzed, as published in the PhD thesis of Ângela Fernandes (*The functional crosstalk of proteolytic systems and metabolism in acute myeloid leukemia*, 2016, University of Minho). Of these 196 AML individuals, we only had access to BM samples of 82 AML subjects, who make up the AML cohort studied in the present work. The 82 BM samples were extracted at diagnosis and classified according to the FAB classification system as represented in Table 4. AML with myelodysplastic-related changes and non-classified AML were included in the category "Others" (Table 4). From 2005 to 2014, 0 (0.0%) individuals were diagnosed with FAB-M6 AML disorder (Table 4). Consistently, the FAB-M6 AML is a well-documented uncommon subtype of AML [189]. Indeed, due to its rarity, the clinical experience with this subtype of AML is limited [189]. Based on the cytogenetic risk group and karyotype, the 82 AML individuals were stratified as described in Table 4. At diagnosis, 49 (59.8%) AML individuals had less than 60 years and 33 (40.2%) had more than 60 years, being the median age 52 years with a range between 21 and 79 years (Table 4). Importantly, the most recent "*Registo Oncológico Nacional*", data published in 2015 and referring to 2010, identifies 65 years as the median age at diagnosis of the Portuguese AML patients [19]. Note that the reduced median age at diagnosis of the AML patients enrolled in the present study (52 years) may reflect a bias, since the elderly may not have been admitted to intensive therapy. The distribution of AML cases according to age at diagnosis showed, as expected, an increase AML incidence with age (Fig. 17). In the present cohort, 41 (50.0%) AML donors were males and 41 (50.0%) were females (Table 4). Interestingly, these values agree with data reported by the "*Registo Oncológico Nacional*", which described a similar number of men and women affected by AML (3.8 males and 3.1 females per 100.000 individuals) [19].

Table 4. Clinical characteristics of 82 acute myeloid leukemia patients at diagnosis (IPO-Porto from 2005 to 2014).

Clinical characteristics	Total of AML cases (n=82)
AML subtypes (FAB classification)	
M0 (n; %)	1; 1.2
M1 (n; %)	8; 9.8
M2 (n; %)	11; 13.4
M3 (n; %)	16; 19.5
M4 (n; %)	8; 9.8
M5 (n; %)	7; 8.5
M6 (n; %)	0; 0.0
Others (n; %)	31; 37.8
Cytogenetic risk group	
Favorable (n; %)	24; 29.3
Intermediate I (n; %)	29; 35.4
Intermediate II (n; %)	7; 8.5
Adverse (n; %)	20; 24.4
No information (n; %)	2; 2.4
Karyotype	
Normal karyotype (n; %)	40; 48.8
Abnormal karyotype (n; %)	36; 43.9
No information (n; %)	6; 7.3
Age (mean; range)	52; 21-79
<60 (n; %)	49; 59.8
≥60 (n; %)	33; 40.2
Gender	
Male (n; %)	41; 50.0
Female (n; %)	41; 50.0

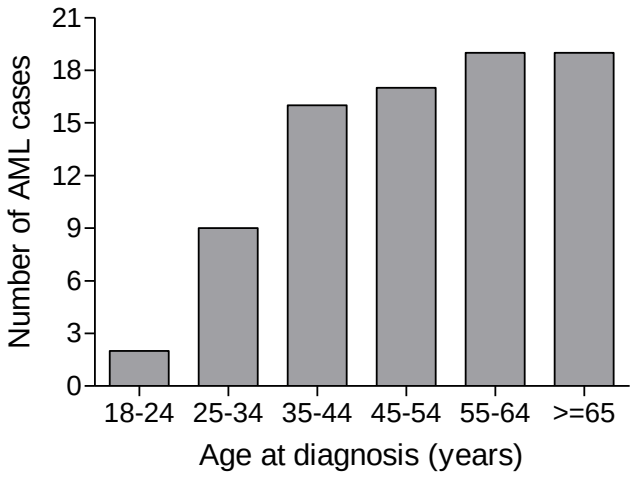

Fig. 17. Distribution of acute myeloid leukemia (AML) cases according to age at diagnosis. The horizontal axis shows 5-year age intervals. The vertical axis shows the number of AML cases in a given age group. A total of 82 AML individuals diagnosed and treated at IPO-Porto from 2005 to 2014 are included in this analysis.

MNCs were also isolated from the BM samples of 39 individuals without hematological malignancy to be used as control. Extraction of the BM samples was performed during a routine cardiac surgery at Hospital da Arrábida - Porto from 2014 to 2016. At the time of BM samples collection, 11 (28.2%) control individuals had less than 60 years and 28 (71.8%) had more than 60 years, being the median age 71 years with a range between 40 and 87 years (Table 5). Plus, 31 (79.5%) control donors were male and 8 (20.5%) were female (Table 5).

Table 5. Clinical characteristics of 39 donors without hematological malignancy (Hospital da Arrábida - Porto from 2014 to 2016).

Clinical characteristics	Total of control cases (n=39)
Age (mean; range)	71; 40-87
<60 (n; %)	11; 28.2
≥60 (n; %)	28; 71.8
Gender	
Male (n; %)	31; 79.5
Female (n; %)	8; 20.5

3.4.2. Autophagy signature in acute myeloid leukemia individuals

3.4.2.1. Expression of autophagy-related genes in acute myeloid leukemia

To better characterize the autophagy profile among distinct AML subtypes, a retrospective cohort study was conducted with mRNA samples extracted from the bone marrow mononuclear cells (BM-MNCs) of 82 AML patients (described in Table 4) and kindly provided from IPO-Porto. Due to the inherent limitations of a retrospective cohort study only mRNA samples were obtained. Accordingly, to minimize the impossibility of studying autophagy at the protein level, transcriptionally regulated genes, *MAP1LC3B* (*microtubule associated protein 1 light chain 3 beta*), *ATG12* (*autophagy related 12 homolog*), *ATG5* (*autophagy related 5 homolog*), *BECLIN1* (*coiled-coil myosin-like BCL2-interacting protein*) and *BCL2* (*B-cell lymphoma/leukemia 2*), were selected. mRNA samples were also extracted from the BM-MNCs of 39 individuals without hematological malignancy (described in Table 5) to be used as control (these mRNA specimens were also used in the PhD thesis of Ângela Fernandes - *The functional crosstalk of proteolytic systems and metabolism in acute myeloid leukemia*, 2016, University of Minho). A lower *MAP1LC3B* (Fig. 18A) and *ATG12* (Fig. 18B) gene expression was detected in the BM-MNCs of AML subjects than in the BM-MNCs of control donors, while a similar *ATG5* gene expression (Fig. 18C) was observed between the two tested groups. Consistently, Watson, A. S. *et al.* [93], Radwan, S. M. *et al.* [190] and Liang, P. Q. *et al.*

[191] reported decreased *MAP1LC3B* mRNA expression levels in the BM-MNCs of AML patients when compared to the BM-MNCs of control donors. Reduced *ATG12* gene expression was also detected by Watson, A. S. *et al.* [93] and Walter, M. J. *et al.* [192] in the AML scenario. Plus, identical *ATG5* mRNA expression levels were noticed by Watson, A. S. *et al.* [93] and Lian, Y. *et al.* [193] between the BM-MNCs of AML and control individuals. Data herein obtained point to a reduced expression of autophagy-related genes in the BM-MNCs of AML patients when compared to the BM-MNCs of control donors. Interestingly, by quantifying the LC3 co-localization with lysosomal markers by flow cytometry and the positive p62 staining by immunohistochemistry, Watson, A. S. *et al.* showed reduced autophagy at the functional level in the AML patients [93]. Data concerning *BECLIN1* gene expression did not reveal statistical differences between the two tested groups (Fig. 18D). Nevertheless, a tendency for increased *BECLIN1* gene expression was detected in the BM-MNCs of AML individuals in comparison to the BM-MNCs of control donors (Fig. 18D). In agreement, Hu, X. Y. *et al.* also found elevated *BECLIN1* mRNA expression levels in the BM-MNCs of AML subjects when compared to the BM-MNCs of control donors [194]. However, reduced *BECLIN1* mRNA expression levels were detected by Watson, A. S. *et al.* [93], Radwan, S. M. *et al.* [190] and Liang, P. Q. *et al.* [191] in the BM-MNCs of AML patients. A study conducted by Lian, Y. *et al.* also showed similar *BECLIN1* mRNA expression levels between the BM-MNCs of AML and control individuals [193]. Accordingly, the *BECLIN1* expression pattern in the BM-MNCs of AML subjects appears to be controversial. A recent study described that interaction of the Beclin-1 BH3 domain with Bcl-2 is fundamental for the anti-apoptotic activity of Bcl-2 [195]. Thus, unlike other BH3-only proteins, which act as pro-apoptotic molecules, Beclin-1 has been recognized as an anti-apoptotic protein [196-198]. Since Beclin-1 participates not only in autophagy but also in regulated cell death [198], the increased *BECLIN1* gene expression observed in the BM-MNCs of AML patients (Fig. 18D) may indicate a high Beclin-1 recruitment for the apoptotic process. In agreement, an elevated *BCL2* gene expression was noticed in the BM-MNCs of AML subjects when compared to the BM-MNCs of control donors (Fig. 18E). Augmented Bcl-2 mRNA and protein levels have been widely described in AML patients [199], further supporting a fundamental crosstalk between these two players in the AML scenario. Autophagy has been robustly shown as exerting a paradoxical role in the AML scenario, acting both as tumor-suppressor and -promoter [93, 147, 148, 152, 153, 169-172]. In the present work, the reduced *MAP1LC3B* (Fig. 18A) and *ATG12* (Fig. 18B) gene expression observed in the BM-MNCs of AML patients when compared to the BM-MNCs of control individuals points to these autophagy-related players as tumor suppressor genes

in the AML context. The higher *BCL2* gene expression detected in the BM-MNCs of AML individuals than in the BM-MNCs of control donors (Fig. 18E) proposes *BCL2* as a tumor promoter gene in the presented AML cohort, in agreement with several reported studies [199]. The tendency for augmented *BECLIN1* gene expression in the BM-MNCs of AML subjects (Fig. 18D) also suggests *BECLIN1* as an oncogene in the AML disorder, which may result from a high Beclin-1 recruitment to prevent apoptosis.

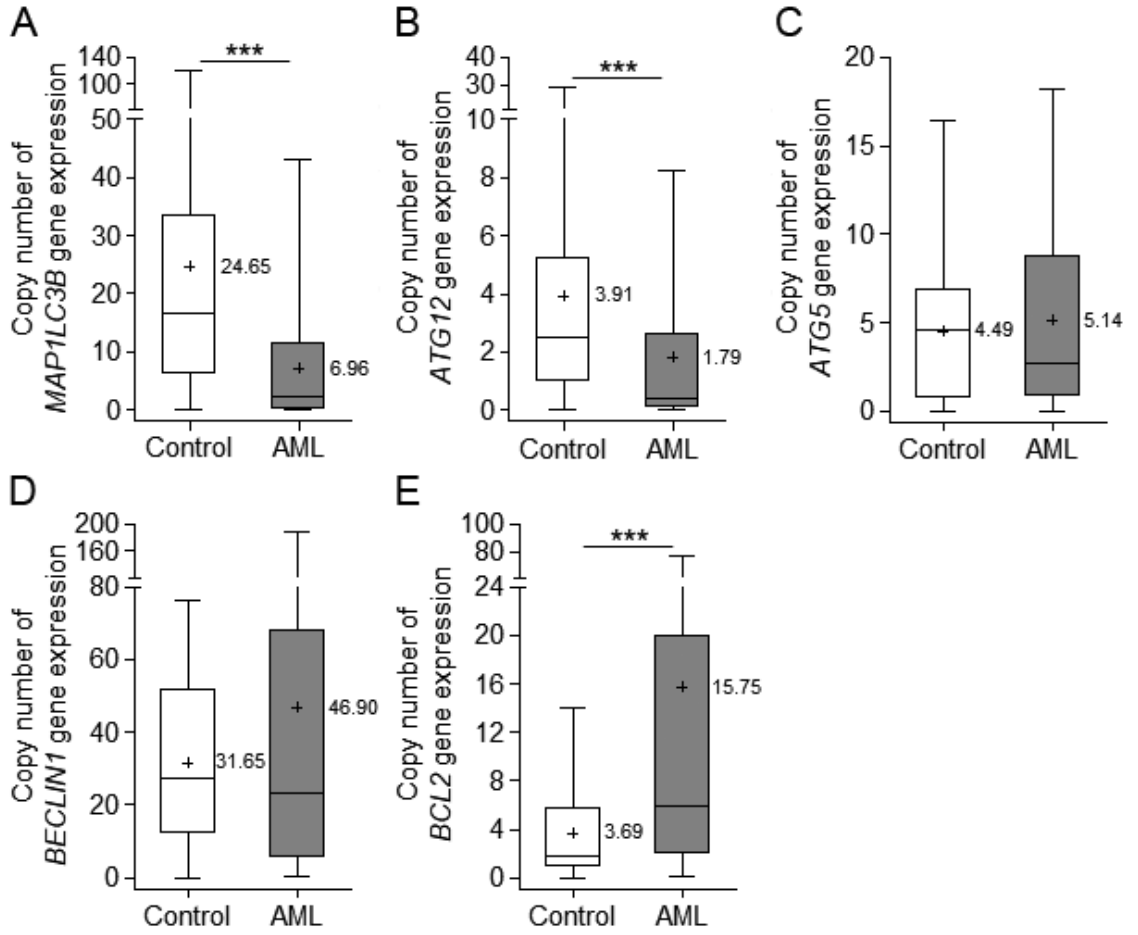

Fig. 18. Acute myeloid leukemia individuals present a distinct autophagy-related genes expression profile in comparison to control donors. Mononuclear cells (MNCs) were isolated from the bone marrow (BM) samples of both donors without hematological malignancy (Control) and patients with acute myeloid leukemia (AML). mRNA was then extracted from the bone marrow mononuclear cells (BM-MNCs) and the expression levels of the autophagy-related genes (A) *MAP1LC3B*, (B) *ATG12*, (C) *ATG5*, (D) *BECLIN1* and (E) *BCL2* were determined by qPCR. BM samples from a total of 39 control individuals and 82 AML subjects were enrolled in this study. The copy number gene expression was calculated by the standard quantity copy number curve, previous defined for each gene. Student's t-test and Mann-Whitney post hoc test were used to compare the mRNA expression levels of the *MAP1LC3B*, *ATG12*, *ATG5*, *BECLIN1* and *BCL2* between the control and AML individuals. ***p <0.001. The mean is shown as "+" and the respective value (*MAP1LC3B*: Control=24.65 vs AML=6.96; *ATG12*: Control=3.91 vs AML=1.79; *ATG5*: Control=4.49 vs AML=5.14; *BECLIN1*: Control=31.65 vs AML=46.90; *BCL2*: Control=3.69 vs AML=15.75).

It is widely described that binding of Bcl-2 to Beclin-1 may disrupt the formation of the Beclin-1-hVps34 complex, reducing the Beclin-1's capacity to induce autophagy [198]. To get some clues about this mechanism in the BM-MNCs of AML subjects, the degree of association between the mRNA expression levels of *BCL2* and *MAP1LC3B*, *ATG12, ATG5* or *BECLIN1* was calculated using the Spearman's rank correlation method, a non-parametric statistical test used to measure the strength of association between two ranked variables through the Spearman's rank correlation coefficient (r). Indeed, while r=+1 denotes a perfect positive correlation between two variables, r=0 represents no correlation and r=-1 indicates a perfect negative correlation. A significant positive correlation was detected in all tested conditions, *BCL2/ MAP1LC3B*: r=0.8640, p<0.0001 (Fig. 19A); *BCL2/ ATG12*: r=0.8325, p<0.0001 (Fig. 19B); *BCL2/ ATG5*: r=0.9065, p<0.0001 (Fig. 19C); *BCL2/ BECLIN1*: r=0.9011, p<0.0001 (Fig. 19D), indicating that the mRNA expression levels of *BCL2* and *MAP1LC3B*, *ATG12*, *ATG5* or *BECLIN1* move in tandem - the *BCL2* mRNA expression levels increase/decrease as the *MAP1LC3B*, *ATG12*, *ATG5* or *BECLIN1* mRNA expression levels increase/decrease. Accordingly, if a similar correlation analysis was obtained at the protein level, it could suggest that Beclin-1 is interacting with Bcl-2 to prevent apoptosis and that Bcl-2/Beclin-1 interaction is not impairing autophagy in the BM-MNCs of AML individuals. Nevertheless, such an approach is impossible to perform due to the unavailability of protein samples, an intrinsic limitation to the retrospective cohort study.

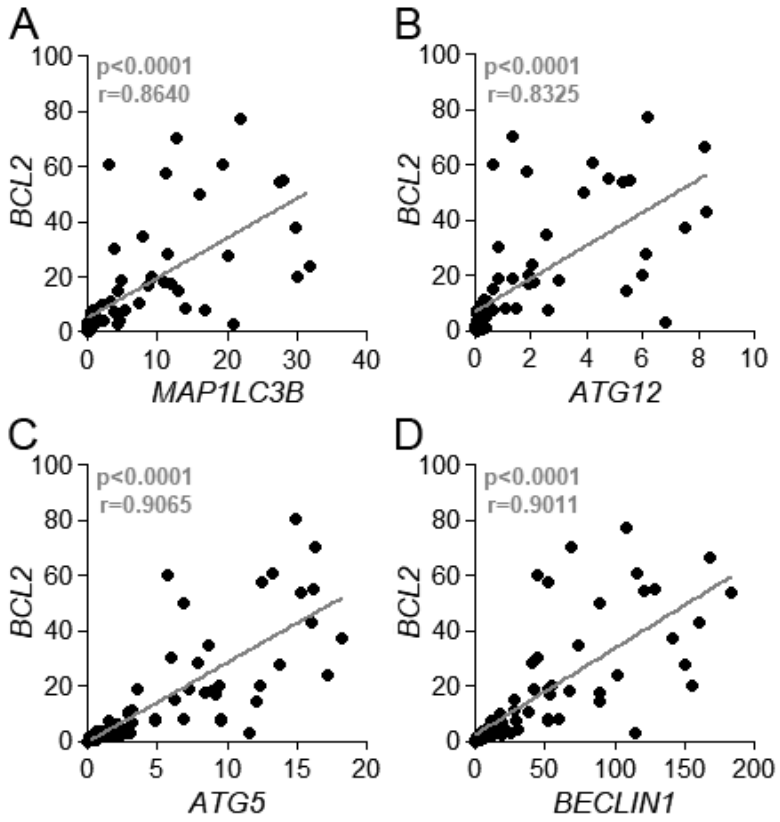

Fig. 19. Acute myeloid leukemia patients exhibit a significant positive correlation between the mRNA expression levels of *BCL2* and (A) *MAP1LC3B*, (B) *ATG12*, (C) *ATG5* or (D) *BECLIN1*. Mononuclear cells (MNCs) were isolated from the bone marrow (BM) samples of 82 individuals diagnosed with acute myeloid leukemia (AML). mRNA was then extracted from the bone marrow mononuclear cells (BM-MNCs) and the expression levels of the autophagy-related genes *MAP1LC3B*, *ATG12*, *ATG5*, *BECLIN1* and *BCL2* were determined by qPCR. The copy number gene expression was calculated by the standard quantity copy number curve, previous defined for each gene. The Spearman's rank correlation method was then applied to determine the strength of association between the mRNA expression levels of *BCL2* and *MAP1LC3B*, *ATG12*, *ATG5* or *BECLIN1*. A significant positive correlation was obtained in all tested conditions: *BCL2/ MAP1LC3B*: r=0.8640, p<0.0001; *BCL2/ ATG12*: r=0.8325, p<0.0001; *BCL2/ ATG5*: r=0.9065, p<0.0001; *BCL2/ BECLIN1*: r=0.9011, p<0.0001.

The retrospective cohort study herein conducted with human mRNA samples proposes autophagy as a tumor suppressor mechanism in the AML scenario, by showing a reduced expression of autophagy-related genes in the BM-MNCs of AML patients when compared to the BM-MNCs of control individuals. As expected, the expression of anti-apoptotic genes was shown to be increased in the BM-MNCs of the AML subjects, as widely reported in other AML cohorts. Since AML is a heterogeneous group of hematological disorders, the assessment of the autophagy-related genes expression among the different AML subtypes is needed to better understand the disease development, progression and chemoresistance.

3.4.2.2. Expression of autophagy-related genes among distinct subtypes of acute myeloid leukemia

To unravel the autophagy status among distinct subtypes of AML, an *in silico* analysis was performed by clustering the previously determined *MAP1LC3B*, *ATG12*, *ATG5*, *BECLIN1* and *BCL2* mRNA expression levels (Fig. 18) according to the FAB AML subtype, FAB-M1 to FAB-M5 (Table 4). The AML group defined as "Others" (Table 4) comprises miscellaneous AML cases and therefore was not included in this analysis. The FAB-M0 and FAB-M6 AML subtypes (Table 4) were also not studied due to the reduced and absent number of AML cases, respectively. Although without statistical differences, a higher *MAP1LC3B* (Fig. 20A, left panel), *ATG12* (Fig. 20B, left panel) and *ATG5* (Fig. 20C, left panel) gene expression was noticed in the BM-MNCs of the FAB-M2 and FAB-M3 AML patients than in the BM-MNCs of the other tested FAB AML individuals. A trend towards increased *MAP1LC3B*, *ATG12* and *ATG5* gene expression (Fig. 20A-C, left panel) was also detected in the BM-MNCs of the FAB-M3 AML subjects when compared to the BM-MNCs of the FAB-M2 AML patients. Data point therefore to a differential autophagic signature among distinct subtypes of AML, by showing the FAB-M3 AML patients as those who exhibit the highest autophagy-related genes expression followed by the FAB-M2 AML individuals and finally the FAB-M1, FAB-M4 and FAB-M5 AML subjects. Nevertheless, the BM-MNCs of the FAB-M3 AML individuals still presented a trend towards reduced expression of autophagy-related genes when compared to the BM-MNCs of the control donors (Fig. 20A-B, right panel). Indeed, the successful treatment of the FAB-M3 AML patients consists in the induction of autophagy by the all-trans retinoic acid (ATRA), which leads to the autophagic degradation of the PML/RARα oncoprotein with consequent differentiation of promyelocytes into mature granulocytes [200]. This therapeutic approach, specifically applied to the FAB-M3 AML individuals, results in high complete remission rate (80-90%) [69]. Data concerning *BECLIN1* (Fig. 20D, left panel) and *BCL2* (Fig. 20E, left panel) gene expression did not reveal statistical differences between the tested FAB AML subtypes. Nevertheless, similar to the gene expression pattern of the *MAP1LC3B*, *ATG12* and *ATG5* (Fig. 20A-C, left panel), the BM-MNCs of the FAB-M3 AML patients displayed the highest *BECLIN1* and *BCL2* gene expression followed by the BM-MNCs of the FAB-M2 AML individuals and finally the BM-MNCs of the other studied FAB AML subjects (Fig. 20D-E, left panel). A distinct anti-apoptotic gene profile appears therefore to occur among different subtypes of AML. Although without statistical significance, when compared to the BM-MNCs of the control donors, the BM-MNCs of the FAB-M1, FAB-M4 and FAB-M5 AML individuals presented reduced *BECLIN1* gene expression whereas the BM-MNCs of the FAB-M2 and FAB-M3 AML patients displayed augmented *BECLIN1*

mRNA expression levels (Fig. 20D, right panel). These findings together with the data obtained in Fig. 18D clearly illustrate the importance of clustering and scrutinizing each subtype of AML. Indeed, the tendency for increased *BECLIN1* gene expression observed in the BM-MNCs of the AML individuals when compared to the BM-MNCs of the control donors (Fig. 18D) only represents the FAB-M2 and FAB-M3 AML patients, with the other tested FAB AML subtypes being neglected (Fig. 20D, right panel). By comparing with the BM-MNCs of the control donors, a trend towards augmented *BCL2* gene expression was also detected in the BM-MNCs of the FAB-M2 and FAB-M3 AML patients while no major differences were noticed in the BM-MNCs of the FAB-M1, FAB-M4 and FAB-M5 AML subjects (Fig. 20E, right panel). These data together with the results obtained in Fig. 18E, which revealed a higher *BCL2* gene expression in the BM-MNCs of the AML individuals than in the BM-MNCs of the control donors, reinforce the need to individually analyze each subtype of AML.

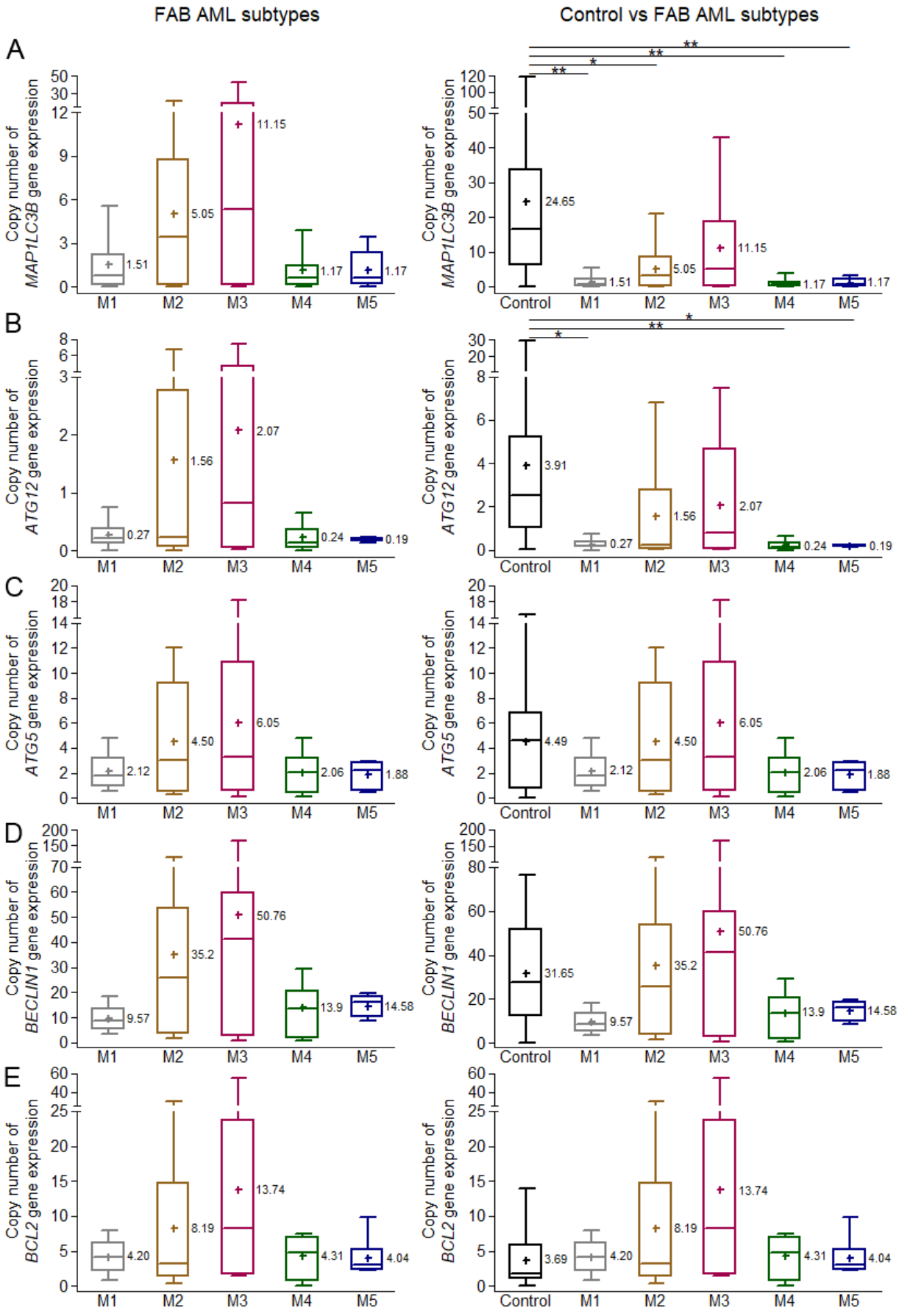

Fig. 20. Patients with distinct subtypes of acute myeloid leukemia exhibit a differential autophagy-related genes expression signature. Mononuclear cells (MNCs) were isolated from the bone marrow (BM) samples of both donors

without hematological malignancy (Control) and patients with distinct subtypes of acute myeloid leukemia (AML). mRNA was then extracted from the bone marrow mononuclear cells (BM-MNCs) and the expression levels of the autophagy-related genes (A) *MAP1LC3B*, (B) *ATG12*, (C) *ATG5*, (D) *BECLIN1* and (E) *BCL2* were determined by qPCR. BM samples from a total of 39 control individuals and 50 AML subjects, distributed according to the French-American-British (FAB) classification system as FAB-M1: 8; FAB-M2: 11; FAB-M3: 16; FAB-M4: 8 and FAB-M5: 7, were enrolled in this study. The copy number gene expression was calculated by the standard quantity copy number curve, previous defined for each gene. One-way ANOVA and Dunns post hoc test were used to compare the mRNA expression levels of the *MAP1LC3B*, *ATG12*, *ATG5*, *BECLIN1* and *BCL2* between the studied groups. *p <0.05; **p <0.01. The mean is shown as "+" and the respective value (*MAP1LC3B*: Control=24.65 vs M1=1.51 vs M2=5.05 vs M3=11.15 vs M4=1.17 vs M5=1.17; *ATG12*: Control=3.91 vs M1=0.27 vs M2=1.56 vs M3=2.07 vs M4=0.24 vs M5=0.19; *ATG5*: Control=4.49 vs M1=2.12 vs M2=4.50 vs M3=6.05 vs M4=2.06 vs M5=1.88; *BECLIN1*: Control=31.65 vs M1=9.57 vs M2=35.2 vs M3=50.76 vs M4=13.9 vs M5=14.58; *BCL2*: Control=3.69 vs M1=4.20 vs M2=8.19 vs M3=13.74 vs M4=4.31 vs M5=4.04).

The increased *BECLIN1* and *BCL2* gene expression (Fig. 20D-E, right panel) associated with the decreased *MAP1LC3B* and *ATG12* gene expression (Fig. 20A-B, right panel) in the BM-MNCs of the FAB-M2 and FAB-M3 AML patients when compared to the BM-MNCs of the control donors may indicate an impairment of autophagy as a result of the Beclin-1 recruitment to prevent apoptosis. Indeed, the Beclin-1 network regulates both autophagy and apoptosis, with a possible decline in autophagy due to the anti-apoptotic activity of Beclin-1 [198]. To get some clues about this process in the BM-MNCs of the FAB-M2 and FAB-M3 AML subjects, the strength of association between the mRNA expression levels of *BCL2* and *MAP1LC3B*, *ATG12*, *ATG5* or *BECLIN1* was calculated using the Spearman's rank correlation method. A significant positive correlation was noticed in all tested conditions of the FAB-M3 AML individuals, *BCL2*/*MAP1LC3B*: r=0.9341, p<0.0001 (Fig. 21A); *BCL2*/*ATG12*: r=0.8364, p=0.0022 (Fig. 21B); *BCL2*/*ATG5*: r=0.8846, p<0.0001 (Fig. 21C); *BCL2*/*BECLIN1*: r=0.8681, p=0.0001 (Fig. 21D), proposing that the *BCL2* gene expression increases/decreases as the *MAP1LC3B*, *ATG12*, *ATG5* or *BECLIN1* gene expression increases/decreases. Although the FAB-M2 AML subjects presented both the Spearman's rank correlation coefficient (r) and the probability value (p) lower than the FAB-M3 AML individuals, a significant positive correlation was also detected - *BCL2*/*MAP1LC3B*: r=0.7000, p=0.0204 (Fig. 21A); *BCL2*/*ATG12*: r=0.7091, p=0.0268 (Fig. 21B); *BCL2*/*ATG5*: r=0.7818, p=0.0064 (Fig. 21C); *BCL2*/*BECLIN1*: r=0.7727, p=0.0074 (Fig. 21D). If an identical correlation analysis was detected at the protein level, it could infer that Beclin-1 is interacting with Bcl-2 to prevent apoptosis and that Bcl-2/Beclin-1 interaction is not disrupting autophagy in the BM-MNCs of the FAB-M2 and FAB-M3 AML patients. However, as previously mentioned, such a study is impossible to perform due to the absence of protein specimens.

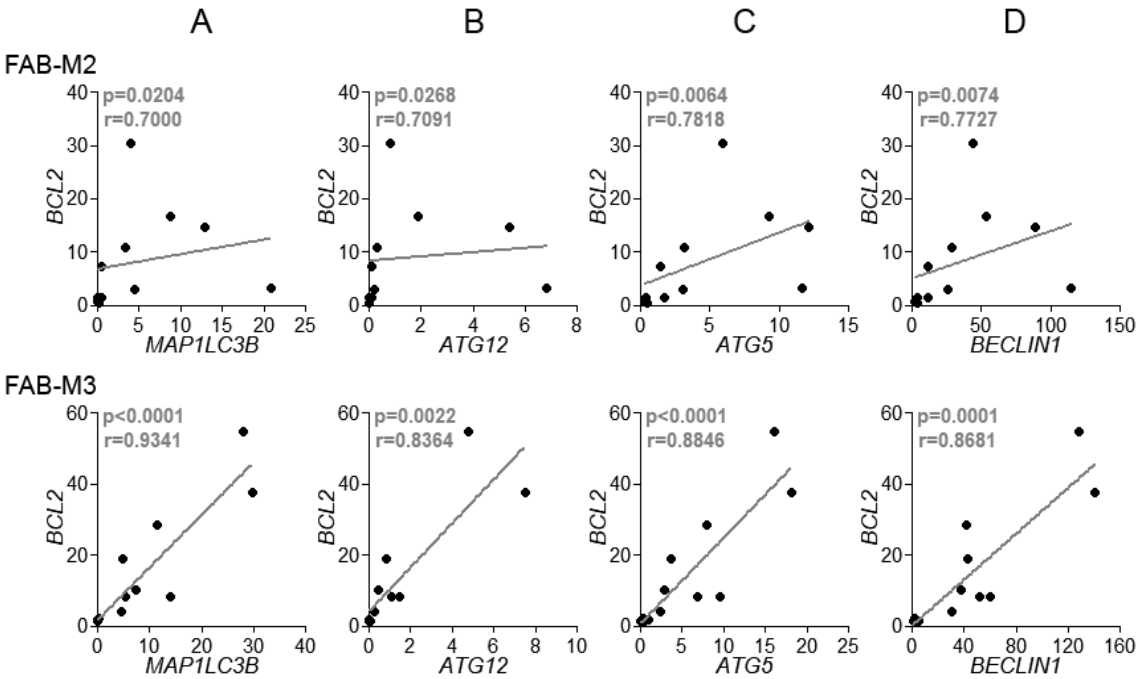

Fig. 21. FAB-M2 and FAB-M3 acute myeloid leukemia patients exhibit a significant positive correlation between the mRNA expression levels of *BCL2* and (A) *MAP1LC3B*, (B) *ATG12*, (C) *ATG5* or (D) *BECLIN1*. Mononuclear cells (MNCs) were isolated from the bone marrow (BM) samples of 27 individuals diagnosed with distinct subtypes of acute myeloid leukemia (AML), distributed according to the French-American-British (FAB) classification system as FAB-M2: n=11 and FAB-M3: n=16. mRNA was then extracted from the bone marrow mononuclear cells (BM-MNCs) and the expression levels of the autophagy-related genes *MAP1LC3B*, *ATG12*, *ATG5*, *BECLIN1* and *BCL2* determined by qPCR. The copy number gene expression was calculated by the standard quantity copy number curve, previous defined for each gene. The Spearman's rank correlation method was then applied to determine the strength of association between the mRNA expression levels of *BCL2* and *MAP1LC3B*, *ATG12*, *ATG5* or *BECLIN1*. A significant positive correlation was obtained in all tested conditions: FAB-M2 (*BCL2*/*MAP1LC3B*: r=0.7000, p=0.0204; *BCL2*/*ATG12*: r=0.7091, p=0.0268; *BCL2*/*ATG5*: r=0.7818, p=0.0064; *BCL2*/*BECLIN1*: r=0.7727, p=0.0074) and FAB-M3 (*BCL2*/*MAP1LC3B*: r=0.9341, p<0.0001; *BCL2*/*ATG12*: r=0.8364, p=0.0022; *BCL2*/*ATG5*: r=0.8846, p<0.0001; *BCL2*/*BECLIN1*: r=0.8681, p=0.0001).

Results herein obtained with AML patients diagnosed and treated at IPO-Porto from 2005 to 2014 propose a differential autophagic signature among distinct FAB AML subtypes, exposing the relevance of clustering and analyzing AML according to its subtype. The stratification of AML may therefore allow not only remarkable advances in the understanding of the AML pathogenesis but also the development of molecularly targeted and effective therapies.

3.4.2.3. Expression of autophagy-related genes based on the cytogenetic risk group or karyotype of acute myeloid leukemia

Although the FAB classification system is still currently incorporated in the AML treatment protocols of several cooperative study groups for patient stratification purposes, it is falling into disuse and

being replaced by the World Health Organization (WHO) classification [23, 24]. The latter takes into account several parameters that are not considered by the FAB classification system and that allow the design of more targeted and effective AML treatments, such as cytogenetic and immunophenotypic features, molecular genetic studies and patient's clinical data [23, 24]. The AML patients enrolled in this retrospective cohort study were classified using the FAB classification system, making it impossible to characterize autophagy according to the WHO classification. Nevertheless, the expression of autophagy-related genes was evaluated based on the cytogenetic risk group or karyotype. When the AML patients were categorized according to the cytogenetic risk group into favorable (F), intermediate I (I), intermediate II (II) and adverse (A) (Table 4), the BM-MNCs of the favorable cytogenetic risk group displayed a trend towards increased *MAP1LC3B* (Fig. 22A), *ATG12* (Fig. 22B), *ATG5* (Fig. 22C), *BECLIN1* (Fig. 22D) and *BCL2* (Fig. 22E) gene expression when compared to the BM-MNCs of the other tested cytogenetic risk groups. Although without statistical differences, a reduced autophagy-related genes expression was clearly noticed in the BM-MNCs of the intermediate II cytogenetic risk group (Fig. 22). A similar *MAP1LC3B*, *ATG12*, *ATG5*, *BECLIN1* and *BCL2* gene expression was also detected between the BM-MNCs of the intermediate I and adverse cytogenetic risk groups (Fig. 22). Data propose therefore a differential expression of core autophagy genes among distinct cytogenetic risk groups, with the BM-MNCs of the favorable and intermediate II cytogenetic risk groups exhibiting the highest and lowest autophagy-related genes profile, respectively. In line with these observations, Zare-Abdollahi, D. *et al.* revealed a higher *BECLIN1* gene expression in the BM-MNCs of the favorable cytogenetic risk group than in the BM-MNCs of the intermediate (I+II) and adverse cytogenetic risk groups, which displayed a similar *BECLIN1* gene expression among them [201]. Interestingly, when the AML patients described in Table 4 were only categorized into favorable, intermediate (I+II) and adverse cytogenetic risk groups, an identical *BECLIN1* gene expression was also found between the BM-MNCs of the intermediate (I+II) and adverse cytogenetic risk groups (Mean: I+II - 38.89; A - 41.40). A similar expression was also obtained for all the other tested autophagy-related genes (*MAP1LC3B*: I+II - 5.25, A - 5.16; *ATG12*: I+II - 1.58, A - 1.69; *ATG5*: I+II - 4.29, A - 4.51; *BCL2*: I+II - 13.31, A - 15.29). These findings clearly illustrate the need to dissect AML into several cytogenetic risk groups, by showing relevant differences in the expression of autophagy-related genes between the intermediate I and intermediate II cytogenetic risk groups, which have often been studied as a single group. By clustering the AML individuals into favorable and adverse cytogenetic risk groups, Liang, P. Q., *et al.* reported a trend towards increased *MAP1LC3B*,

BECLIN1 and *BCL2* gene expression in the BM-MNCs of the favorable cytogenetic risk group [191], corroborating the results herein obtained (Fig. 22A, D, E). Curiously, functional studies performed by Folkerts, H. *et al.* revealed higher autophagy levels in the AML cells of the adverse cytogenetic risk group than in the AML cells of the intermediate (I+II) and favorable cytogenetic risk groups [202]. A trend towards augmented autophagy levels was also described in the AML cells of the intermediate (I+II) cytogenetic risk group when compared to the AML cells of the favorable cytogenetic risk group [202].

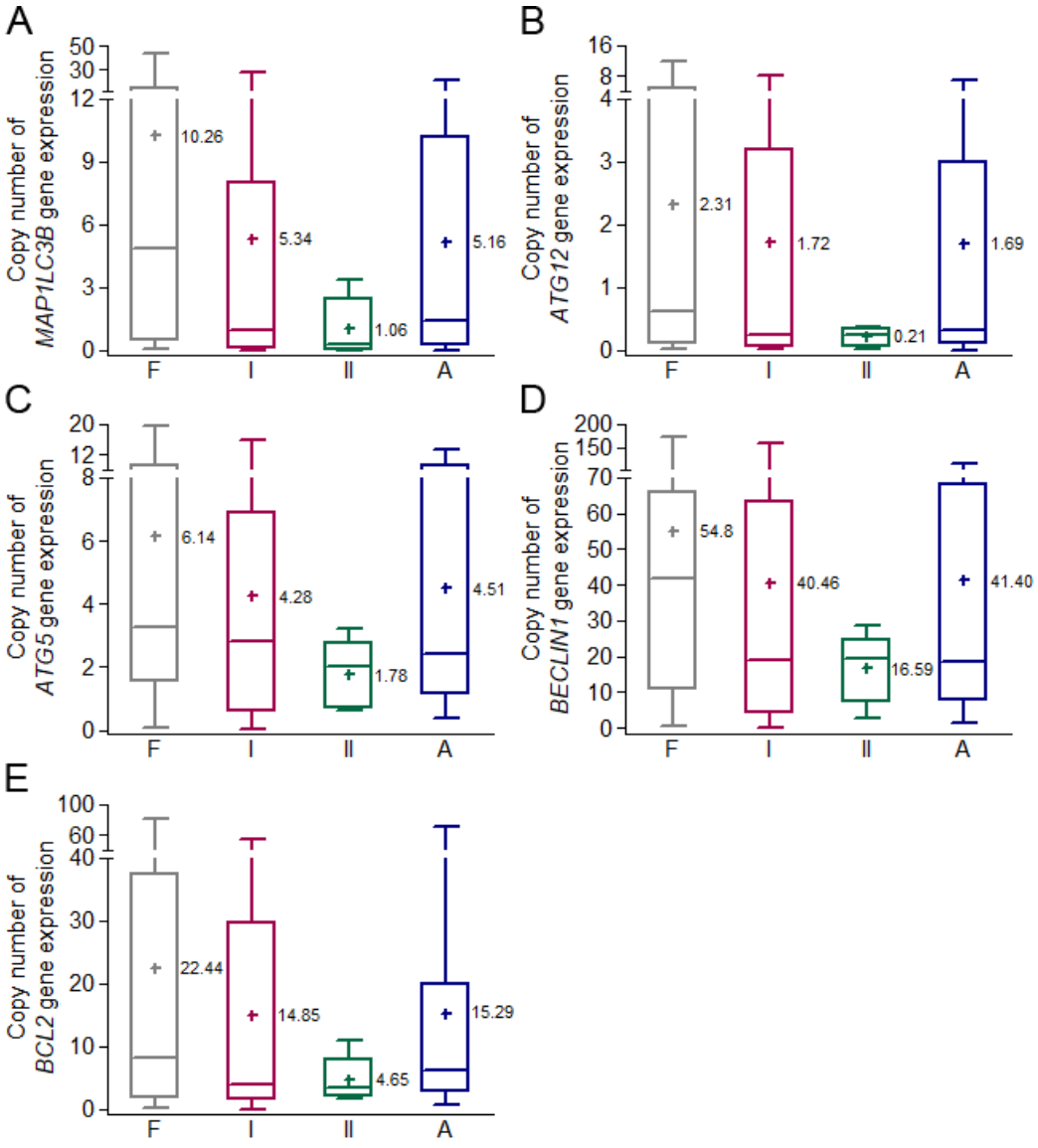

Fig. 22. Acute myeloid leukemia individuals with different cytogenetic risk groups present a distinct autophagy-related genes expression pattern. Mononuclear cells (MNCs) were isolated from the bone marrow (BM) samples of patients with acute myeloid leukemia (AML). mRNA was then extracted from the bone marrow mononuclear cells (BM-MNCs) and the expression levels of the autophagy-related genes (A) *MAP1LC3B*, (B) *ATG12*, (C) *ATG5*, (D) *BECLIN1* and (E) *BCL2* were determined by qPCR. BM samples from a total of 80 AML subjects, distributed according to the cytogenetic risk group as Favorable (F): 24, Intermediate I (I): 29, Intermediate II (II); 7 and Adverse (A): 20, were enrolled in this study. The copy number gene expression was calculated by the standard quantity copy number curve, previous defined

for each gene. One-way ANOVA and Dunns post hoc test were used to compare the mRNA expression levels of the *MAP1LC3B*, *ATG12*, *ATG5*, *BECLIN1* and *BCL2* between the studied groups. The mean is shown as "+" and the respective value (*MAP1LC3B*: F=10.26 vs I=5.34 vs II=1.06 vs A=5.16; *ATG12*: F=2.31 vs I=1.72 vs II=0.21 vs A=1.69; *ATG5*: F=6.14 vs I=4.28 vs II=1.78 vs A=4.51; *BECLIN1*: F=54.80 vs I=40.46 vs II=16.59 vs A=41.40; *BCL2*: F=22.44 vs I=14.85 vs II=4.65 vs A=15.29).

When the AML patients were stratified according to the karyotype into normal and abnormal (Table 4), differences in the expression of core autophagy genes were revealed (Fig. 23A-E). Indeed, a higher expression of the *MAP1LC3B* (Fig. 23A) and *ATG5* (Fig. 23C) autophagy-associated genes was found in the BM-MNCs of the abnormal karyotype than in the BM-MNCs of the normal karyotype. A trend towards augmented *BECLIN1* gene expression was also noticed in the BM-MNCs of the abnormal karyotype in comparison to the BM-MNCs of the normal karyotype (Fig. 23D). A similar *ATG12* (Fig. 23B) and *BCL2* (Fig. 23E) gene expression was observed between the tested groups. Overall, the results herein obtained indicate an increased autophagic signature in the AML individuals with abnormal karyotype when compared to those with normal karyotype. Interestingly, by using AML blasts isolated from the BM-MNCs of AML subjects, Folkerts, H. *et al.* described a higher autophagy flux in patients with abnormal karyotype than with normal karyotype [202]. The authors proposed that the high autophagy flux displayed by AML cells might be an intrinsec property to cope with constitutive metabolic stress linked to the genetic alterations [202]. Data herein presented emphasize that differences in the clinical characteristics of AML patients, as karyotype classification, should be considered in their evaluation and management to develop personalized therapies and to benefit patient outcomes.

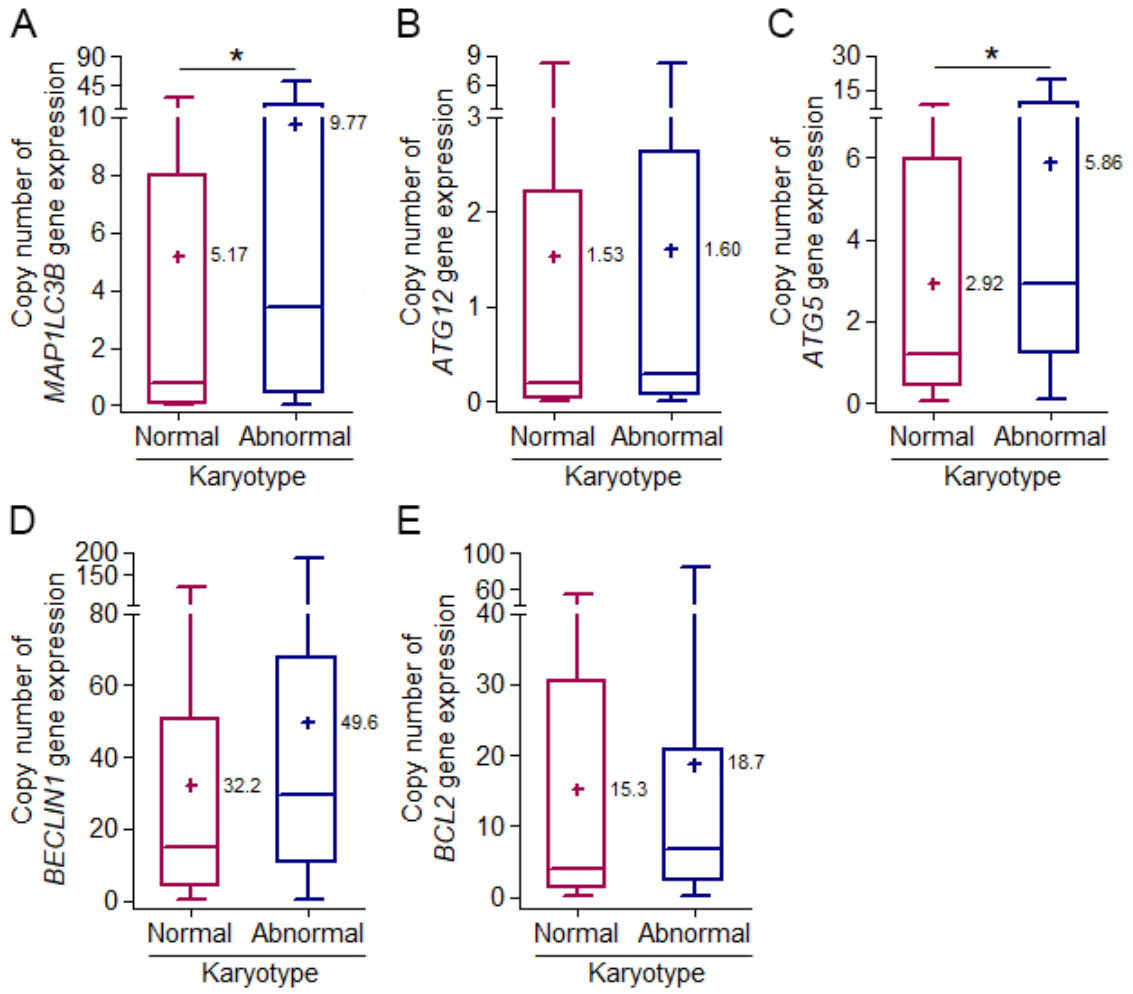

Fig. 23. Acute myeloid leukemia individuals with abnormal karyotype present increased expression of core autophagy genes. Mononuclear cells (MNCs) were isolated from the bone marrow (BM) samples of patients with acute myeloid leukemia (AML). mRNA was then extracted from the bone marrow mononuclear cells (BM-MNCs) and the expression levels of the autophagy-related genes (A) *MAP1LC3B*, (B) *ATG12*, (C) *ATG5*, (D) *BECLIN1* and (E) *BCL2* were determined by qPCR. BM samples from a total of 76 AML subjects, distributed according to the karyotype as normal (40) and abnormal (36), were enrolled in this study. The copy number gene expression was calculated by the standard quantity copy number curve, previous defined for each gene. Student's t-test and Mann-Whitney post hoc test were used to compare the mRNA expression levels of the *MAP1LC3B*, *ATG12*, *ATG5*, *BECLIN1* and *BCL2* between the normal and abnormal groups. *p <0.05. The mean is shown as "+" and the respective value (*MAP1LC3B*: Normal=5.17 vs Abnormal=9.77; *ATG12*: Normal=1.53 vs Abnormal=1.60; *ATG5*: Normal=2.92 vs Abnormal=5.86; *BECLIN1*: Normal=32.2 vs Abnormal=49.6; *BCL2*: Normal=15.3 vs Abnormal=18.7).

The *in silico* analysis presented in this section reinforces the clinical heterogeneity of AML, by showing a differential expression of essential autophagy genes among distinct cytogenetic risk groups or karyotypes. Indeed, while the BM-MNCs of the intermediated II cytogenetic risk group seem to display the lowest expression of autophagy-related genes, the BM-MNCs of the favorable cytogenetic risk group appear to exhibit the highest autophagy gene profile. The BM-MNCs of AML

patients with abnormal karyotype also present higher expression of autophagy-associated genes than the BM-MNCs of AML patients with normal karyotype.

Data obtained in this chapter clearly indicate the need of taking into consideration several clinical parameters in the AML context, supporting the relevance of looking at AML as a highly heterogeneous group of hematological disorders.

CHAPTER 4

Human bone marrow mesenchymal stromal cells under high glucose concentrations: impact on the tumorigenicity of distinct acute myeloid leukemia cell types

4.1. Abstract

Acute myeloid leukemia (AML) is an aggressive and rapidly lethal blood cancer that, if untreated, has a median survival of 3 months or less. The interplay between AML cells and bone marrow mesenchymal stromal cells (BM-MSCs) has been implicated in the AML development, progression and therapy resistance. Epidemiological data have also shown an increased incidence of AML in patients with type 2 diabetes *mellitus* (hereinafter called DM), which has been identified as promoting disturbances in the BM-MSCs function. The present work aimed to clarify the impact of DM-induced changes in the BM-MSCs on the development and progression of distinct subtypes of AML. Three different human AML cell lines representative of three distinct AML subtypes, HL-60 (FAB-M2 AML), NB-4 (FAB-M3 AML) and KG-1 (FAB-M6 AML), were acutely and chronically exposed to the conditioned medium (CM) produced by non-diabetic human BM-MSCs under regular or high glucose levels (RG or HG, respectively). An augmented tumorigenic phenotype was displayed by the different tested AML cell types upon chronic exposure to the CM-HG, proposing that in response to elevated glucose concentrations the BM-MSCs change their secretome and/or extracellular vesicles (EVs) profile by releasing soluble signaling molecules and/or EVs that, upon prolonged contact, increase the tumorigenicity of distinct AML cell types. A higher tumorigenic profile was also exhibited by NB-4 cells followed by HL-60 and KG-1 cells upon long-term exposure to the CM-HG, indicating that the soluble factors and/or EVs secreted by the BM-MSCs under high glucose levels have a differential impact on the tumorigenicity of distinct AML cell types by favoring those with increased glycolytic metabolism. The results herein obtained indicate that chronic exposure to the alterations promoted by high glucose levels in the BM-MSCs secretome and/or BM-MSCs-derived EVs profile contributes to the development and progression of different AML subtypes, in a cell type-dependent manner. These data provide evidence for a positive impact of metabolic disorders, as DM, on the pathogenesis of distinct AML subtypes.

Keywords: Acute myeloid leukemia (AML) ▪ Diabetes *mellitus* (DM) ▪ Hematopoietic niche ▪ Bone marrow mesenchymal stromal cells (BM-MSCs) ▪ Cancer cells tumorigenicity.

4.2. Introduction

Acute myeloid leukemia (AML) is a fatal disorder that, if untreated, has a median survival of 3 months or less, being the early diagnosis and treatment imperative to obtain better outcomes [8, 10]. The basis for the current AML treatment was developed more than 40 years ago and consists in the combination of an anthracycline antibiotic, such as doxorubicin, with high doses of a cytosine

analog, such as cytarabine [155-157]. While young patients tolerate intensified therapeutic regimens and have good outcomes, the AML treatment is highly toxic and presents limited application and poor outcomes among old individuals, the most affected population [155-157]. Yet, due to the lack of a better therapeutic strategy and given that if untreated AML is rapidly fatal, this approach remains the worldwide AML gold standard of care [155-157]. Accordingly, the elucidation of the mechanisms underlying AML development, progression and chemoresistance is fundamental to develop more effective and targeted therapies.

The interaction between AML cells and the bone marrow (BM) microenvironment has been extensively implicated in the survival, proliferation and drug resistance of the leukemic cells [203-211]. Indeed, the communication between AML cells and the surrounding BM mesenchymal stromal cells (BM-MSCs), either through physic contact and/or paracrine signaling, has been described as up-regulating multiple survival, proliferative and/or anti-apoptotic signaling pathways in the AML cells [203, 205-207, 210, 211]. This crosstalk has also been referred as promoting the adhesion/homing of AML cells within the BM niche, which protects the leukemic cells from chemotherapy conferring a drug-resistance phenotype [204, 205, 208-210]. The leukemic stem cells sheltered within the BM microenvironment have also been identified as giving rise to persistence of minimal residual disease, which in turn, contributes to the relapse of AML patients after a variable period of remission [204]. The BM comprises therefore a dynamic network of growth factors, cytokines and stromal cells that provide a permissive environment for the AML development, progression and therapy resistance as well as for the AML patients relapse. Thus, the interplay between AML cells and the adjacent BM-MSCs is of utmost importance in the AML scenario.

By performing a meta-analysis of observational studies, Castillo, J. J. and co-workers reported an increased incidence of hematological malignancies, namely AML, in patients with type 2 diabetes *mellitus* (hereinafter called DM) [212], a metabolic disorder characterized by chronic hyperglycemia [213] that affects millions of people worldwide [214, 215]. It was also concluded that patients who develop leukemia after a pre-condition of DM were associated with a poorer AML prognosis [212]. In the context of chronic lymphocytic leukemia (CLL), Seymour, E. K. *et al.*, by performing a retrospective cohort study, also described a shorter disease-specific survival and a shorter overall survival in patients with both CLL and DM when compared to CLL patients without DM, identifying DM as a predictor of poor outcome in the context of this hematological malignancy [216]. However, to date, no clear association was established between the presence of DM and

the development, progression and chemoresistance of hematological malignancies, namely AML. Nevertheless, it is well known that DM severely affects the function of several organs, namely BM [217]. Indeed, by using a mouse model of DM, Ferraro, F. *et al.* showed an impaired egress of hematopoietic stem and progenitor cells (HSPCs) from the BM of these animals as result of DM-induced changes in the BM niche [218]. Interestingly, by performing a retrospective analysis of BM transplant patient records, Ferraro, F. *et al.* also found an elevated correlation between DM and diminished HSPCs mobilization [218]. A reduced egress of endothelial progenitor cells (EPC) from the BM to the circulation was also verified by Westerweel, P.E. *et al.* in diabetic mice as response to DM-promoted disturbances in the BM stromal compartment [219]. Keats, E. *et al.* also revealed a detrimental impact of hyperglycemia in human BM-MSCs, by showing their reduced growth and aberrant differentiation (enhanced adipogenesis as well as impaired chondrogenesis and osteogenesis) in response to *in vitro* high glucose concentrations [220]. A prolonged exposure to elevated glucose levels was also extensively implicated in the premature senescence, genomic instability and telomere changes of BM-MSCs [221-225]. It is therefore critical to elucidate the relevance of diabetes-induced alterations in the BM microenvironment on the development, progression and drug resistance of AML.

Results herein obtained suggest that prolonged exposure to the soluble factors and/or extracellular vesicles (EVs) secreted by the BM-MSCs under high glucose levels contributes to the development and progression of distinct AML subtypes, by favoring those with augmented glycolytic profile. Indeed, upon chronic exposure to the conditioned medium produced by non-diabetic human BM-MSCs under high glucose levels, NB-4 cells, a glycolysis-dependent AML cell type, and KG-1 cells, an OXPHOS-dependent AML cell type, exhibited the highest and lowest tumorigenic phenotype, respectively. HL-60 cells, a moderate glycolysis-dependent AML cell type, displayed an intermediate tumorigenic profile.

4.3. Material and methods

4.3.1. Cell cultures

4.3.1.1. Human bone marrow mesenchymal stromal cells

Mesenchymal stromal cells (MSCs) were isolated from non-diabetic human bone marrow (BM) samples collected during a routine cardiac surgery at Hospital da Arrábida - Porto from 2014 to 2016 (BM samples are included in the control cohort referred in chapter 3). Briefly, mononuclear cells (MNCs) were isolated from the BM samples using the standard density gradient centrifugation,

as referred in section 3.3.2, and cultured in Dulbecco's Modified Eagle Medium (DMEM) containing 5mM of D-glucose (Gibco®) and supplemented with 20% heat-inactivated fetal bovine serum (FBS) (Biochrom® - Merck Millipore) and 1% antibiotic-antimycotic solution (Invitrogen®) in a humidified, 37°C, 5% CO_2 atmosphere. The nonadherent cells were removed upon 7 days of culture. At 70-80% of cell confluence, the adherent cells (BM-MSCs) were trypsinized with Trypsin-EDTA solution (Gibco®) and further expanded. BM-MSCs with 3 to 5 passages were used for the experimental approaches presented in this chapter.

4.3.1.2. Human acute myeloid leukemia cell lines

Three different human acute myeloid leukemia (AML) cell lines representative of three distinct AML subtypes, NB-4 (FAB-M3 AML), HL-60 (FAB-M2 AML) and KG-1 (FAB-M6 AML), were used in this work (detailed characteristics of the tested AML cell lines are described in section 2.3.1). NB-4, HL-60 and KG-1 cell lines were obtained from the German Collection of Microorganisms and Cell cultures (DSMZ® - Deutsche Sammlung von Mikroorganismen und Zellkulturen - German). Cells were maintained in Roswell Park Memorial Institute (RPMI) 1640 medium (Biochrom® - Merck Millipore) supplemented with 10% heat-inactivated FBS (Biochrom® - Merck Millipore) and 1% antibiotic-antimycotic solution (Invitrogen®) in a humidified, 37°C, 5% CO_2 atmosphere. AML cells with 5 to 20 passages were used for the experimental approaches presented in this chapter.

4.3.2. Production of conditioned medium by human bone marrow mesenchymal stromal cells

The resulting medium from the BM-MSCs culture is called conditioned medium (CM), which contains a broad spectrum of BM-MSCs-secreted soluble factors, such as cytokines, chemokines and growth factors, as well as, BM-MSCs-derived extracellular vesicles (EVs) containing proteins, mRNAs and miRNAs [226].

Non-diabetic human BM-MSCs were resuspended in DMEM containing regular (5mM) or high (25mM) levels of D-glucose (Gibco®) and supplemented with 20% FBS (Biochrom® - Merck Millipore) and 1% antibiotic-antimycotic solution (Invitrogen®). Upon 4 days of incubation in a humidified, 37ºC and 5% CO_2 atmosphere, the cell culture medium (conditioned medium; CM) was collected, filtered and stored at 4ºC. The CM produced by the non-diabetic human BM-MSCs under regular or high glucose levels (CM-RG or CM-HG, respectively) was thus obtained. A schematic representation of the CM production is illustrated in Fig. 24.

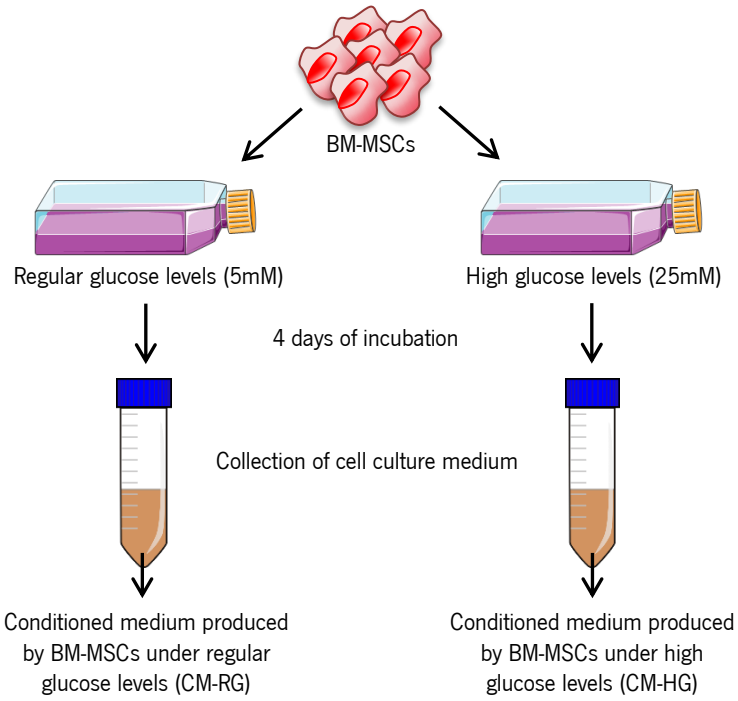

Fig. 24. Schematic representation of the conditioned medium production by human bone marrow mesenchymal stromal cells. Non-diabetic human bone marrow mesenchymal stromal cells (BM-MSCs) were resuspended in DMEM containing regular (5mM) or high (25mM) glucose levels and subsequently incubated for 4 days in a humidified, 37ºC and 5% CO_2 atmosphere. The cell culture medium (conditioned medium) was then collected, filtered and stored at 4ºC. The conditioned medium (CM) produced by the non-diabetic human BM-MSCs under regular or high glucose levels (CM-RG or CM-HG, respectively) was thus obtained.

4.3.3. Assessment of acute myeloid leukemia cells tumorigenicity

4.3.3.1. Measurement of cell viability

NB-4, HL-60 and KG-1 cells were resuspended in the CM-RG or CM-HG. AML cells resuspended in DMEM containing regular (5mM) or high (25mM) glucose levels (DMEM-RG or DMEM-HG, respectively) were also tested. NB-4, HL-60 and KG-1 cells were then plated at $0.5x10^6$ cells/mL/well and incubated for 2, 4 and 7 days in a humidified, 37ºC and 5% CO_2 atmosphere. Upon the incubation periods, the number of viable cells was counted using the trypan blue dye exclusion assay. At least, three independent biological replicates were performed. The number of viable cells is shown as absolute values.

4.3.3.2. Determination of migration capacity

4.3.3.2.1. Acute exposure model

NB-4, HL-60 and KG-1 cells were starved overnight in starvation medium (DMEM containing 5mM of glucose with no FBS and 0.5% BSA; Sigma-Aldrich®). AML cells ($3x10^5$ cells in 100µL) were

then added to the top chamber of 24-transwell culture inserts with 8µm pore size (Biosciences®), which were placed in wells containing 500µL of CM-RG, CM-HG, DMEM-RG or DMEM-HG. NB-4, HL-60 and KG-1 cells were subsequently incubated for 24h in a humidified, 37ºC and 5% CO_2 atmosphere. The AML migrating cells were finally collected and counted using the trypan blue dye exclusion method. At least, three independent biological replicates were performed. The number of migrating cells is shown as absolute values. A schematic representation of the acute exposure model is shown in Fig. 25.

4.3.3.2.2. Chronic/prolonged exposure model

NB-4, HL-60 and KG-1 cells were pre-exposed for 7 days to CM-RG, CM-HG, DMEM-RG or DMEM-HG. Upon this incubation period (not applied to the acute exposure model), the remaining experimental procedure was performed as described for the acute exposure model. At least, three independent biological replicates were performed. The number of migrating cells is shown as absolute values. A schematic representation of the chronic exposure model is illustrated in Fig. 25.

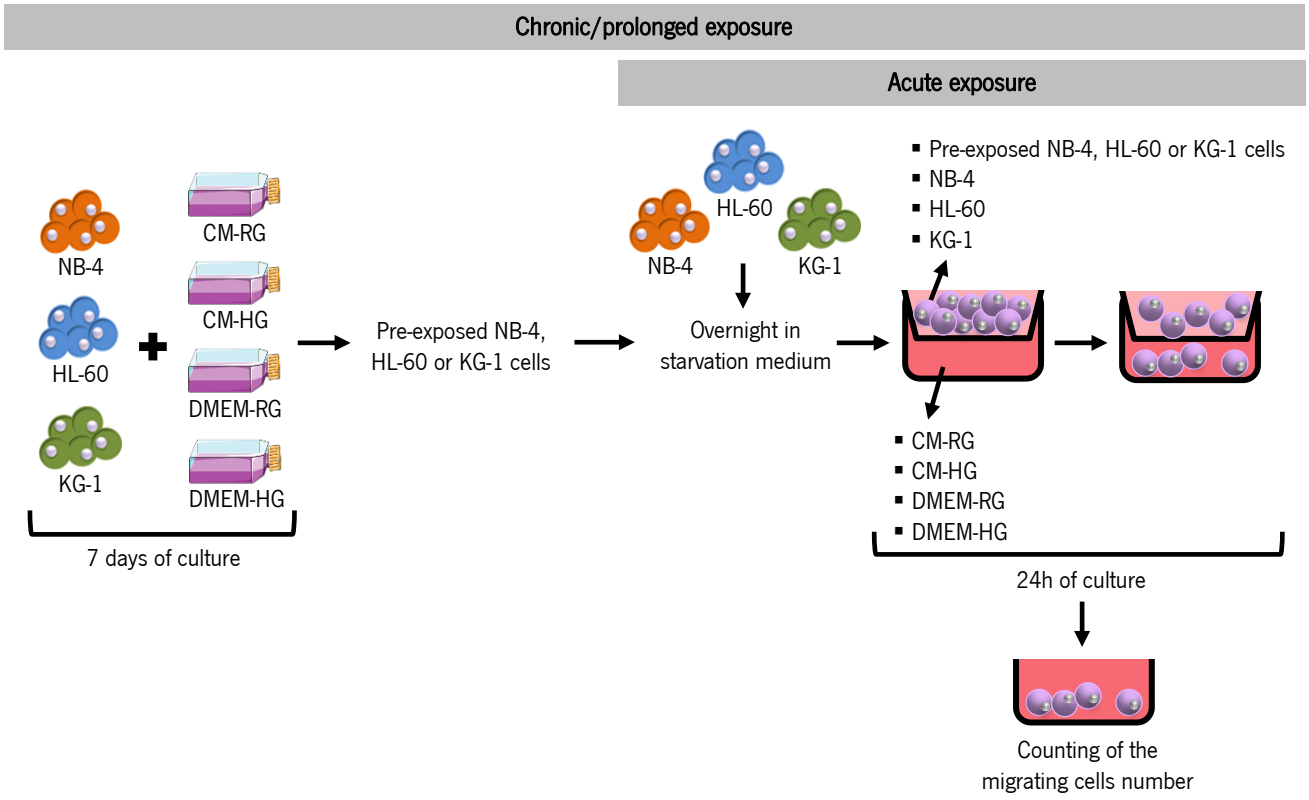

Fig. 25. Schematic representation of the acute and chronic exposure models used to determine the migratory capacity of distinct acute myeloid leukemia cell types. In the acute exposure scenario, NB-4, HL-60 or KG-1 cells were starved overnight in starvation medium and subsequently added to the top chamber of 24-transwell culture inserts which were placed in wells containing different culture media: conditioned medium produced by non-diabetic human bone marrow

mesenchymal stromal cells (BM-MSCs) under regular glucose levels (CM-RG), conditioned medium produced by non-diabetic human BM-MSCs under high glucose levels (CM-HG), DMEM with regular glucose levels (DMEM-RG) or DMEM with high glucose levels (DMEM-HG). Upon 24h of culture, the number of NB-4, HL-60 or KG-1 migrating cells was counted. In the chronic/prolonged exposure model, NB-4, HL-60 or KG-1 cells were pre-exposed for 7 days to CM-RG, CM-HG, DMEM-RG or DMEM-HG and then submitted to the same experimental approach described for the acute exposure model.

4.3.4. Isolation of acute myeloid leukemia cells-derived extracellular vesicles by differential ultracentrifugation

Extracellular vesicles (EVs) were isolated from the conditioned medium (CM) of HL-60 or KG-1 cells upon 24h of culture via differential ultracentrifugation, as described by Lasser, C. and co-workers [227]. To remove cellular debris and larger particles, the supernatants were filtered with a 0.22μm filter unit and then ultracentrifuged at 120.000g for 70min. The resultant pellets were washed with phosphate-buffered saline (PBS) and, after a second ultracentrifugation, the EVs derived from HL-60 or KG-1 cells were resuspended in PBS for subsequent characterization by immunoblotting analysis and nanotracking analysis (NTA).

4.3.5. Characterization of acute myeloid leukemia cells-derived extracellular vesicles

4.3.5.1. Immunoblotting analysis

HL-60 and KG-1 cells-derived EVs as well as HL-60 and KG-1 cells were lysed with radioimmunoprecipitation assay (RIPA) buffer (10mM Tris-HCl at pH 7.4, 150mM NaCl, 1mM EDTA, 0.1% SDS, 1% Triton X-100 and 1% sodium deoxycholate) supplemented with Complete Protease Inhibitor Mixture tablets (Roche Diagnostics). Protein concentration was then determined using the Pierce™ BCA Protein Assay Kit (Thermo Fisher Scientific®). 20μg of the total protein were resolved in a 8% sodium dodecyl sulfate (SDS) polyacrylamide gel and electrophoretically transferred onto polyvinylidene fluoride (PVDF) membranes using the Trans Blot protein transfer system (Bio-Rad®). Membranes were blocked for 1h in tris-buffered saline (TBS) with 0.1% tween 20 (TBS-T) containing 5% non-fat milk and afterwards incubated overnight at 4°C with the polyclonal primary antibodies at 1:1000 in 1% non-fat milk - Mouse anti-Alix antibody (Cell Signaling Technology®), Goat anti-CD63 antibody (SICGEN), Goat anti-Calnexin antibody (SICGEN), Rabbit anti-Flotilin-1 antibody (Santa Cruz Biotechnology®) and Goat anti-GAPDH antibody (SICGEN). After washing with TBS-T, membranes were incubated with the respective secondary antibodies, IgG anti-Mouse antibody (Bio-Rad®) for Alix, IgG anti-Rabbit antibody (Bio-Rad®) for Flotilin-1 and IgG anti-Goat antibody (Bio-Rad®) for all the others, at 1:5000 in 1% non-fat milk for 1h at room

temperature. Protein levels were detected after incubation with Clarity Western ECL Substrate (Bio-Rad®) or SuperSignal West Femto Maximum Sensitivity Substrate (Thermo Fisher Scientific®). Digital images were obtained in the ImageQuant™ LAS 500 System (GE Healthcare®). One independent biological replicate was performed.

4.3.5.2. Nanotracking analysis (measurement of particle size and concentration)

EVs isolated from the CM of HL-60 or KG-1 cells were resuspended in 1mL of PBS. NTA was subsequently performed using the NanoSight LM 10 instrument (NanoSight Ltd). The analysis settings were optimized and kept constant between samples and each video was analyzed to give the mean size and estimated concentration of particles. Data were processed using the NTA 2.2 analytical software. One independent biological replicate was performed.

4.3.6. Statistical analysis

All data is reported as the mean ± standard error of the mean (SEM). Statistical analysis was performed using the one-way ANOVA and Tukey post hoc tests to compare the CM-HG/CM-RG or DMEM-HG/DMEM-RG ratios between the NB-4, HL-60 and KG-1 cells in what concerns the cell migration capacity in response to both acute and chronic exposure models. The two-away ANOVA and Bonferroni post hoc tests were used to compare the tested groups for all the other analysis. A *p* value lower than 0.05 was assumed to denote a significant difference. Statistical analysis was conducted using Prism software (GraphPad Software, San Diego, CA®).

4.4. Results and discussion

4.4.1. Long-term exposure to high glucose concentrations: impact on the tumorigenicity of acute myeloid leukemia cells

Type 2 diabetes *mellitus* (hereinafter called DM) is a metabolic disorder characterized by chronic/prolonged hyperglycemia [213] that has been assigned as a potential risk factor for the development and poorer prognosis of acute myeloid leukemia (AML) [212]. Indeed, data obtained by our group revealed a trend towards reduced overall survival (OS) and relapse-free survival (RFS) in patients with both AML and DM when compared to AML patients without DM (Fig. 26), pointing to DM as a predictor for worse outcome in the AML scenario, as reported by other studies [212].

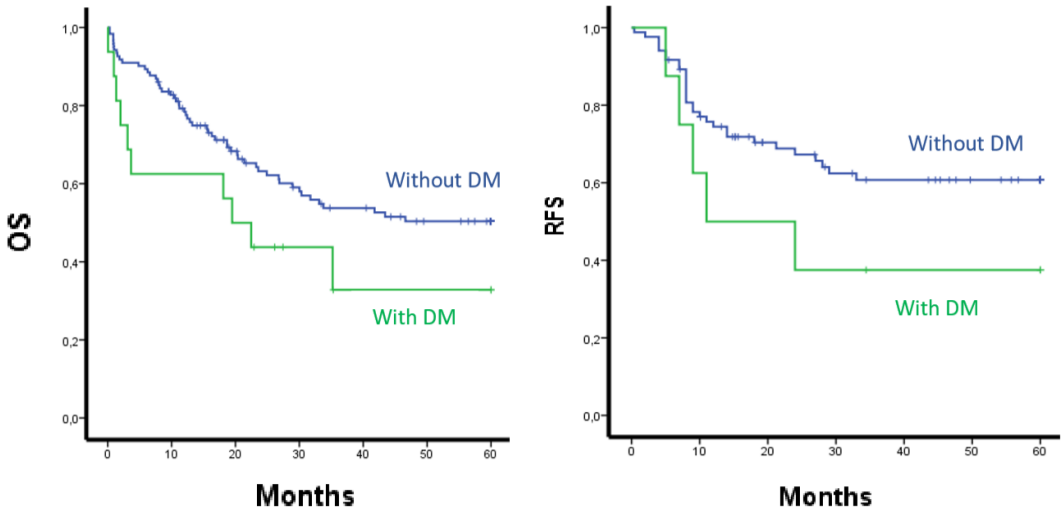

Fig. 26. Curves based on the Kaplan-Meier analysis to determine the impact of type 2 diabetes *mellitus* on the overall survival and relapse-free survival of acute myeloid leukemia patients. Number of acute myeloid leukemia (AML) cases included on the overall survival (OS) analysis: 122 cases without type 2 diabetes *mellitus* (DM) and 16 cases with DM; *p* value=0.090. Number of AML cases included on the relapse-free survival (RFS) analysis: 84 cases without DM and 8 cases with DM; *p* value=0.159. The AML patients enrolled in this study were diagnosed and treated at IPO-Porto from 2005 to 2014. Results published in the PhD thesis of Ângela Fernandes (*The functional crosstalk of proteolytic systems and metabolism in acute myeloid leukemia*, 2016, University of Minho).

Data obtained with different human AML cell lines representative of distinct AML subtypes, HL-60 (FAB-M2 AML), NB-4 (FAB-M3 AML) and KG-1 (FAB-M6 AML), revealed different energy requirements among the tested AML cell types, by showing a glycolytic phenotype for NB-4 cells, an oxidative metabolism for KG-1 cells and a glycolytic-oxidative intermediate state for HL-60 cells (Chapter 2; Fig. 8, 9). Altogether, results presented in Fig. 8, 9 and 26 highlight the need to clarify the impact of DM on the development and progression of distinct AML subtypes. NB-4, HL-60 and KG-1 cells were chronically exposed to DMEM containing high glucose levels (DMEM-HG), to mimic an *in vitro* condition of increased glucose concentrations, or regular glucose levels (DMEM-RG), to be used as control. Cell viability and *in vitro* migration capacity were then assessed to determine the AML cells tumorigenicity. A higher number of NB-4 and HL-60 viable cells was noticed in response to DMEM-HG than to DMEM-RG upon 2, 4 and 7 days of culture (Fig. 27A), pointing to elevated glucose concentrations as a beneficial condition for the survival and/or proliferation of AML cell types with augmented glycolytic dependence. Indeed, KG-1 cells, a non-glycolysis-dependent AML cell type, displayed a similar and even lower viability profile in response to DMEM-HG than to DMEM-RG (Fig. 27A). The positive impact of high glucose levels on the survival and/or proliferation of AML cell types with exacerbated glycolytic phenotype was supported by the ratio obtained between the number of AML viable cells in the DMEM-HG and in the DMEM-RG (DMEM-

HG/DMEM-RG) upon 2, 4 and 7 days of incubation, which was highest for NB-4 cells followed by HL-60 and KG-1 cells (Fig. 27B). An increased DMEM-HG/DMEM-RG ratio was also verified for NB-4 cells over the 7 days of culture (Fig. 27B), suggesting that chronic exposure to high glucose levels improves the survival and/or proliferation of AML cell types with elevated glycolytic metabolism. In agreement, KG-1 cells exhibited a reduced DMEM-HG/DMEM-RG ratio over the 7 days of incubation (Fig. 27B). Concerning the migration capacity of the tested AML cell types, a higher number of NB-4 and HL-60, but not KG-1, migrating cells was noticed upon prolonged exposure to DMEM-HG than to DMEM-RG (Fig. 27C, D), indicating that chronic exposure to elevated glucose concentrations preferentially improves the migration capacity of glycolysis-dependent AML cell types. These observations were reinforced by the ratio obtained between the number of AML migrating cells in the DMEM-HG and in the DMEM-RG (DMEM-HG/DMEM-RG), which was highest for NB-4 cells followed by HL-60 cells and finally KG-1 cells (Fig. 27E). Altogether, data herein obtained propose that long-term exposure to high glucose levels, as observed in DM, potentiates the tumorigenicity of different AML cell types, especially those with exacerbated glycolytic profile. Curiously, little is known about the role of chronic exposure to increased glucose concentrations on the tumorigenicity of hematological malignant cells, namely AML. Nevertheless, the long-term exposure to high glucose levels has been extensively described as beneficial for the tumorigenicity of innumerous solid tumor types [228-233]. Indeed, augmented proliferation, migration, drug-resistance as well as reduced apoptosis has been identified in breast [228, 229], colorectal [230], ovarian [231], pancreatic [232] and hepatocytes [233] cancer cells submitted to prolonged hyperglycemia.

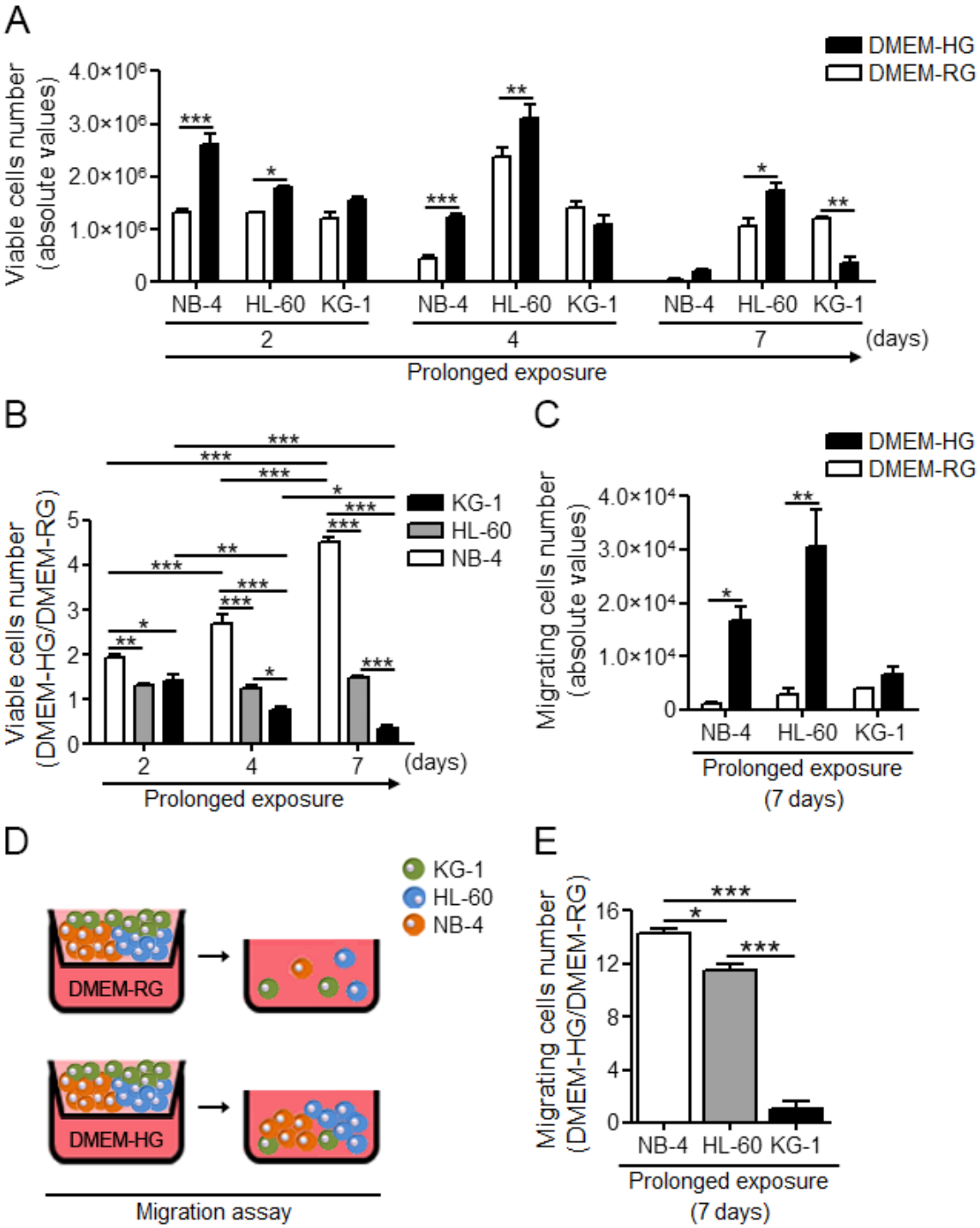

Fig. 27. Chronic exposure to culture medium containing high glucose levels promotes increased survival and/or proliferation as well as elevated migration capacity of NB-4 and HL-60 cells but not KG-1 cells. (A) NB-4, HL-60 and KG-1 cells were cultured in DMEM containing regular or high glucose levels (DMEM-RG or DMEM-HG, respectively) for 2, 4 and 7 days. Upon the incubation periods, cell viability was assessed by counting the number of viable cells using the trypan blue dye exclusion assay. The results are shown as mean+/-SEM of, at least, three independent biological replicates. Two-way ANOVA and Bonferroni post hoc test were used to compare the number of NB-4, HL-60 or KG-1 viable cells between the DMEM-RG and the DMEM-HG upon 2, 4 or 7 days of culture. *p <0.05; **p <0.01; ***p <0.001. (B) The ratio between the number of NB-4, HL-60 or KG-1 viable cells obtained in the DMEM-HG and in the DMEM-RG (DMEM-HG/DMEM-RG) upon 2, 4 or 7 days of incubation was calculated. The results are shown as mean+/-SEM of, at least, three independent biological replicates. Two-way ANOVA and Bonferroni post hoc test were used to

compare the DMEM-HG/DMEM-RG ratio between NB-4, HL-60 and KG-1 cells upon 2, 4 and 7 days of culture. *p <0.05; **p <0.01; ***p <0.001. (C) NB-4, HL-60 and KG-1 cells were pre-exposed to DMEM-RG or DMEM-HG for 7 days followed by an overnight starvation period. The migration assay was then performed for 24h, cells were added to the top chamber of 24-transwell culture inserts with 8μm pore size which were placed in wells containing DMEM-RG or DMEM-HG, and the number of migrating cells towards DMEM-RG or DMEM-HG was counted using the trypan blue dye exclusion assay. The results are shown as mean+/-SEM of, at least, three independent biological replicates. Two-way ANOVA and Bonferroni post hoc test were used to compare the number of NB-4, HL-60 or KG-1 migrating cells between the DMEM-RG and the DMEM-HG. *p <0.05; **p <0.01. (D) Schematic representation of the NB-4, HL-60 and KG-1 cells migration capacity upon prolonged exposure to DMEM-RG or to DMEM-HG. (E) The ratio between the number of NB-4, HL-60 or KG-1 migrating cells obtained in the DMEM-HG and in the DMEM-RG (DMEM-HG/DMEM-RG) was calculated. The results are shown as mean+/-SEM of, at least, three independent biological replicates. One-way ANOVA and Tukey post hoc test were used to compare the DMEM-HG/DMEM-RG ratio between NB-4, HL-60 and KG-1 cells. *p <0.05; ***p <0.001.

To better elucidate the relevance of long-term exposure to high glucose levels on the tumorigenicity of distinct AML cell types, the migration capacity of NB-4, HL-60 and KG-1 cells was assessed upon acute exposure to DMEM-RG or to DMEM-HG. A similar number of HL-60 and KG-1 migrating cells was noticed between the DMEM-RG and the DMEM-HG, while a trend towards augmented NB-4 migrating cells was detected in response to DMEM-HG than to DMEM-RG (Fig. 28A, B). In agreement, no statistical differences were observed between NB-4, HL-60 and KG-1 cells in what concerns the DMEM-HG/DMEM-RG ratio (Fig. 28C). Results indicate therefore that short-term exposure to elevated glucose concentrations has no major impact on the tumorigenicity of different AML cell types, highlighting the contribution of chronic exposure to the increased tumorigenicity of glycolysis-dependent AML cell types.

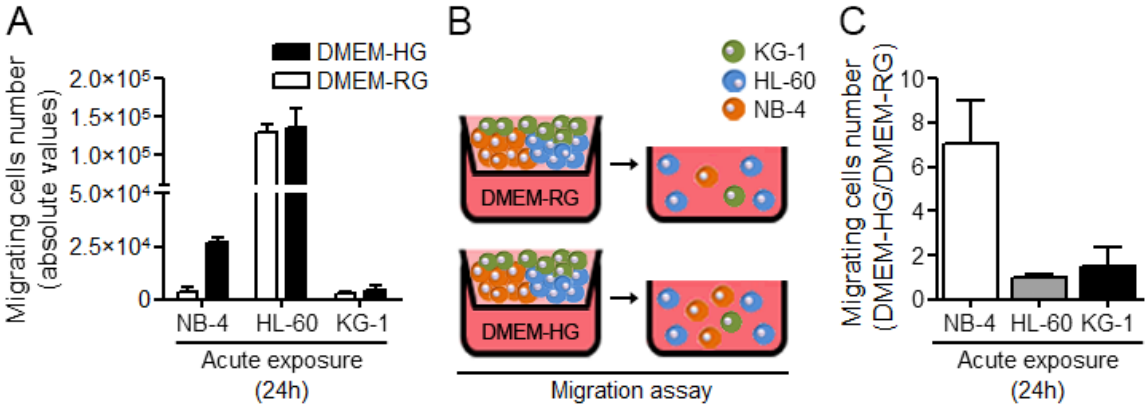

Fig. 28. Acute exposure to culture medium containing high glucose levels has no major impact on the migration capacity of distinct acute myeloid leukemia cell types. (A) NB-4, HL-60 and KG-1 cells were starved overnight in starvation medium. The migration assay was then performed for 24h, cells were added to the top chamber of 24-transwell culture inserts with 8μm pore size which were placed in wells containing DMEM with regular or high glucose levels (DMEM-RG or DMEM-HG, respectively), and the number of migrating cells towards DMEM-RG or DMEM-HG was counted using the trypan blue dye exclusion assay. The results are shown as mean+/-SEM of, at least, three independent biological replicates. Two-way ANOVA and Bonferroni post hoc test were used to compare the number of

NB-4, HL-60 or KG-1 migrating cells between the DMEM-RG and the DMEM-HG. (B) Schematic representation of the NB-4, HL-60 and KG-1 cells migration capacity upon acute exposure to DMEM-RG or to DMEM-HG. (C) The ratio between the number of NB-4, HL-60 or KG-1 migrating cells obtained in the DMEM-HG and in the DMEM-RG (DMEM-HG/DMEM-RG) was calculated. The results are shown as mean+/-SEM of, at least, three independent biological replicates. One-way ANOVA and Tukey post hoc test were used to compare the DMEM-HG/DMEM-RG ratio between NB-4, HL-60 and KG-1 cells.

Data presented in this section propose that chronic exposure to high glucose levels exerts a beneficial role on the development and progression of different AML subtypes, by favoring AML cell subsets with increased glycolytic phenotype.

4.4.2. Long-term exposure to conditioned medium produced by non-diabetic human bone marrow mesenchymal stromal cells under high glucose levels: impact on the tumorigenicity of acute myeloid leukemia cells

The bone marrow (BM) is the organ that hosts hematopoiesis and is therefore the hotspot for the development of hematopoietic disorders, namely AML [234]. The complex and dynamic crosstalk between the AML cells and the cellular components of the adjacent BM niche, namely BM mesenchymal stromal cells (BM-MSCs), has been widely recognized as playing a critical role in the AML development, progression and response to therapy [203-211]. Indeed, the BM stromal compartment has been claimed as a tumor sanctuary in which AML cells, either through physic contact and/or paracrine signaling, can acquire survival, proliferative and drug resistance phenotypes [203-211]. Interestingly, DM has not only been identified as a potential risk factor for the development and poorer prognosis of AML ([212] and Fig. 26) but also as a disturber of the BM-MSCs function [218-225]. It is therefore critical to elucidate the impact of DM-promoted alterations in the BM-MSCs on the development and progression of distinct AML subtypes. NB-4, HL-60 and KG-1 cells were chronically exposed to the conditioned medium (CM) produced by non-diabetic human BM-MSCs under high or regular glucose levels (CM-HG or CM-RG, respectively). Cell viability and *in vitro* migration capacity were then evaluated to determine the AML cells tumorigenicity. A higher number of NB-4, HL-60 and KG-1 viable cells was noticed in response to CM-HG than to CM-RG upon 2, 4 and 7 days of culture (Fig. 29A), proposing that in response to elevated glucose concentrations the BM-MSCs change their secretome and/or extracellular vesicles (EVs) profile by releasing soluble signaling molecules and/or EVs that up-regulate the survival and/or proliferation of distinct AML cell types. Nevertheless, these BM-MSCs-secreted soluble factors and/or -derived EVs appear to preferentially enhance the survival and/or proliferation of

AML cell types with augmented glycolytic metabolism, as showed by the ratio obtained between the number of AML viable cells in the CM-HG and in the CM-RG (CM-HG/CM-RG) upon 4 and 7 days of incubation, which was highest for NB-4 cells followed by HL-60 cells and ultimately KG-1 cells (Fig. 29B). An increased CM-HG/CM-RG ratio was also verified for NB-4 and HL-60 cells, but not for KG-1 cells, over the 7 days of culture (Fig. 29B), indicating that long-term exposure to the soluble factors and/or EVs released by the BM-MSCs under high glucose levels exerts a positive impact on the survival and/or proliferation of glycolysis-dependent AML cell types. Concerning the migration assay, a higher number of NB-4 and HL-60, but not KG-1, migrating cells was detected upon chronic exposure to the CM-HG than to the CM-RG (Fig. 29C, D), suggesting that in response to elevated glucose concentrations the BM-MSCs release soluble signaling molecules and/or EVs that, upon prolonged contact, promote the attraction of different AML cell types, mainly those with exacerbated glycolytic dependence. This theory was supported by the ratio obtained between the number of AML migrating cells in the CM-HG and in the CM-RG (CM-HG/CM-RG), which was highest for NB-4 cells followed by HL-60 cells and finally KG-1 cells (Fig. 29E). Knowing that the BM-MSCs are placed within the BM microenvironment, these results indicate that AML cell types with augmented glycolytic signature may be easily attracted/retained into the BM niche under a chronic hyperglycemia scenario. Notice that the adhesion/homing of AML cells within the BM niche contributes to their increased survival, proliferative, anti-apoptotic and/or drug resistance phenotypes [204, 205, 208-210]. Altogether, data herein obtained suggest that CM from BM-MSCs grown in high glucose levels contains soluble signaling molecules and/or EVs that, upon long-term exposure, improve the tumorigenicity of AML cells in a cell type-dependent manner. To the best of our knowledge, this is the first study trying to understand the impact of high glucose-induced disturbances in the BM-MSCs on the development and progression of distinct AML subtypes.

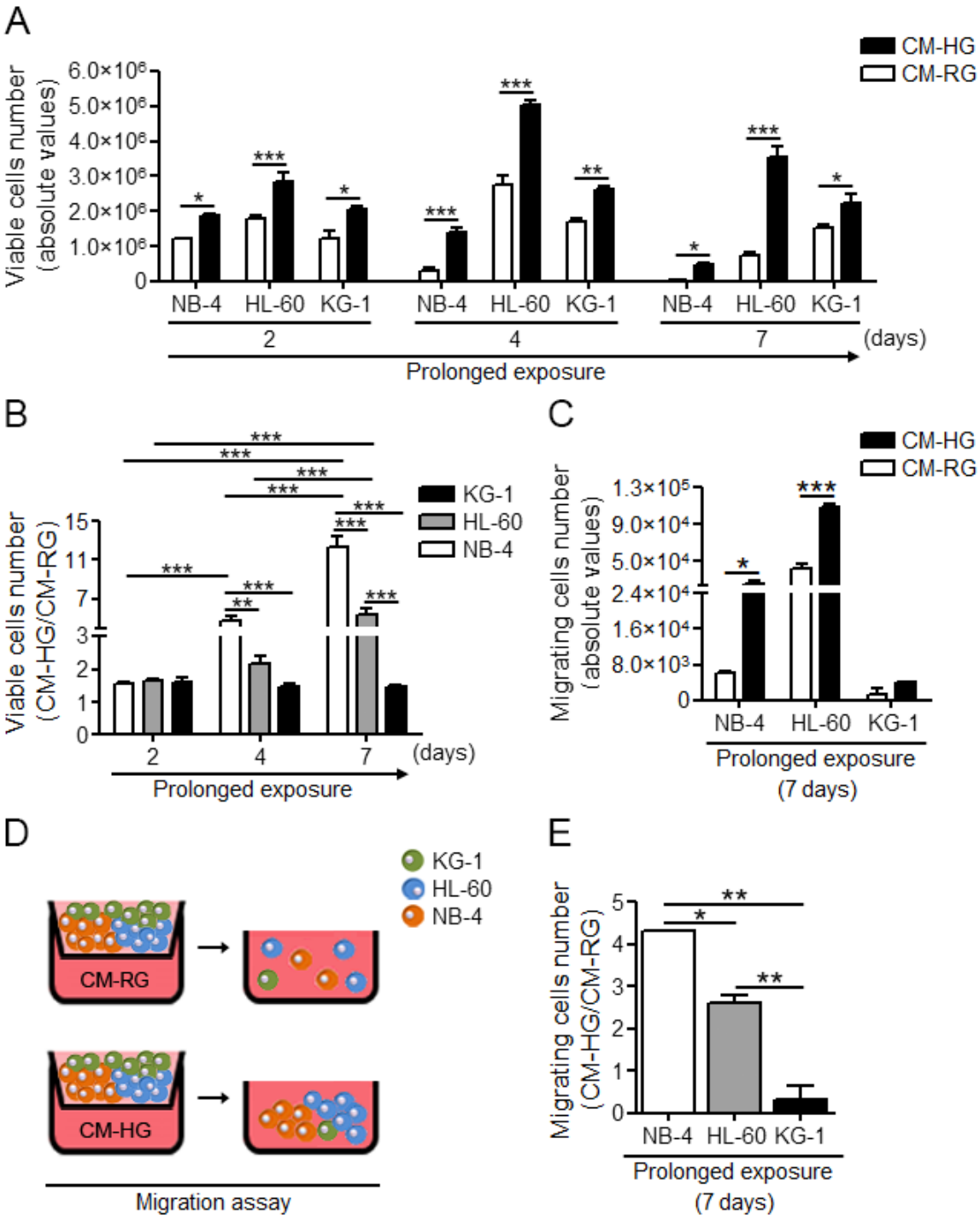

Fig. 29. Chronic exposure to conditioned medium produced by non-diabetic human bone marrow mesenchymal stromal cells under high glucose levels promotes increased survival and/or proliferation as well as augmented migration capacity of NB-4 and HL-60 cells but not KG-1 cells. (A) NB-4, HL-60 and KG-1 cells were cultured in the conditioned medium (CM) produced by non-diabetic human bone marrow mesenchymal stromal cells submitted to DMEM containing regular or high glucose levels (CM-RG or CM-HG, respectively) for 2, 4 and 7 days. Upon the incubation periods, cell viability was assessed by counting the number of viable cells using the trypan blue dye exclusion assay. The results are shown as mean+/-SEM of, at least, three independent biological replicates. Two-way ANOVA and Bonferroni post hoc test were used to compare the number of NB-4, HL-60 or KG-1 viable cells between the CM-RG and the CM-HG upon 2, 4 or 7 days of culture. *p <0.05; **p <0.01; ***p <0.001. (B) The ratio between the number of NB-4, HL-60 or KG-1 viable cells obtained in the CM-HG and in the CM-RG (CM-HG/CM-RG) upon 2, 4 or 7 days of incubation was calculated. The results are shown as mean+/-SEM of, at least, three independent biological

replicates. Two-way ANOVA and Bonferroni post hoc test were used to compare the CM-HG/CM-RG ratio between NB-4, HL-60 and KG-1 cells upon 2, 4 and 7 days of culture. **p <0.01; ***p <0.001. (C) NB-4, HL-60 and KG-1 cells were pre-exposed to CM-RG or CM-HG for 7 days followed by an overnight starvation period. The migration assay was then performed for 24h, cells were added to the top chamber of 24-transwell culture inserts with 8µm pore size which were placed in wells containing CM-RG or CM-HG, and the number of migrating cells towards CM-RG or CM-HG was counted using the trypan blue dye exclusion assay. The results are shown as mean+/-SEM of, at least, three independent biological replicates. Two-way ANOVA and Bonferroni post hoc test were used to compare the number of NB-4, HL-60 or KG-1 migrating cells between the CM-RG and the CM-HG. *p <0.05; ***p <0.001. (D) Schematic representation of the NB-4, HL-60 and KG-1 cells migration capacity upon prolonged exposure to CM-RG or to CM-HG. (E) The ratio between the number of NB-4, HL-60 or KG-1 migrating cells obtained in the CM-HG and in the CM-RG (CM-HG/CM-RG) was calculated. The results are shown as mean+/-SEM of, at least, three independent biological replicates. One-way ANOVA and Tukey post hoc test were used to compare the CM-HG/CM-RG ratio between NB-4, HL-60 and KG-1 cells. *p <0.05; **p <0.01.

To further investigate the relevance of the chronic exposure to the soluble factors and/or EVs secreted by the BM-MSCs under high glucose levels on the tumorigenicity of different AML cell types, the migration capacity of NB-4, HL-60 and KG-1 cells was evaluated upon acute exposure to CM-RG or to CM-HG. A similar number of NB-4, HL-60 and KG-1 migrating cells was detected between the CM-RG and the CM-HG (Fig. 30A, B). As expected, no statistical differences were obtained between NB-4, HL-60 and KG-1 cells in what concerns the CM-HG/CM-RG ratio (Fig. 30C). Data indicate therefore that short-term exposure to the soluble signaling molecules and/or EVs released by the BM-MSCs under elevated glucose concentrations has no major impact on the tumorigenicity of distinct AML cell types, reinforcing the positive role of prolonged exposure in the augmented tumorigenicity of glycolysis-dependent AML cell types.

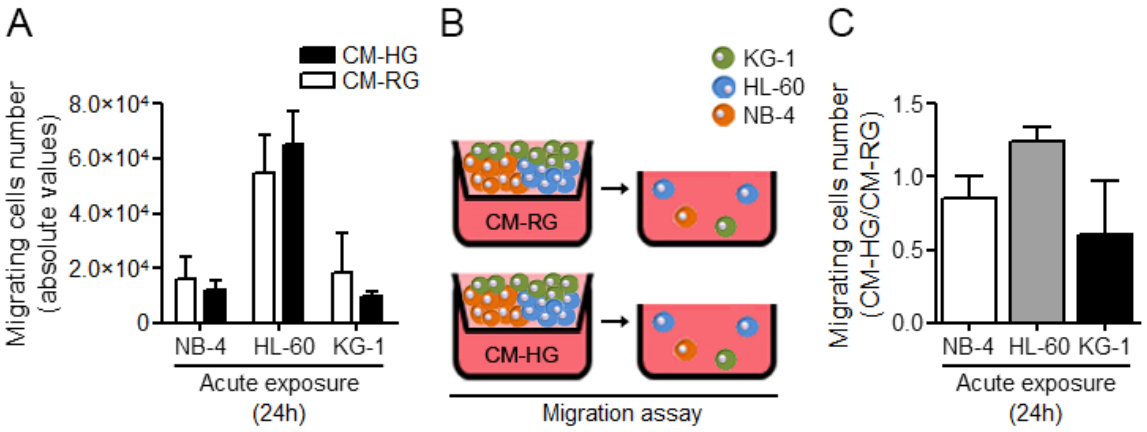

Fig. 30. Acute exposure to conditioned medium produced by non-diabetic human bone marrow mesenchymal stromal cells under high glucose levels has no major impact on the migration capacity of distinct acute myeloid leukemia cell types. (A) NB-4, HL-60 and KG-1 cells were starved overnight in starvation medium. The migration assay was then performed for 24h, cells were added to the top chamber of 24-transwell culture inserts with 8µm pore size which were placed in wells containing conditioned medium (CM) produced by non-diabetic human bone marrow mesenchymal stromal cells submitted to DMEM with regular or high glucose levels (CM-RG or CM-HG, respectively), and the number

of migrating cells towards CM-RG or CM-HG was counted using the trypan blue dye exclusion assay. The results are shown as mean+/-SEM of, at least, three independent biological replicates. Two-way ANOVA and Bonferroni post hoc test were used to compare the number of NB-4, HL-60 or KG-1 migrating cells between the CM-RG and the CM-HG. (B) Schematic representation of the NB-4, HL-60 and KG-1 cells migration capacity upon acute exposure to CM-RG or to CM-HG. (C) The ratio between the number of NB-4, HL-60 or KG-1 migrating cells obtained in the CM-HG and in the CM-RG (CM-HG/CM-RG) was calculated. The results are shown as mean+/-SEM of, at least, three independent biological replicates. One-way ANOVA and Tukey post hoc test were used to compare the CM-HG/CM-RG ratio between NB-4, HL-60 and KG-1 cells.

Results obtained in this section propose that long-term exposure to the changes promoted by high glucose levels in the BM-MSCs secretome and/or BM-MSCs-derived EVs profile contributes to the development and progression of distinct AML subtypes, manly those with increased glycolytic phenotype.

A detailed characterization of the CM produced by the non-diabetic human BM-MSCs upon exposure to high or regular glucose levels would be critical to identify BM-MSCs-secreted soluble factors as well as BM-MSCs-derived EVs responsible for the elevated tumorigenicity displayed by the different tested AML cell types in response to CM-HG (Fig. 29). A co-culture system involving non-diabetic versus diabetic human BM-MSCs and different AML cell types would also be fundamental. Indeed, it is well documented that communication between AML cells and BM-MSCs is bidirectional: not only the BM-MSCs modulate the AML cells phenotype but also the AML cells are able to reprogram the BM-MSCs behavior into a leukemia growth-permissive and normal hematopoiesis-suppressive profile [235-241]. EVs secreted by AML cells have been identified as key mediators of the AML cells-to-BM-MSCs communication, playing a critical role on the AML initiation, progression and chemoresistance [235, 238-241]. Accordingly, the characterization of EVs derived from different AML cell lines, HL-60 and KG-1, was conducted to illustrate the EVs profile of distinct AML cell types. Immunoblotting analysis was initially performed to confirm the isolation and purification of the AML cells-secreted EVs. The expression of CD63, alix and flotillin-1, well-recognized EVs marker proteins [242, 243], was noticed in the HL-60 and KG-1 cells-derived EVs (Fig. 31A), indicating the presence of EVs in both isolates. As expected, the expression of the studied EVs markers was also observed in the corresponding cell lysate samples (Fig. 31A). The purification of both EVs isolates was demonstrated by the absence of calnexin, an endoplasmic reticulum (ER) stress marker protein [244], in the HL-60 and KG-1 cells-derived EVs (Fig. 31A). As anticipated, calnexin was enriched in whole cell lysates (Fig. 31A). Taken together, data suggest that the applied isolation process gives rise to purified EVs, free from other membrane vesicles or

protein aggregates. Upon isolation, nanotracking analysis (NTA) was performed to determine the size and concentration of the HL-60 or KG-1 cells-secreted EVs. The isolated EVs presented similar size (HL-60=136nM vs KG-1=134nM) and concentration (HL-60= 7,37±0,35x10^{8}particles/mL vs KG-1=7,45±0,2x10^{8}particles/mL)(Fig. 31B), proposing that under basal state different AML cell types release EVs with an identical profile.

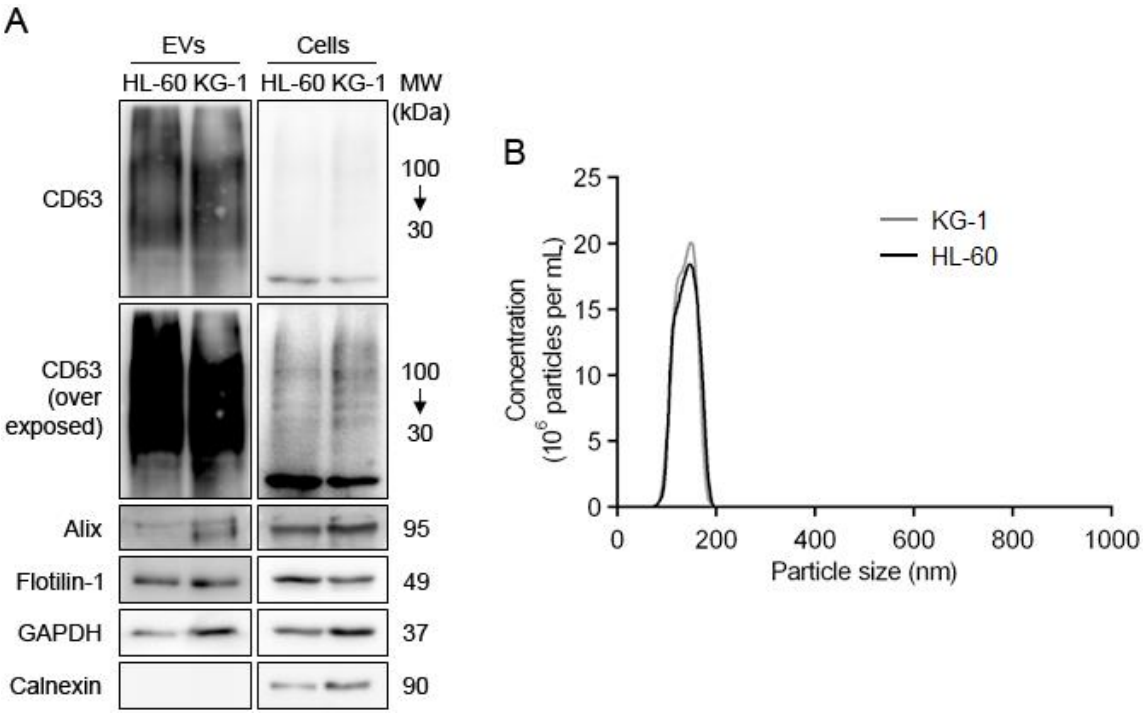

Fig. 31. Extracellular vesicles released by HL-60 and KG-1 cells under basal state exhibit similar size and concentration. Extracellular vesicles (EVs) were isolated from the conditioned medium (CM) of HL-60 or KG-1 cells upon 24h of culture via differential ultracentrifugation. EVs were then characterized by (A) immunoblotting analysis and (B) nanotracking analysis (NTA). The expression of proteins typically enriched in EVs, as CD63, alix and flotillin-1, and endoplasmic reticulum (ER), as calnexin, was assessed by immunoblotting analysis in HL-60 or KG-1 cells-derived EVs as well as in the corresponding cell lysate samples. GAPDH was used as loading control. The results are representative of one independent biological replicate. The size (nm) and concentration (10^6 particles/mL) of HL-60 or KG-1 cells-derived EVs was determined by NTA. The results were processed using the NTA 2.2 analytical software and are representative of one independent biological replicate.

The results obtained in this chapter provide evidence for a critical role of DM in the AML context, by remodeling the BM niche to support leukemic persistence at the expense of homeostatic function. Indeed, chronic exposure to high glucose concentrations, a metabolic condition observed in DM, promotes changes in the BM-MSCs phenotype which, in turn, increases the tumorigenic phenotype of diverse AML cell types. As DM is increasing at an alarming rate and is becoming a

metabolic disorder of great magnitude, a deep understanding of the molecular basis involved in the DM contribution to AML initiation, progression and chemoresistance is fundamental.

CHAPTER 5

General discussion and conclusions

The genetic and epigenetic heterogeneity, compromising differentiation, proliferation and self-renewal of hematopoietic stem cells (HSCs) and/or myeloid progenitors, is a fundamental property of acute myeloid leukemia (AML) [8-11, 245]. This multitude of AML scenarios has not only hampering the understanding of the AML pathogenesis but also the development of efficient therapeutic strategies. The metabolic rewiring characterized by alterations in cellular energy metabolism, nutrient-sensing pathways, as AMPK, mTORC1 and AKT, and/or macroautophagy (hereinafter called autophagy) has been reported in several types of tumor cells, namely in AML [86-93, 120, 122, 123, 128, 130, 147, 148, 152, 153, 164-172]. Nevertheless, the heterogeneous nature of this group of hematological disorders has been responsible for the current controversial literature (either using cell lines, animal models or patient-derived samples), which has pointed to diverse nutrient-sensing players and autophagy as "double-edged swords" in the AML context [92, 93, 120, 122, 123, 128, 130, 147, 148, 152, 153, 164-172]. The impact of metabolic transformations on the pathogenesis of each subtype of AML remains therefore unclear. Accordingly, the work presented in this thesis aimed to obtain new insights on the contribution of metabolic changes to the development of distinct subtypes of AML.

In vitro approaches were initially performed using three different human AML cell lines representative of three distinct AML subtypes (HL-60 - FAB-M2 subtype; NB-4 - FAB-M3 subtype; KG-1 - FAB-M6 subtype). These cell lines were chosen because they are very well characterized and widely used as representative of different AML subtypes. Cell lines are advantageous cellular models that allow the reduction of the human burden associated with ethical considerations as well as the decrease of the variability between samples [246]. The continuous proliferation of these immortalized cells also facilitates *in vitro* studies, unlike primary cells that cannot survive in these conditions for long time periods. Plus, cell lines are useful to identify molecular targets/potential candidates to be explored in patient's samples context [246]. Cell lines also present important limitations as the inability to recapitulate the complexity of the primary tumor cells and to review the multiple interactions with the tumoral microenvironment [246]. Results herein obtained with different AML cell lines highlight the multitude of metabolic cellular scenarios that might arise even in very closely related cell lines, such as NB-4 and HL-60, which belong to a different genetic cluster when compared to KG-1 [247]. Distinct energetic, metabolic and autophagic networks are suggested among different subtypes of AML, with the activated AKT/mTORC1 axis being claimed as a positive regulator of glycolysis and a negative regulator of autophagy in certain AML subtypes and the activated AMPK being pointed as a positive regulator of both oxidative metabolism and

autophagy in other AML scenarios. Recent publications from Kishton, R. J. and co-workers proposed AMPK as supporting the oxidative metabolism of T cell acute lymphoblastic leukemia (T-ALL) cells [163]. The role of AKT [96] or mTORC1 [94] in sustaining glycolysis of AML cells was also recently described. To the best of our knowledge, findings obtained in this thesis show for the first time a constitutive co-activation of AMPK and mTORC1, often perceived as antagonists [184], in a specific subtype of AML cells, with AMPK imposing its action on mTORC1. A similar contradictory metabolic scenario was already reported by Pezze, P. D. *et al.* in myocytes responding to amino acids supplementation [248]. The authors proposed that the concomitant activation of AMPK and mTORC1 is implicated in the maintenance of protein homoeostasis and on the fuel of metabolites for biosynthetic processes [248]. The relevance of amino acid signaling and mTORC1 AKT-independent activation in the context of AML remains to be explored. In the present thesis, autophagy is also recognized as controlling the energy metabolism of different AML cell types through negative regulation of glycolysis. Indeed, autophagy was recently identified by Watson, A.S. and co-workers as limiting the glycolytic metabolism of AML cells [93]. Interestingly, data on the inhibition of nutrient-sensing pathways identify AKT as a potential candidate for the treatment of specific AML subtypes, while propose AMPK and mTORC1 as ineffective therapeutic targets in other AML scenarios. The results obtained in this thesis indicate that exclusive metabolic frames sustain the survival and proliferation of distinct AML cell types, elucidating the heterogenicity of distinct AML subtypes. The therapeutic approach to AML disorders must therefore pass through personalized therapy adapted to the heterogeneity of this group of hematological malignancies. The genetically, metabolically and clinically heterogeneity of AML should be considered. Indeed, such heterogeneity might justify the general modest growth-inhibitory effects of mTOR inhibition in preclinical AML models and clinical trials [125, 167]. Importantly, the results presented in this thesis highlight the relevance that comparative studies implying AML cell lines have on the determination of the anti-leukemia efficacy, particularly, of the effectiveness of combinatory therapy with conventional and new targeted agents.

The relevance of autophagy in health and disease was recently highlighted when Yoshinori Ohsumi was awarded the Nobel Prize for Physiology or Medicine for his work elucidating the mechanism of autophagy [249]. Advancements in the understanding of autophagy and how this pathway can be used to improve the clinical outcomes of AML patients have come a long way. Nevertheless, the role of autophagy in the AML disorder remains controversial, with interventions to both stimulate and inhibit autophagy being proposed as cancer therapies [93, 147, 148, 152, 153, 169-172].

The precise mechanism of autophagy in the AML context requires therefore further study. To validate the *in vitro* findings obtained with AML cell lines, it would be important to conduct the same experimental approaches with human primary AML cells. Nevertheless, such studies were impossible to perform due to the unavailability of the biological specimens. Instead, mRNA samples extracted from the bone marrow mononuclear cells (BM-MNCs) of AML patients, diagnosed and treated at IPO-Porto from 2005 to 2014, were used and the expression levels of essential autophagy-related genes were determined. Transcriptionally regulated genes were selected to minimize the impossibility of studying autophagy at the protein level. In this thesis, by comparing AML subjects with control donors, a reduced autophagy phenotype is suggested for AML. Indeed, the mRNA expression levels of the *MAP1LC3B* and *ATG12* autophagy-associated genes were shown to be statistically decreased in the BM-MNCs of the AML individuals when compared to the BM-MNCs of the control donors, as reported by other studies [93, 190-192]. A crosstalk between Beclin-1 and Bcl-2 to prevent the apoptosis of AML cells is also proposed in this thesis, after observing a higher *BECLIN1* and *BCL2* gene expression in the BM-MNCs of the AML patients than in the BM-MNCs of the control individuals. Indeed, in addition to its autophagic role, Beclin-1 has been recognized as fundamental for the anti-apoptotic activity of Bcl-2 [198]. In agreement with the findings herein obtained, increased *BCL2* mRNA expression levels have been extensively reported in the AML context [199]. However, data concerning the expression pattern of *BECLIN1* in the BM-MNCs of AML patients have been debatable, with normal [193], reduced [93, 190, 191] and augmented [194] mRNA expression levels described. The heterogeneous nature of AML has a critical impact on the paradoxical role (both tumor suppressor and promoter) attributed to autophagy. Accordingly, the characterization of the autophagy pattern among different subtypes of AML becomes a pressing demand. In this thesis, by clustering AML patients according to their FAB subtype, a heterogeneous autophagic signature is proposed in the AML scenario, as suggested by the *in vitro* data obtained with AML cell lines. Indeed, a differential expression of core autophagy genes was revealed among the BM-MNCs of the different tested FAB AML subtypes. To the best of our knowledge, this is the first time that a characterization of autophagy among different subtypes of AML is performed. Curiously, authors studying autophagy in AML have clustered the different AML subtypes into the same group, comparing them with control donors. The FAB classification system is falling into disuse and being replaced by the World Health Organization (WHO) classification, a more detailed, complete and modern classification [23, 24]. However, the AML patients used in this thesis were classified at diagnosis using the FAB classification system, making

it impossible to characterize autophagy according to the WHO classification. The heterogeneity of the autophagic status in the AML disorder is once again proposed in this thesis when the AML patients are clustered according to their cytogenetic risk group or karyotype. In fact, a differential expression of essential autophagy genes was noticed among the BM-MNCs of distinct cytogenetic risk groups, as published by other studies [191, 201]. An increased expression of core autophagy genes was also found in the BM-MNCs of AML individuals with abnormal karyotype when compared to those with normal karyotype. In line with these findings, Folkerts, H. and co-workers reported a higher autophagy flux in AML patients with abnormal karyotype than with normal karyotype [202]. Taken together, data on the mRNA expression levels of autophagy-associated genes highlight not only the relevance of autophagy in the AML context but also the autophagic heterogeneity of AML. The molecular and clinical heterogeneity of AML results in varied responses to treatment, posing a challenge to personalized therapeutic schemes. Both patient and disease status should therefore be taken into consideration to make individual-based clinical decisions for AML patients.

Despite advances in the understanding of the molecular mechanisms underlying the AML pathogenesis, the treatment of AML remains a major challenge. Data reported in this thesis, with clinical data of AML patients diagnosed and treated at IPO-Porto from 2005 to 2014, showed a trend towards reduced overall survival (OS) and relapse-free survival (RFS) in patients with both AML and type 2 diabetes *mellitus* (hereinafter called DM) when compared to AML patients without DM, pointing to DM as a predictor of worse outcome in AML, as documented by other authors [212, 250]. It should be noted that the small number of DM individuals in the AML cohort herein studied (OS: n=16; RFS: n=8) makes critical the continuity of this project to achieve statistical relevance. The expected sharp increase of DM in the upcoming decades [251] makes fundamental the elucidation of the mechanisms underlying the AML-DM association. Over the last years, studies have identified DM as a promoter of disturbances in the function of bone marrow mesenchymal stromal cells (BM-MSCs) [219-225]. Plus, the communication between AML cells and BM-MSCs has been widely implicated in the survival, proliferation and drug resistance of AML cells [203-211]. Accordingly, the work herein presented aimed to clarify the impact of DM-induced alterations in the BM-MSCs on the pathogenesis of distinct subtypes of AML. In this thesis, by using human BM-MSCs and distinct AML cell lines, DM is disclosed as contributing to the development and progression of different AML subtypes, by changing the behavior of BM-MSCs. Indeed, in response to high glucose concentrations the BM-MSCs seem to change their secretome and/or extracellular vesicles (EVs) profile by releasing soluble signaling molecules and/or EVs that, upon long-term

contact, favor the survival and/or proliferation as well as the migration capacity of distinct AML cell types, mainly those with glycolytic dependence. The relevance of prolonged exposure to the increased AML cells tumorigenicity is demonstrated when no differences are detected in the tumorigenic phenotype of the different tested AML cell types between regular and high glucose levels upon acute exposure. To the best of our knowledge, this is the first study trying to get some clues about the impact of DM-induced disturbances in the BM-MSCs on the development and progression of distinct AML subtypes. The results herein obtained highlight, once again, the molecular heterogeneity of AML. Efforts to explore and describe the heterogeneous landscape of AML are therefore required for the optimization of AML therapies and the improvement of AML patients outcomes.

In conclusion, the multidisciplinary work developed during this thesis, which proceeds from *in vitro* systems to more patient-based approaches, provides new insights into the contribution of the energetic, metabolic and autophagic networks as well as bone marrow microenvironment to the pathogenesis of distinct subtypes of AML. The heterogeneity of the AML disorder is proposed, with potential targets being identified for the treatment of specific AML subtypes.

REFERENCES

1. Passegue, E. and I.L. Weisman, *Leukemic stem cells: where do they come from?* Stem Cell Rev, 2005. **1**(3): p. 181-8.
2. Passegue, E., et al., *Normal and leukemic hematopoiesis: are leukemias a stem cell disorder or a reacquisition of stem cell characteristics?* Proc Natl Acad Sci U S A, 2003. **100 Suppl 1**: p. 11842-9.
3. Jordan, C.T. and M.L. Guzman, *Mechanisms controlling pathogenesis and survival of leukemic stem cells.* Oncogene, 2004. **23**(43): p. 7178-87.
4. Lane, S.W., et al., *Differential niche and Wnt requirements during acute myeloid leukemia progression.* Blood, 2011. **118**(10): p. 2849-56.
5. Huntly, B.J. and D.G. Gilliland, *Leukaemia stem cells and the evolution of cancer-stem-cell research.* Nat Rev Cancer, 2005. **5**(4): p. 311-21.
6. Piller, G., *Leukaemia - a brief historical review from ancient times to 1950.* Br J Haematol, 2001. **112**(2): p. 282-92.
7. Patlak, M., *Targeting leukemia: from bench to bedside.* FASEB J, 2002. **16**(3): p. 273.
8. Shipley, J.L. and J.N. Butera, *Acute myelogenous leukemia.* Exp Hematol, 2009. **37**(6): p. 649-58.
9. Lowenberg, B., J.R. Downing, and A. Burnett, *Acute myeloid leukemia.* N Engl J Med, 1999. **341**(14): p. 1051-62.
10. Estey, E. and H. Dohner, *Acute myeloid leukaemia.* Lancet, 2006. **368**(9550): p. 1894-907.
11. Caceres-Cortes, J.R., *Blastic leukaemias (AML): a biologist's view.* Cell Biochem Biophys, 2013. **66**(1): p. 13-22.
12. Mittal, P., *The Acute Leukemias.* Hospital Physician, 2001: p. 37-44.
13. Kumar, C.C., *Genetic abnormalities and challenges in the treatment of acute myeloid leukemia.* Genes Cancer, 2011. **2**(2): p. 95-107.
14. Pedersen-Bjergaard, J., et al., *Causality of myelodysplasia and acute myeloid leukemia and their genetic abnormalities.* Leukemia, 2002. **16**(11): p. 2177-84.
15. Leone, G., et al., *Therapy related leukemias: susceptibility, prevention and treatment.* Leuk Lymphoma, 2001. **41**(3-4): p. 255-76.
16. Felix, C.A., *Secondary leukemias induced by topoisomerase-targeted drugs.* Biochim Biophys Acta, 1998. **1400**(1-3): p. 233-55.
17. *SEER Cancer Statistics Review, 1975-2015, National Cancer Institute. Bethesda, MD, https://seer.cancer.gov/csr/1975_2015/, based on November 2017 SEER data submission, posted to the SEER web site, April 2018.*
18. *SEER Cancer Stat Facts: Acute Myeloid Leukemia. National Cancer Institute. Bethesda, MD, https://seer.cancer.gov/statfacts/html/amyl.html.*
19. *Registo Oncológico Nacional 2010, http://www.roreno.com.pt/pt/publicacoes/publicacoes-nacionais.html*. 2015.
20. Jemal, A., et al., *Cancer statistics, 2010.* CA Cancer J Clin, 2010. **60**(5): p. 277-300.
21. Bennett, J.M., et al., *Proposals for the classification of the acute leukaemias. French-American-British (FAB) co-operative group.* Br J Haematol, 1976. **33**(4): p. 451-8.
22. Harris, N.L., et al., *World Health Organization classification of neoplastic diseases of the hematopoietic and lymphoid tissues: report of the Clinical Advisory Committee meeting-Airlie House, Virginia, November 1997.* J Clin Oncol, 1999. **17**(12): p. 3835-49.
23. Arber, D.A., et al., *The 2016 revision to the World Health Organization classification of myeloid neoplasms and acute leukemia.* Blood, 2016. **127**(20): p. 2391-405.

24. Bennett, J.M., et al., *Proposed revised criteria for the classification of acute myeloid leukemia. A report of the French-American-British Cooperative Group.* Ann Intern Med, 1985. **103**(4): p. 620-5.
25. Cheson, B.D., et al., *Report of the National Cancer Institute-sponsored workshop on definitions of diagnosis and response in acute myeloid leukemia.* J Clin Oncol, 1990. **8**(5): p. 813-9.
26. Dohner, H., et al., *Diagnosis and management of acute myeloid leukemia in adults: recommendations from an international expert panel, on behalf of the European LeukemiaNet.* Blood, 2010. **115**(3): p. 453-74.
27. Martens, J.H. and H.G. Stunnenberg, *The molecular signature of oncofusion proteins in acute myeloid leukemia.* FEBS Lett, 2010. **584**(12): p. 2662-9.
28. Look, A.T., *Oncogenic transcription factors in the human acute leukemias.* Science, 1997. **278**(5340): p. 1059-64.
29. Mitelman, F., B. Johansson, and F. Mertens, *The impact of translocations and gene fusions on cancer causation.* Nat Rev Cancer, 2007. **7**(4): p. 233-45.
30. Uribesalgo, I. and L. Di Croce, *Dynamics of epigenetic modifications in leukemia.* Brief Funct Genomics, 2011. **10**(1): p. 18-29.
31. Sell, S., *Leukemia: stem cells, maturation arrest, and differentiation therapy.* Stem Cell Rev, 2005. **1**(3): p. 197-205.
32. Meyers, S., N. Lenny, and S.W. Hiebert, *The t(8;21) fusion protein interferes with AML-1B-dependent transcriptional activation.* Mol Cell Biol, 1995. **15**(4): p. 1974-82.
33. Frank, R., et al., *The AML1/ETO fusion protein blocks transactivation of the GM-CSF promoter by AML1B.* Oncogene, 1995. **11**(12): p. 2667-74.
34. Lutterbach, B., et al., *The inv(16) encodes an acute myeloid leukemia 1 transcriptional corepressor.* Proc Natl Acad Sci U S A, 1999. **96**(22): p. 12822-7.
35. Lutterbach, B. and S.W. Hiebert, *Role of the transcription factor AML-1 in acute leukemia and hematopoietic differentiation.* Gene, 2000. **245**(2): p. 223-35.
36. Mrozek, K., H. Dohner, and C.D. Bloomfield, *Influence of new molecular prognostic markers in patients with karyotypically normal acute myeloid leukemia: recent advances.* Curr Opin Hematol, 2007. **14**(2): p. 106-14.
37. Kantarjian, H., et al., *Therapeutic advances in leukemia and myelodysplastic syndrome over the past 40 years.* Cancer, 2008. **113**(7 Suppl): p. 1933-52.
38. Roboz, G.J., *Novel approaches to the treatment of acute myeloid leukemia.* Hematology Am Soc Hematol Educ Program, 2011. **2011**: p. 43-50.
39. Tallman, M.S., D.G. Gilliland, and J.M. Rowe, *Drug therapy for acute myeloid leukemia.* Blood, 2005. **106**(4): p. 1154-63.
40. Wang, L.M., J.C. White, and R.L. Capizzi, *The effect of ara-C-induced inhibition of DNA synthesis on its cellular pharmacology.* Cancer Chemother Pharmacol, 1990. **25**(6): p. 418-24.
41. Ross, D.D., et al., *Mechanistic implications of alterations in HL-60 cell nascent DNA after exposure to 1-beta-D-arabinofuranosylcytosine.* Cancer Chemother Pharmacol, 1992. **31**(1): p. 61-70.
42. Fram, R.J. and D.W. Kufe, *DNA strand breaks caused by inhibitors of DNA synthesis: 1-beta-D-arabinofuranosylcytosine and aphidicolin.* Cancer Res, 1982. **42**(10): p. 4050-3.
43. Minotti, G., et al., *Anthracyclines: molecular advances and pharmacologic developments in antitumor activity and cardiotoxicity.* Pharmacol Rev, 2004. **56**(2): p. 185-229.
44. Phillips, D.R., P.C. Greif, and R.C. Boston, *Daunomycin-DNA dissociation kinetics.* Mol Pharmacol, 1988. **33**(2): p. 225-30.

45. Sordet, O., et al., *Apoptosis induced by topoisomerase inhibitors.* Curr Med Chem Anticancer Agents, 2003. **3**(4): p. 271-90.
46. Larsen, A.K., A.E. Escargueil, and A. Skladanowski, *Catalytic topoisomerase II inhibitors in cancer therapy.* Pharmacol Ther, 2003. **99**(2): p. 167-81.
47. Cowell, I.G. and C.A. Austin, *Mechanism of generation of therapy related leukemia in response to anti-topoisomerase II agents.* Int J Environ Res Public Health, 2012. **9**(6): p. 2075-91.
48. Cheson, B.D., et al., *Revised recommendations of the International Working Group for Diagnosis, Standardization of Response Criteria, Treatment Outcomes, and Reporting Standards for Therapeutic Trials in Acute Myeloid Leukemia.* J Clin Oncol, 2003. **21**(24): p. 4642-9.
49. Stone, R.M., M.R. O'Donnell, and M.A. Sekeres, *Acute myeloid leukemia.* Hematology Am Soc Hematol Educ Program, 2004: p. 98-117.
50. Erba, H.P., *Has there been progress in the treatment of older patients with acute myeloid leukemia?* Best Pract Res Clin Haematol, 2010. **23**(4): p. 495-501.
51. Dombret, H., E. Raffoux, and C. Gardin, *Acute myeloid leukemia in the elderly.* Semin Oncol, 2008. **35**(4): p. 430-8.
52. Pollyea, D.A., H.E. Kohrt, and B.C. Medeiros, *Acute myeloid leukaemia in the elderly: a review.* Br J Haematol, 2011. **152**(5): p. 524-42.
53. Kohrt, H.E. and S.E. Coutre, *Optimizing therapy for acute myeloid leukemia.* J Natl Compr Canc Netw, 2008. **6**(10): p. 1003-16.
54. Cassileth, P.A., et al., *Chemotherapy compared with autologous or allogeneic bone marrow transplantation in the management of acute myeloid leukemia in first remission.* N Engl J Med, 1998. **339**(23): p. 1649-56.
55. Burnett, A.K., et al., *Randomised comparison of addition of autologous bone-marrow transplantation to intensive chemotherapy for acute myeloid leukaemia in first remission: results of MRC AML 10 trial. UK Medical Research Council Adult and Children's Leukaemia Working Parties.* Lancet, 1998. **351**(9104): p. 700-8.
56. Jones, C.V. and E.A. Copelan, *Treatment of acute myeloid leukemia with hematopoietic stem cell transplantation.* Future Oncol, 2009. **5**(4): p. 559-68.
57. Estey, E., *Acute myeloid leukemia and myelodysplastic syndromes in older patients.* J Clin Oncol, 2007. **25**(14): p. 1908-15.
58. O'Donnell, M.R., et al., *Acute myeloid leukemia.* J Natl Compr Canc Netw, 2011. **9**(3): p. 280-317.
59. Stapnes, C., et al., *Targeted therapy in acute myeloid leukaemia: current status and future directions.* Expert Opin Investig Drugs, 2009. **18**(4): p. 433-55.
60. Lowenberg, B., et al., *Cytarabine dose for acute myeloid leukemia.* N Engl J Med, 2011. **364**(11): p. 1027-36.
61. Fernandez, H.F., et al., *Anthracycline dose intensification in acute myeloid leukemia.* N Engl J Med, 2009. **361**(13): p. 1249-59.
62. Licht, J.D., *Reconstructing a disease: What essential features of the retinoic acid receptor fusion oncoproteins generate acute promyelocytic leukemia?* Cancer Cell, 2006. **9**(2): p. 73-4.
63. de The, H., et al., *The t(15;17) translocation of acute promyelocytic leukaemia fuses the retinoic acid receptor alpha gene to a novel transcribed locus.* Nature, 1990. **347**(6293): p. 558-61.
64. Kwok, C., et al., *Forced homo-oligomerization of RARalpha leads to transformation of primary hematopoietic cells.* Cancer Cell, 2006. **9**(2): p. 95-108.

65. Sternsdorf, T., et al., *Forced retinoic acid receptor alpha homodimers prime mice for APL-like leukemia.* Cancer Cell, 2006. **9**(2): p. 81-94.
66. Warrell, R.P., Jr., et al., *Differentiation therapy of acute promyelocytic leukemia with tretinoin (all-trans-retinoic acid).* N Engl J Med, 1991. **324**(20): p. 1385-93.
67. Castaigne, S., et al., *All-trans retinoic acid as a differentiation therapy for acute promyelocytic leukemia. I. Clinical results.* Blood, 1990. **76**(9): p. 1704-9.
68. Degos, L., et al., *Treatment of first relapse in acute promyelocytic leukaemia with all-trans retinoic acid.* Lancet, 1990. **336**(8728): p. 1440-1.
69. Sanz, M.A., *Treatment of acute promyelocytic leukemia.* Hematology Am Soc Hematol Educ Program, 2006: p. 147-55.
70. Fenaux, P., et al., *A randomized comparison of all transretinoic acid (ATRA) followed by chemotherapy and ATRA plus chemotherapy and the role of maintenance therapy in newly diagnosed acute promyelocytic leukemia. The European APL Group.* Blood, 1999. **94**(4): p. 1192-200.
71. Sanz, M.A., et al., *Arsenic trioxide in the treatment of acute promyelocytic leukemia. A review of current evidence.* Haematologica, 2005. **90**(9): p. 1231-5.
72. Douer, D. and M.S. Tallman, *Arsenic trioxide: new clinical experience with an old medication in hematologic malignancies.* J Clin Oncol, 2005. **23**(10): p. 2396-410.
73. Shen, Z.X., et al., *All-trans retinoic acid/As2O3 combination yields a high quality remission and survival in newly diagnosed acute promyelocytic leukemia.* Proc Natl Acad Sci U S A, 2004. **101**(15): p. 5328-35.
74. Pfeiffer, T., S. Schuster, and S. Bonhoeffer, *Cooperation and competition in the evolution of ATP-producing pathways.* Science, 2001. **292**(5516): p. 504-7.
75. Barer, A.P., *A Study of Glycolysis.* J Clin Invest, 1931. **10**(3): p. 507-20.
76. Osellame, L.D., T.S. Blacker, and M.R. Duchen, *Cellular and molecular mechanisms of mitochondrial function.* Best Pract Res Clin Endocrinol Metab, 2012. **26**(6): p. 711-23.
77. Locasale, J.W. and L.C. Cantley, *Altered metabolism in cancer.* BMC Biol, 2010. **8**: p. 88.
78. Zheng, J., *Energy metabolism of cancer: Glycolysis versus oxidative phosphorylation (Review).* Oncol Lett, 2012. **4**(6): p. 1151-1157.
79. Warburg, O., *On the origin of cancer cells.* Science, 1956. **123**(3191): p. 309-14.
80. Griguer, C.E., C.R. Oliva, and G.Y. Gillespie, *Glucose metabolism heterogeneity in human and mouse malignant glioma cell lines.* J Neurooncol, 2005. **74**(2): p. 123-33.
81. Fantin, V.R., J. St-Pierre, and P. Leder, *Attenuation of LDH-A expression uncovers a link between glycolysis, mitochondrial physiology, and tumor maintenance.* Cancer Cell, 2006. **9**(6): p. 425-34.
82. Hsu, P.P. and D.M. Sabatini, *Cancer cell metabolism: Warburg and beyond.* Cell, 2008. **134**(5): p. 703-7.
83. Lim, H.Y., et al., *Respiratory competent mitochondria in human ovarian and peritoneal cancer.* Mitochondrion, 2011. **11**(3): p. 437-43.
84. Scott, D.A., et al., *Comparative metabolic flux profiling of melanoma cell lines: beyond the Warburg effect.* J Biol Chem, 2011. **286**(49): p. 42626-34.
85. Moreno-Sanchez, R., et al., *Energy metabolism in tumor cells.* FEBS J, 2007. **274**(6): p. 1393-418.
86. Chen, W.L., et al., *A distinct glucose metabolism signature of acute myeloid leukemia with prognostic value.* Blood, 2014. **124**(10): p. 1645-54.
87. Herst, P.M., et al., *Glycolytic metabolism confers resistance to combined all-trans retinoic acid and arsenic trioxide-induced apoptosis in HL60rho0 cells.* Leuk Res, 2008. **32**(2): p. 327-33.

88. Song, K., et al., *Resistance to chemotherapy is associated with altered glucose metabolism in acute myeloid leukemia.* Oncol Lett, 2016. **12**(1): p. 334-342.
89. Ohayon, D., et al., *Cytoplasmic proliferating cell nuclear antigen connects glycolysis and cell survival in acute myeloid leukemia.* Sci Rep, 2016. **6**: p. 35561.
90. Ju, H.Q., et al., *ITD mutation in FLT3 tyrosine kinase promotes Warburg effect and renders therapeutic sensitivity to glycolytic inhibition.* Leukemia, 2017. **31**(10): p. 2143-2150.
91. Wang, Y.H., et al., *Cell-state-specific metabolic dependency in hematopoiesis and leukemogenesis.* Cell, 2014. **158**(6): p. 1309-1323.
92. Saito, Y., et al., *AMPK Protects Leukemia-Initiating Cells in Myeloid Leukemias from Metabolic Stress in the Bone Marrow.* Cell Stem Cell, 2015. **17**(5): p. 585-96.
93. Watson, A.S., et al., *Autophagy limits proliferation and glycolytic metabolism in acute myeloid leukemia.* Cell Death Discov, 2015. **1**.
94. Poulain, L., et al., *High mTORC1 activity drives glycolysis addiction and sensitivity to G6PD inhibition in acute myeloid leukemia cells.* Leukemia, 2017. **31**(11): p. 2326-2335.
95. Lagadinou, E.D., et al., *BCL-2 inhibition targets oxidative phosphorylation and selectively eradicates quiescent human leukemia stem cells.* Cell Stem Cell, 2013. **12**(3): p. 329-41.
96. Scotland, S., et al., *Mitochondrial energetic and AKT status mediate metabolic effects and apoptosis of metformin in human leukemic cells.* Leukemia, 2013. **27**(11): p. 2129-38.
97. Molina, J.R., et al., *An inhibitor of oxidative phosphorylation exploits cancer vulnerability.* Nat Med, 2018. **24**(7): p. 1036-1046.
98. Farge, T., et al., *Chemotherapy-Resistant Human Acute Myeloid Leukemia Cells Are Not Enriched for Leukemic Stem Cells but Require Oxidative Metabolism.* Cancer Discov, 2017. **7**(7): p. 716-735.
99. Lunt, S.Y. and M.G. Vander Heiden, *Aerobic glycolysis: meeting the metabolic requirements of cell proliferation.* Annu Rev Cell Dev Biol, 2011. **27**: p. 441-64.
100. Ahn, C.S. and C.M. Metallo, *Mitochondria as biosynthetic factories for cancer proliferation.* Cancer Metab, 2015. **3**(1): p. 1.
101. Owen, O.E., S.C. Kalhan, and R.W. Hanson, *The key role of anaplerosis and cataplerosis for citric acid cycle function.* J Biol Chem, 2002. **277**(34): p. 30409-12.
102. Chan, S.M., et al., *Isocitrate dehydrogenase 1 and 2 mutations induce BCL-2 dependence in acute myeloid leukemia.* Nat Med, 2015. **21**(2): p. 178-84.
103. Wang, F., et al., *Targeted inhibition of mutant IDH2 in leukemia cells induces cellular differentiation.* Science, 2013. **340**(6132): p. 622-6.
104. Stein, E.M., et al., *Enasidenib in mutant IDH2 relapsed or refractory acute myeloid leukemia.* Blood, 2017. **130**(6): p. 722-731.
105. Stein, E.M., *Enasidenib, a targeted inhibitor of mutant IDH2 proteins for treatment of relapsed or refractory acute myeloid leukemia.* Future Oncol, 2018. **14**(1): p. 23-40.
106. Figueroa, M.E., et al., *Leukemic IDH1 and IDH2 mutations result in a hypermethylation phenotype, disrupt TET2 function, and impair hematopoietic differentiation.* Cancer Cell, 2010. **18**(6): p. 553-67.
107. Kats, L.M., et al., *Proto-oncogenic role of mutant IDH2 in leukemia initiation and maintenance.* Cell Stem Cell, 2014. **14**(3): p. 329-41.
108. Ward, P.S., et al., *The common feature of leukemia-associated IDH1 and IDH2 mutations is a neomorphic enzyme activity converting alpha-ketoglutarate to 2-hydroxyglutarate.* Cancer Cell, 2010. **17**(3): p. 225-34.
109. Castro, I., B. Sampaio-Marques, and P. Ludovico, *Targeting Metabolic Reprogramming in Acute Myeloid Leukemia.* Cells, 2019. **8**(9).

110. Emadi, A., et al., *Inhibition of glutaminase selectively suppresses the growth of primary acute myeloid leukemia cells with IDH mutations.* Exp Hematol, 2014. **42**(4): p. 247-51.
111. Matre, P., et al., *Inhibiting glutaminase in acute myeloid leukemia: metabolic dependency of selected AML subtypes.* Oncotarget, 2016. **7**(48): p. 79722-79735.
112. Vander Heiden, M.G., *Targeting cancer metabolism: a therapeutic window opens.* Nat Rev Drug Discov, 2011. **10**(9): p. 671-84.
113. Sanz, P., *AMP-activated protein kinase: structure and regulation.* Curr Protein Pept Sci, 2008. **9**(5): p. 478-92.
114. Hardie, D.G., F.A. Ross, and S.A. Hawley, *AMPK: a nutrient and energy sensor that maintains energy homeostasis.* Nat Rev Mol Cell Biol, 2012. **13**(4): p. 251-62.
115. Saxton, R.A. and D.M. Sabatini, *mTOR Signaling in Growth, Metabolism, and Disease.* Cell, 2017. **168**(6): p. 960-976.
116. Bar-Peled, L. and D.M. Sabatini, *Regulation of mTORC1 by amino acids.* Trends Cell Biol, 2014. **24**(7): p. 400-6.
117. Shaw, R.J., *LKB1 and AMP-activated protein kinase control of mTOR signalling and growth.* Acta Physiol (Oxf), 2009. **196**(1): p. 65-80.
118. Liao, Y. and M.C. Hung, *Physiological regulation of Akt activity and stability.* Am J Transl Res, 2010. **2**(1): p. 19-42.
119. Manning, B.D. and A. Toker, *AKT/PKB Signaling: Navigating the Network.* Cell, 2017. **169**(3): p. 381-405.
120. Green, A.S., et al., *The LKB1/AMPK signaling pathway has tumor suppressor activity in acute myeloid leukemia through the repression of mTOR-dependent oncogenic mRNA translation.* Blood, 2010. **116**(20): p. 4262-73.
121. Kawashima, I., et al., *Negative regulation of the LKB1/AMPK pathway by ERK in human acute myeloid leukemia cells.* Exp Hematol, 2015. **43**(7): p. 524-33 e1.
122. Sujobert, P., et al., *Co-activation of AMPK and mTORC1 Induces Cytotoxicity in Acute Myeloid Leukemia.* Cell Rep, 2015. **11**(9): p. 1446-57.
123. Tabe, Y., et al., *Inhibition of mTOR kinase as a therapeutic target for acute myeloid leukemia.* Expert Opin Ther Targets, 2017. **21**(7): p. 705-714.
124. Rizzieri, D.A., et al., *A phase 2 clinical trial of deforolimus (AP23573, MK-8669), a novel mammalian target of rapamycin inhibitor, in patients with relapsed or refractory hematologic malignancies.* Clin Cancer Res, 2008. **14**(9): p. 2756-62.
125. Yee, K.W., et al., *Phase I/II study of the mammalian target of rapamycin inhibitor everolimus (RAD001) in patients with relapsed or refractory hematologic malignancies.* Clin Cancer Res, 2006. **12**(17): p. 5165-73.
126. Amadori, S., et al., *Temsirolimus, an mTOR inhibitor, in combination with lower-dose clofarabine as salvage therapy for older patients with acute myeloid leukaemia: results of a phase II GIMEMA study (AML-1107).* Br J Haematol, 2012. **156**(2): p. 205-12.
127. Park, S., et al., *A phase Ib GOELAMS study of the mTOR inhibitor RAD001 in association with chemotherapy for AML patients in first relapse.* Leukemia, 2013. **27**(7): p. 1479-86.
128. Xu, Q., et al., *Survival of acute myeloid leukemia cells requires PI3 kinase activation.* Blood, 2003. **102**(3): p. 972-80.
129. Min, Y.H., et al., *Constitutive phosphorylation of Akt/PKB protein in acute myeloid leukemia: its significance as a prognostic variable.* Leukemia, 2003. **17**(5): p. 995-7.
130. Tamburini, J., et al., *Constitutive phosphoinositide 3-kinase/Akt activation represents a favorable prognostic factor in de novo acute myelogenous leukemia patients.* Blood, 2007. **110**(3): p. 1025-8.

131. Papa, V., et al., *Proapoptotic activity and chemosensitizing effect of the novel Akt inhibitor perifosine in acute myelogenous leukemia cells.* Leukemia, 2008. **22**(1): p. 147-60.
132. Bortul, R., et al., *Deguelin, A PI3K/AKT inhibitor, enhances chemosensitivity of leukaemia cells with an active PI3K/AKT pathway.* Br J Haematol, 2005. **129**(5): p. 677-86.
133. Gojo, I., et al., *Phase I study of UCN-01 and perifosine in patients with relapsed and refractory acute leukemias and high-risk myelodysplastic syndrome.* Invest New Drugs, 2013. **31**(5): p. 1217-27.
134. Sampath, D., et al., *Phase I clinical, pharmacokinetic, and pharmacodynamic study of the Akt-inhibitor triciribine phosphate monohydrate in patients with advanced hematologic malignancies.* Leuk Res, 2013. **37**(11): p. 1461-7.
135. Wunderle LM, B.S., Lang F, Wolf A, Schleyer E, Serve H, et al. , *Safety and efficacy of BEZ235, a dual PI3-kinase/mTOR inhibitor, in adult patients with relapsed or refractory acute leukemia: results of a phase I study.* ASH annual meeting and exposition. New Orleans: ASH., 2013.
136. Nepstad, I., et al., *Resistance to the Antiproliferative In Vitro Effect of PI3K-Akt-mTOR Inhibition in Primary Human Acute Myeloid Leukemia Cells Is Associated with Altered Cell Metabolism.* Int J Mol Sci, 2018. **19**(2).
137. Glick, D., S. Barth, and K.F. Macleod, *Autophagy: cellular and molecular mechanisms.* J Pathol, 2010. **221**(1): p. 3-12.
138. Yin, Z., C. Pascual, and D.J. Klionsky, *Autophagy: machinery and regulation.* Microb Cell, 2016. **3**(12): p. 588-596.
139. Parzych, K.R. and D.J. Klionsky, *An overview of autophagy: morphology, mechanism, and regulation.* Antioxid Redox Signal, 2014. **20**(3): p. 460-73.
140. Egan, D., et al., *The autophagy initiating kinase ULK1 is regulated via opposing phosphorylation by AMPK and mTOR.* Autophagy, 2011. **7**(6): p. 643-4.
141. Zhao, M. and D.J. Klionsky, *AMPK-dependent phosphorylation of ULK1 induces autophagy.* Cell Metab, 2011. **13**(2): p. 119-20.
142. Jung, C.H., et al., *mTOR regulation of autophagy.* FEBS Lett, 2010. **584**(7): p. 1287-95.
143. Wang, R.C., et al., *Akt-mediated regulation of autophagy and tumorigenesis through Beclin 1 phosphorylation.* Science, 2012. **338**(6109): p. 956-9.
144. Mizushima, N., T. Yoshimori, and B. Levine, *Methods in mammalian autophagy research.* Cell, 2010. **140**(3): p. 313-26.
145. Murrow, L. and J. Debnath, *Autophagy as a stress-response and quality-control mechanism: implications for cell injury and human disease.* Annu Rev Pathol, 2013. **8**: p. 105-37.
146. Maiuri, M.C. and G. Kroemer, *Autophagy in stress and disease.* Cell Death Differ, 2015. **22**(3): p. 365-6.
147. Mortensen, M., et al., *The autophagy protein Atg7 is essential for hematopoietic stem cell maintenance.* J Exp Med, 2011. **208**(3): p. 455-67.
148. Brigger, D., et al., *Inhibition of GATE-16 attenuates ATRA-induced neutrophil differentiation of APL cells and interferes with autophagosome formation.* Biochem Biophys Res Commun, 2013. **438**(2): p. 283-8.
149. Liu, Q., et al., *Atg5-dependent autophagy contributes to the development of acute myeloid leukemia in an MLL-AF9-driven mouse model.* Cell Death Dis, 2016. **7**(9): p. e2361.
150. Porter, A.H., et al., *Acute myeloid leukemia stem cell function is preserved in the absence of autophagy.* Haematologica, 2017. **102**(9): p. e344-e347.
151. Chen, X., et al., *Autophagy is dispensable for Kmt2a/Mll-Mllt3/Af9 AML maintenance and anti-leukemic effect of chloroquine.* Autophagy, 2017. **13**(5): p. 955-966.

152. Sumitomo, Y., et al., *Cytoprotective autophagy maintains leukemia-initiating cells in murine myeloid leukemia.* Blood, 2016. **128**(12): p. 1614-24.
153. Dirkje, W.H., et al., *Autophagy Promotes the Survival and Therapy Resistance of Human Acute Myeloid Leukemia Cells Under Hypoxia.* Blood, 2014. **124**(21): p. 2236.
154. Rubnitz, J.E., *How I treat pediatric acute myeloid leukemia.* Blood, 2012. **119**(25): p. 5980-8.
155. Buchner, T., et al., *Acute Myeloid Leukemia (AML): different treatment strategies versus a common standard arm–combined prospective analysis by the German AML Intergroup.* J Clin Oncol, 2012. **30**(29): p. 3604-10.
156. Rowe, J.M. and M.S. Tallman, *How I treat acute myeloid leukemia.* Blood, 2010. **116**(17): p. 3147-56.
157. Ravandi, F., et al., *Progress in the treatment of acute myeloid leukemia.* Cancer, 2007. **110**(9): p. 1900-10.
158. Frohling, S., et al., *Genetics of myeloid malignancies: pathogenetic and clinical implications.* J Clin Oncol, 2005. **23**(26): p. 6285-95.
159. Cantor, J.R. and D.M. Sabatini, *Cancer cell metabolism: one hallmark, many faces.* Cancer Discov, 2012. **2**(10): p. 881-98.
160. Hanahan, D. and R.A. Weinberg, *Hallmarks of cancer: the next generation.* Cell, 2011. **144**(5): p. 646-74.
161. Kroemer, G. and J. Pouyssegur, *Tumor cell metabolism: cancer's Achilles' heel.* Cancer Cell, 2008. **13**(6): p. 472-82.
162. Vander Heiden, M.G., L.C. Cantley, and C.B. Thompson, *Understanding the Warburg effect: the metabolic requirements of cell proliferation.* Science, 2009. **324**(5930): p. 1029-33.
163. Kishton, R.J., et al., *AMPK Is Essential to Balance Glycolysis and Mitochondrial Metabolism to Control T-ALL Cell Stress and Survival.* Cell Metab, 2016. **23**(4): p. 649-62.
164. Park, S., et al., *Role of the PI3K/AKT and mTOR signaling pathways in acute myeloid leukemia.* Haematologica, 2010. **95**(5): p. 819-28.
165. Sujobert, P. and J. Tamburini, *Co-activation of AMPK and mTORC1 as a new therapeutic option for acute myeloid leukemia.* Mol Cell Oncol, 2016. **3**(4): p. e1071303.
166. Willems, L., et al., *The dual mTORC1 and mTORC2 inhibitor AZD8055 has anti-tumor activity in acute myeloid leukemia.* Leukemia, 2012. **26**(6): p. 1195-202.
167. Recher, C., et al., *Antileukemic activity of rapamycin in acute myeloid leukemia.* Blood, 2005. **105**(6): p. 2527-34.
168. Fernandes, A., et al., *Proteolytic systems and AMP-activated protein kinase are critical targets of acute myeloid leukemia therapeutic approaches.* Oncotarget, 2015. **6**(31): p. 31428-40.
169. Altman, J.K., et al., *Autophagy is a survival mechanism of acute myelogenous leukemia precursors during dual mTORC2/mTORC1 targeting.* Clin Cancer Res, 2014. **20**(9): p. 2400-9.
170. Auberger, P. and A. Puissant, *Autophagy, a key mechanism of oncogenesis and resistance in leukemia.* Blood, 2017. **129**(5): p. 547-552.
171. Kung, C.P., et al., *Autophagy in tumor suppression and cancer therapy.* Crit Rev Eukaryot Gene Expr, 2011. **21**(1): p. 71-100.
172. Evangelisti, C., et al., *Autophagy in acute leukemias: a double-edged sword with important therapeutic implications.* Biochim Biophys Acta, 2015. **1853**(1): p. 14-26.
173. Dalton, W.T., Jr., et al., *HL-60 cell line was derived from a patient with FAB-M2 and not FAB-M3.* Blood, 1988. **71**(1): p. 242-7.

174. Birnie, G.D., *The HL60 cell line: a model system for studying human myeloid cell differentiation.* Br J Cancer Suppl, 1988. **9**: p. 41-5.
175. Koeffler, H.P. and D.W. Golde, *Human myeloid leukemia cell lines: a review.* Blood, 1980. **56**(3): p. 344-50.
176. Zhou, G., et al., *Role of AMP-activated protein kinase in mechanism of metformin action.* J Clin Invest, 2001. **108**(8): p. 1167-74.
177. Barban, S. and H.O. Schulze, *The effects of 2-deoxyglucose on the growth and metabolism of cultured human cells.* J Biol Chem, 1961. **236**: p. 1887-90.
178. Li, J., S.G. Kim, and J. Blenis, *Rapamycin: one drug, many effects.* Cell Metab, 2014. **19**(3): p. 373-9.
179. Mauvezin, C. and T.P. Neufeld, *Bafilomycin A1 disrupts autophagic flux by inhibiting both V-ATPase-dependent acidification and Ca-P60A/SERCA-dependent autophagosome-lysosome fusion.* Autophagy, 2015. **11**(8): p. 1437-8.
180. Yap, T.A., et al., *First-in-man clinical trial of the oral pan-AKT inhibitor MK-2206 in patients with advanced solid tumors.* J Clin Oncol, 2011. **29**(35): p. 4688-95.
181. Magnuson, B., B. Ekim, and D.C. Fingar, *Regulation and function of ribosomal protein S6 kinase (S6K) within mTOR signalling networks.* Biochem J, 2012. **441**(1): p. 1-21.
182. Vazquez-Martin, A., et al., *Serine79-phosphorylated acetyl-CoA carboxylase, a downstream target of AMPK, localizes to the mitotic spindle poles and the cytokinesis furrow.* Cell Cycle, 2013. **12**(10): p. 1639-41.
183. Stein, S.C., et al., *The regulation of AMP-activated protein kinase by phosphorylation.* Biochem J, 2000. **345 Pt 3**: p. 437-43.
184. Hindupur, S.K., A. Gonzalez, and M.N. Hall, *The opposing actions of target of rapamycin and AMP-activated protein kinase in cell growth control.* Cold Spring Harb Perspect Biol, 2015. **7**(8): p. a019141.
185. Mihaylova, M.M. and R.J. Shaw, *The AMPK signalling pathway coordinates cell growth, autophagy and metabolism.* Nat Cell Biol, 2011. **13**(9): p. 1016-23.
186. Klionsky, D.J., et al., *Guidelines for the use and interpretation of assays for monitoring autophagy (3rd edition).* Autophagy, 2016. **12**(1): p. 1-222.
187. Ichimura, Y. and M. Komatsu, *Selective degradation of p62 by autophagy.* Semin Immunopathol, 2010. **32**(4): p. 431-6.
188. Mizushima, N., et al., *A protein conjugation system essential for autophagy.* Nature, 1998. **395**(6700): p. 395-8.
189. Santos, F.P., et al., *Adult acute erythroleukemia: An analysis of 108 patients treated at a single institution.* Leukemia, 2009. **23**(12): p. 2275-80.
190. Radwan, S.M., et al., *Beclin-1 and hypoxia-inducible factor-1alpha genes expression: Potential biomarkers in acute leukemia patients.* Cancer Biomark, 2016. **16**(4): p. 619-26.
191. Liang, P.Q., et al., *Expression of autophagy genes in acute myeloid leukemia: associations with clinical characteristics and prognosis.* Neoplasma, 2018.
192. Walter, M.J., et al., *Acquired copy number alterations in adult acute myeloid leukemia genomes.* Proc Natl Acad Sci U S A, 2009. **106**(31): p. 12950-5.
193. Lian, Y., et al., *Clinical significance of BECLIN1 and ATG5 expression in acute myeloid leukemia patients* Int J Clin Exp Pathol 2018. **11**(3): p. 1529-1537.
194. Hu, X.Y., et al., *[Expression of autophagy related gene Beclin1 and MAPLC3 in bone marrow mononuclear cells isolated from acute leukemia patients and its significance].* 2011. **19**(3): p. 598-601.

195. Vazquez, C.L. and M.I. Colombo, *Beclin 1 modulates the anti-apoptotic activity of Bcl-2: insights from a pathogen infection system.* Autophagy, 2010. **6**(1): p. 177-8.
196. Ciechomska, I.A., et al., *Bcl-2 complexed with Beclin-1 maintains full anti-apoptotic function.* Oncogene, 2009. **28**(21): p. 2128-41.
197. Ciechomska, I.A., C.G. Goemans, and A.M. Tolkovsky, *Why doesn't Beclin 1, a BH3-only protein, suppress the anti-apoptotic function of Bcl-2?* Autophagy, 2009. **5**(6): p. 880-1.
198. Kang, R., et al., *The Beclin 1 network regulates autophagy and apoptosis.* Cell Death Differ, 2011. **18**(4): p. 571-80.
199. Yogarajah, M. and R.M. Stone, *A concise review of BCL-2 inhibition in acute myeloid leukemia.* Expert Rev Hematol, 2018. **11**(2): p. 145-154.
200. Boe, S.O. and A. Simonsen, *Autophagic degradation of an oncoprotein.* Autophagy, 2010. **6**(7): p. 964-5.
201. Zare-Abdollahi, D., et al., *Expression analysis of BECN1 in acute myeloid leukemia: association with distinct cytogenetic and molecular abnormalities.* Int J Lab Hematol, 2016. **38**(2): p. 125-32.
202. Folkerts, H., et al., *Inhibition of autophagy as a treatment strategy for p53 wild-type acute myeloid leukemia.* Cell Death Dis, 2017. **8**(7): p. e2927.
203. Ayala, F., et al., *Contribution of bone microenvironment to leukemogenesis and leukemia progression.* Leukemia, 2009. **23**(12): p. 2233-41.
204. Becker, P.S., *Dependence of acute myeloid leukemia on adhesion within the bone marrow microenvironment.* ScientificWorldJournal, 2012. **2012**: p. 856467.
205. Meads, M.B., L.A. Hazlehurst, and W.S. Dalton, *The bone marrow microenvironment as a tumor sanctuary and contributor to drug resistance.* Clin Cancer Res, 2008. **14**(9): p. 2519-26.
206. Zeng, Z., et al., *Targeting of mTORC1/2 by the mTOR kinase inhibitor PP242 induces apoptosis in AML cells under conditions mimicking the bone marrow microenvironment.* Blood, 2012. **120**(13): p. 2679-89.
207. Blau, O., *Bone marrow stromal cells in the pathogenesis of acute myeloid leukemia.* Front Biosci (Landmark Ed), 2014. **19**: p. 171-80.
208. Macanas-Pirard, P., et al., *Bone marrow stromal cells modulate mouse ENT1 activity and protect leukemia cells from cytarabine induced apoptosis.* PLoS One, 2012. **7**(5): p. e37203.
209. Guan, D., et al., *Bone marrow stromal-cell line HS-5 affects apoptosis of acute myeloid leukemia cells HL-60 through GLI1 activation.* Biomedical Research, 2018. **29**(5): p. 865-868.
210. Rashidi, A. and J.F. DiPersio, *Targeting the leukemia-stroma interaction in acute myeloid leukemia: rationale and latest evidence.* Ther Adv Hematol, 2016. **7**(1): p. 40-51.
211. Brenner, A.K., I. Nepstad, and O. Bruserud, *Mesenchymal Stem Cells Support Survival and Proliferation of Primary Human Acute Myeloid Leukemia Cells through Heterogeneous Molecular Mechanisms.* Front Immunol, 2017. **8**: p. 106.
212. Castillo, J.J., et al., *Increased incidence of non-Hodgkin lymphoma, leukemia, and myeloma in patients with diabetes mellitus type 2: a meta-analysis of observational studies.* Blood, 2012. **119**(21): p. 4845-50.
213. Baynest, H.W., *Classification, Pathophysiology, Diagnosis and Management of Diabetes Mellitus.* J Diabetes Metab, 2015. **6**(5).
214. *World Health Organization. Diabetes Fact Sheet n°312.* at <http://www.who.int/mediacentre/factsheets/fs312/en/>.

215. *International Diabetes Federation - IDF Diabetes Atlas 7th Edition*. at <http://www.diabetesatlas.org/>.
216. Seymour, E.K., et al., *The Impact of Diabetes on Clinical Outcomes in Chronic Lymphocytic Leukemia.* Blood, 2015. **126**(23): p. 2095.
217. Fujimiya, M., et al., *Bone marrow stem cell abnormality and diabetic complications.* Anat Rec (Hoboken), 2012. **295**(6): p. 917-21.
218. Ferraro, F., et al., *Diabetes impairs hematopoietic stem cell mobilization by altering niche function.* Sci Transl Med, 2011. **3**(104): p. 104ra101.
219. Westerweel, P.E., et al., *Impaired endothelial progenitor cell mobilization and dysfunctional bone marrow stroma in diabetes mellitus.* PLoS One, 2013. **8**(3): p. e60357.
220. Keats, E. and Z.A. Khan, *Unique responses of stem cell-derived vascular endothelial and mesenchymal cells to high levels of glucose.* PLoS One, 2012. **7**(6): p. e38752.
221. Zhang, D., et al., *High glucose induces the aging of mesenchymal stem cells via Akt/mTOR signaling.* Mol Med Rep, 2017. **16**(2): p. 1685-1690.
222. Chang, T.C., M.F. Hsu, and K.K. Wu, *High glucose induces bone marrow-derived mesenchymal stem cell senescence by upregulating autophagy.* PLoS One, 2015. **10**(5): p. e0126537.
223. Estrada, J.C., et al., *Human mesenchymal stem cell-replicative senescence and oxidative stress are closely linked to aneuploidy.* Cell Death Dis, 2013. **4**: p. e691.
224. Stolzing, A., N. Coleman, and A. Scutt, *Glucose-induced replicative senescence in mesenchymal stem cells.* Rejuvenation Res, 2006. **9**(1): p. 31-5.
225. Parsch, D., et al., *Telomere length and telomerase activity during expansion and differentiation of human mesenchymal stem cells and chondrocytes.* J Mol Med (Berl), 2004. **82**(1): p. 49-55.
226. Gama, K.B., et al., *Conditioned Medium of Bone Marrow-Derived Mesenchymal Stromal Cells as a Therapeutic Approach to Neuropathic Pain: A Preclinical Evaluation.* Stem Cells Int, 2018. **2018**: p. 8179013.
227. Lasser, C., M. Eldh, and J. Lotvall, *Isolation and characterization of RNA-containing exosomes.* J Vis Exp, 2012(59): p. e3037.
228. Hou, Y., et al., *High glucose levels promote the proliferation of breast cancer cells through GTPases.* Breast Cancer (Dove Med Press), 2017. **9**: p. 429-436.
229. Takatani-Nakase, T., et al., *High glucose level promotes migration behavior of breast cancer cells through zinc and its transporters.* PLoS One, 2014. **9**(2): p. e90136.
230. Wu, J., et al., *High glucose induces epithelial-mesenchymal transition and results in the migration and invasion of colorectal cancer cells.* Exp Ther Med, 2018. **16**(1): p. 222-230.
231. Kellenberger, L.D. and J. Petrik, *Hyperglycemia promotes insulin-independent ovarian tumor growth.* Gynecol Oncol, 2018. **149**(2): p. 361-370.
232. Li, W., et al., *Hyperglycemia enhances the invasive and migratory activity of pancreatic cancer cells via hydrogen peroxide.* Oncol Rep, 2011. **25**(5): p. 1279-87.
233. Davidson, M.D., K.R. Ballinger, and S.R. Khetani, *Long-term exposure to abnormal glucose levels alters drug metabolism pathways and insulin sensitivity in primary human hepatocytes.* Sci Rep, 2016. **6**: p. 28178.
234. Wang, L.D. and A.J. Wagers, *Dynamic niches in the origination and differentiation of haematopoietic stem cells.* Nat Rev Mol Cell Biol, 2011. **12**(10): p. 643-55.
235. Kumar, B., et al., *Acute myeloid leukemia transforms the bone marrow niche into a leukemia-permissive microenvironment through exosome secretion.* Leukemia, 2018. **32**(3): p. 575-587.

236. Zhou, H.S., B.Z. Carter, and M. Andreeff, *Bone marrow niche-mediated survival of leukemia stem cells in acute myeloid leukemia: Yin and Yang.* Cancer Biol Med, 2016. **13**(2): p. 248-59.
237. Barrera-Ramirez, J., et al., *Micro-RNA Profiling of Exosomes from Marrow-Derived Mesenchymal Stromal Cells in Patients with Acute Myeloid Leukemia: Implications in Leukemogenesis.* Stem Cell Rev, 2017. **13**(6): p. 817-825.
238. Colmone, A., et al., *Leukemic cells create bone marrow niches that disrupt the behavior of normal hematopoietic progenitor cells.* Science, 2008. **322**(5909): p. 1861-5.
239. Huan, J., et al., *RNA trafficking by acute myelogenous leukemia exosomes.* Cancer Res, 2013. **73**(2): p. 918-29.
240. Boyiadzis, M. and T.L. Whiteside, *Exosomes in acute myeloid leukemia inhibit hematopoiesis.* Curr Opin Hematol, 2018. **25**(4): p. 279-284.
241. Kumar, B., et al., *Exosome-mediated microenvironment dysregulation in leukemia.* Biochim Biophys Acta, 2016. **1863**(3): p. 464-470.
242. Kaur, S., et al., *CD63, MHC class 1, and CD47 identify subsets of extracellular vesicles containing distinct populations of noncoding RNAs.* Sci Rep, 2018. **8**(1): p. 2577.
243. Willms, E., et al., *Cells release subpopulations of exosomes with distinct molecular and biological properties.* Sci Rep, 2016. **6**: p. 22519.
244. Ni, M. and A.S. Lee, *ER chaperones in mammalian development and human diseases.* FEBS Lett, 2007. **581**(19): p. 3641-51.
245. Li, S., C.E. Mason, and A. Melnick, *Genetic and epigenetic heterogeneity in acute myeloid leukemia.* Curr Opin Genet Dev, 2016. **36**: p. 100-6.
246. Kennedy, J.A. and F. Barabe, *Investigating human leukemogenesis: from cell lines to in vivo models of human leukemia.* Leukemia, 2008. **22**(11): p. 2029-40.
247. Rucker, F.G., et al., *Disclosure of candidate genes in acute myeloid leukemia with complex karyotypes using microarray-based molecular characterization.* J Clin Oncol, 2006. **24**(24): p. 3887-94.
248. Dalle Pezze, P., et al., *A systems study reveals concurrent activation of AMPK and mTOR by amino acids.* Nat Commun, 2016. **7**: p. 13254.
249. *The Nobel Assembly. The Nobel Assembly at Karolinska Instiutet has today decided to award the 2016 Nobel Prize in Physiology or Medicine to Yoshinori Ohsumi. 2016 < https://www.nobelprize.org/nobel_prizes/medicine/laureates/2016/press.html>.*
250. Harb, A., et al., *Acute myeloid leukemia and diabetes insipidus with monosomy 7.* Cancer Genet Cytogenet, 2009. **190**(2): p. 97-100.
251. American Diabetes, A., *Diagnosis and classification of diabetes mellitus.* Diabetes Care, 2013. **36 Suppl 1**: p. S67-74.